FINAL
CONTRACT REPORT

# AN EVALUATION
# OF THE PERFORMANCE
# OF EPOXY-COATED REINFORCING STEEL
# IN CONCRETE EXPOSURE SPECIMENS

JERZY ZEMAJTIS
Research Associate
Virginia Polytechnic Institute
and State University

RICHARD E. WEYERS
Professor
Virginia Polytechnic Institute
and State University

MICHAEL M. SPRINKEL
Research Manager
Virginia Transportation Research Council

V · I · R · G · I · N · I · A
VTRC

TRANSPORTATION RESEARCH COUNCIL

VIRGINIA TRANSPORTATION RESEARCH COUNCIL

# FINAL CONTRACT REPORT

# AN EVALUATION OF THE PERFORMANCE OF EPOXY-COATED REINFORCING STEEL IN CONCRETE EXPOSURE SPECIMENS

**Jerzy Zemajtis**
**Research Associate**
**Virginia Polytechnic Institute and State University**

**Richard E. Weyers**
**Professor**
**Virginia Polytechnic Institute and State University**

**Michael M. Sprinkel**
**Research Manager**
**Virginia Transportation Research Council**

(The opinions, findings, and conclusions expressed in this
report are those of the authors and not necessarily
those of the sponsoring agencies.)

# ABSTRACT

This report presents the results of a two-year study of five different epoxy-coated rebar (ECR) specimens in concrete. The purpose of the project was to compare the performance of exposure specimens constructed with ECR to that of specimens constructed with bare steel. Small scale specimens (SSS) and large scale specimens (LSS) were evaluated. LSS were built to simulate exposure conditions typical for concrete bridges located in the coastal region or inland where deicing salts are used. SSS were fabricated with added mechanical damage to the coating. Sodium chloride was added to the concrete mixing water, and the specimens were kept outdoors and exposed to natural weathering only. The LSS were kept inside the laboratory and were exposed to weekly ponding cycles of sodium chloride solution of either three or six percent by weight.

Tests of AC impedance, corrosion rates (3LP), electrochemical impedance spectroscopy (EIS), and visual observations were performed on SSS. The condition of the LSS was assessed through chloride concentration measurements and AC impedance. Additionally, visual observations were performed for identification of rust stains and cracking on concrete surfaces. Corrosion rates and corrosion potential were used to evaluate the performance of the control LSS. The 3LP data was difficult to interpret for the SSS because the corrosion rate was found to be the same for all specimens, even though the corroding area was different. A bare steel specimen cracked after nine months of exposure; no cracks were observed on specimens with ECR during the two-year exposure period. None of the non-destructive techniques used in this study was appropriate for characterization of ECR. Destructive sampling and examination of the bar and coating condition was the best method for evaluating ECR performance. Cracking in the control specimens appeared to be related to rebar corrosion. Most of the ECR specimens had no corrosion-related cracks. Only specimens fabricated with concrete with water to cement ratios larger than 0.7 experienced corrosion-related cracking.

Although the exposure specimens do not simulate actual field conditions because the coatings were well bonded when the salt exposure began, the authors recommend that the SSS and LSS specimens continue to be monitored until cracking has occurred in all specimens. This effort will allow researchers to better estimate the service provided by ECR and will provide useful information on corrosion-induced spalling in specimens with ECR.

# FINAL CONTRACT REPORT

## AN EVALUATION OF THE PERFORMANCE OF EPOXY-COATED REINFORCING STEEL IN CONCRETE EXPOSURE SPECIMENS

**Jerzy Zemajtis**
**Research Associate**
**Virginia Polytechnic Institute and State University**

**Richard E. Weyers**
**Professor**
**Virginia Polytechnic Institute and State University**

**Michael M. Sprinkel**
**Research Manager**
**Virginia Transportation Research Council**

## INTRODUCTION

It is well known that the steel reinforcement in concrete bridges deteriorates rapidly when exposed to chloride ion. As the cause, process and severity of the concrete bridge deterioration problem in the United States became known, a multitude of corrosion abatement techniques were developed for existing and newly constructed bridges. Epoxy-coated reinforcing steel (ECR) and corrosion-inhibiting admixtures are two such techniques developed to extend the service life of newly constructed concrete bridge components. ECR is currently the most common corrosion protection method for concrete bridges in the United States. Corrosion inhibitors have been used for over 20 years but are employed significantly less frequently than ECR.

Until 1986, when Florida reported that the Long Key Bridge showed signs of corrosion only six years after construction, the effectiveness of ECR remained unquestioned. Since then, twelve field studies have been conducted on the corrosion protection effectiveness of ECR.[1] Conclusions have been mixed, from satisfactory corrosion protection performance to date for bridge decks, to poor performance in substructures. Some studies have predicted that ECR will not provide long-term (50 years) of corrosion protection for substructures or decks.[1] The reason for the mixed conclusions included limited or inappropriate evaluation methods which always accompany a lack of knowledge of the cause(s) of failure, and subjectively defined failure criteria. Studies where care and appropriate evaluation methods and failure criteria have been employed have concluded that ECR will not provide 50 years of corrosion-free protection for steel in concrete bridge components.[2, 3] More recent studies, including one in Virginia, support these earlier conclusions that ECR will not provide long term corrosion protection performance.[4,5] As a result, interest in the effectiveness of corrosion-inhibiting admixtures has been renewed.

In response to this interest, the Virginia Department of Transportation (VDOT) initiated an evaluation of corrosion protection performance for newly constructed concrete bridges. The protection systems included in the study are ECR (present and new coatings), galvanized reinforcing steel, three commercial corrosion-inhibiting admixtures, low-permeability concretes, and two dual corrosion protection systems (a corrosion inhibitor and ECR, and a corrosion inhibitor and low permeable concrete). Evaluation of the corrosion protection effectiveness was assessed in both a simulated concrete pore water solution and in concrete exposure specimens. An ECR field study was also included. The field study assessed the condition of three 8 year old substructures in a marine environment and three 17 year old bridge decks that were seasonally exposed to deicer salt. This report presents the results of the study of ECR in concrete exposure specimens.

## PURPOSE & SCOPE

The purpose of this study was fourfold:

1. To identify existing corrosion assessment test methods that could be used to determine instantaneous corrosion states of ECR in concrete

2. To evaluate the short-term laboratory corrosion protection performance of past, current and future ECR samples supplied to VDOT by ECR coaters

3. To compare the short-term laboratory corrosion protection performance of two new epoxy coating systems with the present coatings purchased by VDOT

4. To provide well-characterized ECR specimens for long term evaluation of corrosion protection performance.

The study was limited to the assessment of ECR presently being supplied to Virginia by three coaters and two newly developed epoxy coating systems. Small and large scale specimens were prepared. The objective of the small specimen tests was to evaluate how well non-destructive test methods characterize ECR performance, and whether these tests could be used to evaluate the ECR used in the LSS. The tests included AC impedance, corrosion rates, using the three point linear polarization test (3LP), and electrochemical impedance spectroscopy (EIS). The objective of LSS testing was to investigate ECR as a corrosion protection system and to evaluate its performance in reference to bare steel. The secondary objective was to differentiate between the five types of ECR. Methods used to assess the condition of the LSS included chloride concentration measurements and AC impedance. Additionally, visual observations were performed for identification of rust stains and cracking on concrete surfaces.

# METHODS

## Specimen Design

Two types of specimens were used in this study: small scale specimens (SSS) and large scale specimens (LSS). LSS and SSS had in common the following parameters: water to cement ratio (w/c) of 0.45, concrete mixture proportions, concrete cover depth of 25 mm, and type of the reinforcing steel. However, SSS were kept outdoors and exposed to natural weathering; for part of the research period, the LSS were kept inside the laboratory and exposed to sodium chloride (NaCl) solutions. Concrete for SSS was mixed in the laboratory, NaCl was added to the mixing water and some of the epoxy coating was mechanically removed. In contrast, LSS were cast with concrete that was plant batched and mixed and delivered in a ready-mix truck, and no additional damage was added to the coating other than what would have occurred during the placement of the concrete. Three out of five ECR bar types used for LSS fabrication were in the condition "as received" (Table 1). These samples were purchased from Free State Coaters (FSC), Florida Steel (FS), and Lane Enterprises (LNE). The remaining two types, Canada Green (CGN) and Canada Gray (CGY), were shipped to the Materials Research Laboratory directly from the manufacturer. Each bar was individually wrapped, so that no transportation or handling damage was possible. These bars were in perfect physical condition. Only FS bars were used in fabrication of SSS.

### *Small Scale Specimens*

Small scale specimens were built to evaluate nondestructive test methods for identifying rebar corrosion. Six specimens, each with two No. 5 16 mm diameter FS bars, were used in the study. Each bar was 360 mm long. Only bars with a visually perfect coating were selected for evaluation. The coating from selected bars was then mechanically removed to varying degrees of damage, so that the damaged area of each bar was known prior to concrete placement. The specimens differed not only by the degree of coating damage, but also by the location of the damage in reference to the specimens' top surface. Specimen I had a bare steel bar and an epoxy-coated bar with no visual surface damage (perfect coating). Specimens II, III, IV, V, and VI had epoxy-coated bars with 0.01, 0.2, 0.5, 1, and 2 percent surface damage, respectively. One bar, with the surface damage on top of the bar, was placed so that the damaged area was at 25 mm depth from the specimen's surface. The other bar, with the surface damage on the bottom of the bar, was placed so that the damaged area was at 41 mm depth from the specimen's surface. All specimens were designed to have a 25mm cover depth. The test configuration is presented in Table 2, and Figure 1 shows the typical configuration for each SSS.

Concrete for SSS was mixed in the laboratory and its mixture proportions are presented in Table 3. To accelerate corrosion of the embedded reinforcing bars, sodium chloride was dissolved in mixing water. The resulting admixed chloride ion concentration was 4.8 $kg/m^3$ of concrete. The w/c ratio was 0.45, slump was equal to 190 mm, density was determined to be 2.32 $g/cm^3$, and air content was 7 percent. Compressive strength at 28 days was 34.4 MPa.

The specimens were cast in wooden forms oiled with form release agent. Reinforcing steel was placed at the bottom of the forms to achieve exactly 25 mm cover depth and to prevent subsidence cracking over the bar. After 28 days of wet curing, the four sides of each specimen were painted with epoxy to reduce moisture movement across these faces. Top and bottom of the specimens were left as cast and finished surfaces. The specimens were then stored outdoors at the Civil Engineering Materials Research Laboratory in Blacksburg, Virginia.

*Large Scale Specimens*

To assess performance of epoxy coating, eleven ECR specimens and two control specimens were cast. The eleven ECR specimens were made with five different types of epoxy-coated steel. The parameters that were kept constant for all 13 specimens included 0.45 w/c ratio and 25 mm reinforcing cover depth. In addition to these 13 specimens, 2 specimens with a w/c ratio of 0.74 and 1 specimen with a w/c ratio of 0.71 were cast, for a total of 16 specimens. As shown in Figure 2, each specimen was 1.72 m high, had horizontal dimensions of 1.12 m by 1.12 m, and was designed to simulate four exposure conditions: wetted deck surface (horizontal zone), wetted vertical surfaces of bridge members (vertical zone), tidal zone, and immersion zone. The immersion zone covered an area from the bottom of specimens' legs to the height of 305 mm. The tidal zone was defined as 305 mm to 610 mm from the bottom of specimens' legs. A vertical surface area above 610 mm from the bottom of a specimen corresponded to the vertical zone, and the horizontal zone was the top surface area of the specimen.

The specimens differed by the following parameters (see Table 4):

- Type of the reinforcing steel: bare steel (specimens BS-1, BS-2), five types of epoxy-coated steel designated as FSC (specimens FSC-1, FSC-2, FSC-3, FSC-4, FSC-5, FSC-51), LNE (specimens LNE-1, LNE-2), FS (specimens FS-1, FS-2), CGN (specimens CGN-1, CGN-11), and CGY (specimens CGY-1, CGY-11)

- Configuration of the reinforcing steel (RS) in specimen's legs: type I - RS electrically disconnected in both legs, type II - RS electrically connected in both legs (same bars for vertical, tidal, and immersion zones), type III - RS electrically disconnected in the right leg and RS electrically connected in the left leg (same bars for vertical, tidal, and immersion zones)

- Configuration of the RS in the horizontal zone: each specimen had either both mats with ECR, or top mat - ECR and bottom mat – BS

- Concrete type: VDOT A4 concrete with w/c = 0.45, or concrete with w/c > 0.7

- Concentration of wetting solution: either 3 percent or 6 percent sodium chloride (NaCl) by weight.

Four steel forms were used for LSS preparation. Since each form was used several times, all surfaces were carefully cleaned and then oiled with form release agent before each concrete placement. Specimens were wet cured in the forms for seven days. After removal from the forms, the specimens were wrapped with wet burlap and covered with plastic for additional 21 days of wet curing. The specimens were then air-dried in the laboratory for a minimum of 30 and prepared for wet-dry cycles. All bar ends protruding from specimen legs in the lower part of the legs (0.61 m from the bottom) were protected with plastic tubing, stoppers, and silicone against contact with wetting solution. Plexiglass dikes were assembled on the specimen's top surface so that the salt (NaCl) solution could uniformly wet the legs. Each specimen was placed into a 0.71 m deep high-density polyethylene (HDPE) tank and exposed to wet-dry cycles. The following section includes a description of the specimen wet-dry cycles.

## Experimental Plan

Unlike SSS, all LSS were kept indoors and exposed to wet-dry ponding cycles. Each cycle was one week in duration and was divided into two stages. The specimens were paired so when the wetting solution was at high tide level (610 mm from the bottom of a specimen) for the first specimen, the second specimen had wetting solution at low tide level (305 mm from the bottom of a specimen). When the water was at low tide position, wetting solution was pumped to the top of a specimen, thus wetting specimen surfaces in the horizontal and vertical zones. At the same time, surfaces in the tidal zone were allowed to air dry. While the first specimen from the pair had a dry tidal zone, the other specimen had a wetted tidal zone. Thus, the tidal zone was cyclically submersed and the immersion zone was constantly submersed in the NaCl solution. The horizontal and vertical zones of the specimens were allowed to air dry during the high tide period. Since there was an odd number of specimens, wetting solution from one specimen was pumped to external containers, so that the high tide - low tide levels could easily be adjusted. Horizontal, vertical, and tidal zones were subjected to wetting for an average of 3.5 days in a week and to air drying also for an average of 3.5 days in a week. Immersion zones were subjected to wetting solution for 7 days a week. The wetting solutions used in the study included 3 percent and 6 percent sodium chloride by weight. After approximately 1.5 years of wet-dry cycles, the specimens were removed from the tanks and moved outdoors.

## Evaluation Methods

### Small Scale Specimens

AC impedance and three point linear polarization (3LP) measurements were taken on each SSS bar on a monthly basis, and a set of EIS measurements was taken once. For each bar, AC impedance was recorded at three locations while 3LP and EIS were recorded at one location. In addition to these tests, the authors conducted visual observations in order to identify rust stains and cracking on concrete surfaces.

### Large Scale Specimens

The authors evaluated the LSS for chloride diffusion, AC impedance, corrosion rates and potentials.

Chloride diffusion was monitored by collecting concrete powder samples at three depths: 13 mm, 25 mm, and 38 mm after 33 weeks, one year, and 1.5 years of ponding. To prevent damage to the LSS, the samples collected at 33 weeks and 1 year were obtained from small concrete blocks, 300 mm by 300 mm by 130 mm, placed in the tidal and immersion zones. These blocks were cast from the same batch of concrete as the LSS, cured under the same conditions, and placed into the HDPE tanks at the same time as LSS. After 1.5 years of ponding, chloride samples were collected from all four exposure zones of the LSS. In addition to the chloride samples from the three above-mentioned depths, a chloride sample from the depth of 51 mm was collected in the horizontal zone.

AC impedance measurements in the horizontal zone were taken on a monthly basis and were recorded at 12 locations (4 bars, 3 locations each). For the vertical, tidal, and immersion zones, AC impedance was recorded at 9 locations (3 bars, 3 locations each) for each zone and for each leg of the specimen. The researchers made AC impedance measurements from 66 locations in all (horizontal zone - 12, vertical zone left leg - 9, tidal zone left leg - 9, immersion zone left leg - 9, vertical zone right leg - 9, tidal zone right leg - 9, immersion zone right leg – 9).

In addition to chloride concentrations and AC impedance, corrosion rates and potentials were measured on the control specimens. Potentials were measured with the same frequency and in the same locations as the AC impedance readings. Corrosion rates were measured at three locations for each exposure zone and each leg, for a total of 21 different locations per specimen. Figure 3 presents the measurement location plan for AC impedance, potential, and corrosion rates, in the horizontal zone and vertical, tidal, and immersion zones on the specimen's right leg. Measurement locations on the specimen's left leg were the same as on the right leg.

## Potentials

Corrosion potentials non-destructively identify the probability of active corrosion. The method uses a copper-copper sulfate half-cell electrode (CSE) that is connected to a voltmeter and then to the reinforcing steel. According to the ASTM C 876-80 standard test method, the more negative the voltmeter reading, the greater the chance of corrosion.[6] Table 5 presents the relationship of the potential readings versus probability of corrosion for bare reinforcing steel.

Corrosion potential surveys were conducted only on the control specimens, BS-1 and BS-2, because it has been demonstrated that this test is not reliable on coated bars.[7] Measurement locations on the control specimens are shown in Figure 3.

## AC Impedance

The Nilsson Soil Resistance Meter 400 (97.4 Hz square wave, 12 V) was used for AC impedance monitoring of SSS and LSS. As long as the epoxy coating is intact, impedance values are expected to be very high. Once coating properties change, either due to reinforcement corrosion or other means, AC impedance decreases. The technique requires an AC resistance meter, metal wires, and a sponge probe. One wire is connected to the rebar being investigated, the other one is connected to the sponge probe, which is placed in the desired location above the rebar. The sponge probe used in this study was 50 mm by 70 mm. The sponge was saturated with the soapy water wetting solution used in the corrosion potential method before every measurement. AC impedance measurements on SSS were taken above the rebar at .25, .5, and .75 of specimen length. The locations for AC impedance measurements for LSS are shown in Figure 3.

## Corrosion Current Density

The linear polarization technique is a non-destructive method for assessing the instantaneous corrosion current density. Corrosion current density is directly proportional to the instantaneous rate of metal loss. The corrosion current density is often referred to as the corrosion rate. Several devices based on the linear polarization method have been developed to determine the corrosion current density of steel in concrete. One of the most common is the 3LP device. Corrosion current density measurements are very susceptible to variable field conditions such as concrete temperature, moisture, and oxygen content. The manufacturer's interpretation of measured corrosion current density (rate) is given in Table 6. 3LP readings on SSS were taken above the center of each rebar. The locations of 3LP measurements for LSS are shown in Figure 3.

7

Measuring chloride content is a common technique used to determine the potential for corrosion activity. It is generally known that once the concentration of chloride ions reaches the corrosion threshold level, the greater the chloride ion concentration, the greater the probability of active corrosion. Table 7 provides guidelines for interpretation of chloride content measurements.[8]

No chloride sampling was required for SSS because the amount of chlorides added to the mixture was known. For LSS, samples for chloride concentration were collected as pulverized concrete at three or four average depths. The collection apparatus used an impact drill with 29 mm diameter bit 2.3 times the maximum aggregate size, connected to a vacuum collection unit.[9] The concrete powder was collected in a coffee filter, which was then stored in a plastic container until chemical analysis (chloride ion concentration determination) was performed. A sample set was taken for each concrete type, each solution concentration, and for two exposure conditions (tidal and immersion zone), after 33 weeks and 1 year of ponding from the blocks, and for all exposure conditions after 1.5 years of ponding from the LSS. Each sample set consisted of chloride samples from the following depths: 13 mm - from 6 to 19 mm, 25 mm - from 19 to 32 mm, 38 mm - from 32 to 44 mm, 51 mm - from 44 to 57 mm (only horizontal zone, 1.5 years of ponding). Because of high variability of chloride content close to the surface, powdered concrete samples from the top 6 mm were discarded. Background chloride content measurements were performed by sampling concrete made with compressive strength cylinders.

Measurements of chloride content were carried out according to the ASTM C 114-88.[10] A titration method was used to determine the quantity of acid soluble chlorides in the concrete digestion solution.

*Electrochemical Impedance Spectroscopy*

The electrochemical impedance spectroscopy (EIS) technique is a tool used in the corrosion evaluation of coated steel. This method requires a gain phase analyzer, a potentiostat, and a computer interface.[11] The resulting impedance over a wide frequency range provides valuable information on individual components of the system, as well as a sum of impedances for all system components. By scanning the specimen at various frequencies, The EIS is capable of separating single impedances from each system component. Once coating impedance is determined, information on coating saturation, conductive pore development, or time at which interfacial corrosion starts can be obtained.

For a bare bar, the difference in impedance recorded at the lowest and highest frequencies is the polarization resistance of the bar. For a coated bar, however, an additional component, Warburg impedance, must be added to the circuit.[12] This does not allow for data interpretation as a polarization resistance. The data can be compared by looking at the impedance values at the

frequency of about 0.01 Hz, as suggested by the NCHRP.[11] Coating corrosion resistance is excellent when impedance value is high (see Table 8).

In comparison, AC impedance measurement provides the same result as EIS for the same frequency. The EIS technique was used on all SSS bars.

## Materials

### *Bare Steel*

Two control specimens were constructed with bare steel reinforcement : BS-1 and BS-2. Bare steel was also used as a bottom mat reinforcement in two ECR specimens: FSC-3 and FSC-4. All bare steel was in the form of No. 5 (D = 16 mm) bars, Grade 60, and came from one heat. Physical and chemical properties of bare steel used in this study, based on mill certificates, are presented in Table 9.

### *ECR*

Five types of epoxy-coated No. 5 bars (D = 16 mm) were studied (see Table 1). Three ECR types were from U.S. manufacturers: Free State Coaters (FSC), Lane Enterprises (LNE), and Florida Steel (FS). Two came from Canada: Canadian green (CGN) and Canadian gray (CGY). Of fourteen ECR specimens, six were cast with FSC. Eight others were cast with LNE, FS, CGN, and CGY (two each).

All epoxy-coated bars of U.S. origin were collected at construction sites in Virginia. This approach was necessary so that the damage to the coating due to transportation and handling was the same as for the bars used in actual structures. Total outdoor exposure, at the construction site and at the lab, was one month. After the outdoor exposure period the bars were visually inspected to identify mechanical damage to the coating, discoloration, corrosion, and coating integrity. The results of these inspections are presented in Figure 4. The bars were stored in the laboratory under black plastic (for UV light protection), until specimen preparation.

Two types of Canadian bars were received directly from the manufacturer. Each bar was individually protected against any mechanical damage during transportation and handling. The Canadian bars were not subjected to any outdoor exposure.

Concrete, designated as VDOT A4, was specified for all specimens. Water to cement (w/c) ratio of 0.45, together with the amounts of cement and coarse aggregate equal to 377 and 867 kg/m$^3$ of concrete, respectively, were kept constant for all mixes. Concrete mixture proportions are presented in Table 10. Some specimens had a higher w/c because of batching errors made by the concrete supplier.

Type I/II cement was used for concrete mixes. Its density was 3.15 g/cm$^3$ and was certified to meet ASTM C-150-92, AASHO M-85-88, and Federal SS-C-1960 specifications. Chemical and physical test data are provided in Table 11.

The concrete mix employed a coarse aggregate of No. 78 stone with a unit weight of 96.7. Its density was 2.75 g/cm$^3$ and absorption was measured at 0.66 percent. Natural sand, with a fineness modulus (FM) of 2.7, 2.66 g/cm$^3$ density, and 0.84 percent absorption, was used as fine aggregate. Daravair-M air entraining admixture was used for all mixes in the amount of 65 ml/100 kg of cement. Water reducing admixture, WRDA-19, a high range water reducer, was necessary to keep the w/c ratio constant and to provide adequate workability during placing of the concrete.

Slump, air content, concrete temperature, and concrete density (unit weight) were recorded before concrete placement. Results of these tests are presented in Table 12. While placing concrete, several 100 by 200 mm cylinders were made for compressive strength and rapid chloride permeability tests. Compressive strength was measured after 3, 7, 28, 56 days and 1 year of moist curing. Cylinders were analyzed at the Virginia Transportation Research Council (VTRC) for electrical indication of the concrete's ability to resist chloride ion penetration. The tests were performed according to ASTM C 1202 at 28 days and 1 year of moist curing.[13] Compression and chloride penetration test results are presented in Tables 13 and 14, respectively.

# RESULTS

## Small Scale Specimens

### *Corrosion Rates*

Figure 5 shows the relationship of corrosion rates ($i_{corr}$) versus time for the control specimen I-BS. The first corrosion current density reading was 6.2 $\mu A/cm^2$ and during the first week of exposure it was about 4 $\mu A/cm^2$. After 20 weeks, $i_{corr}$ decreased to below 3 $\mu A/cm^2$ and remained in that range till the first crack developed at about 9-10 months of exposure. After cracking, the corrosion rate increased to 7.7 $\mu A/cm^2$ and fluctuated over time between 3.5 and 8.3 $\mu A/cm^2$, with the exception of two readings, 1.1 $\mu A/cm^2$ at 76th week of exposure and 2.0 $\mu A/cm^2$ at 125th week of exposure. None of the corrosion rate readings for the I-ECR specimen, zero percent area damage, were stable during the evaluation time. Thus, data for this specimen are not presented.

For the bars with the damage on the bottom of the bars, corrosion rates were almost identical at all times and were in the range of 0.004 to 0.07 $\mu A/cm^2$, regardless of the amount of the coating damage. Corrosion rates for the bars with 0.01, 0.2, and 0.5 percent area damage are presented in Figure 6, while Figure 7 presents the bars with 1 and 2 percent area damage.

ECR bars with the coating damaged on the top surfaces showed more variation. Corrosion rates for the bars with the 0.01, 0.2, and 0.5 percent area damage are shown in Figure 8. Corrosion rates for the 0.01 and 0.2 percent area damage were almost constant during the entire time of testing and ranged from 0.003 to 0.02 $\mu A/cm^2$. For the specimen IV-T, 0.5 percent area damage, corrosion rate values were about 0.01 $\mu A/cm^2$ for the first 66 weeks of exposure, and increased an order of magnitude, to 0.14 $\mu A/cm^2$, between 66th and 125th week of exposure. Corrosion current density for specimen V-T, 1 percent area damage, decreased from 0.17 $\mu A/cm^2$ to 0.08 $\mu A/cm^2$ within the first six weeks of exposure. After six weeks, corrosion rates started to increase and after 115 weeks of exposure the corrosion rate was 1.31 $\mu A/cm^2$. The corrosion rates for specimen VI-T, 2 percent area damage, were similar to the results of specimen V-T. Within the first five weeks $i_{corr}$ values decreased from 0.18 $\mu A/cm^2$ to 0.01 $\mu A/cm^2$. After five weeks, the values started to increase, reaching a value of 0.58 $\mu A/cm^2$ after 115 weeks of exposure. Corrosion rate values for specimens V-T and VI-T, together with I-BS for comparison, are presented in Figure 9. A relationship of corrosion rates divided by the percent area damage versus time, for specimens with the damaged areas on top and bottom of the bars, are presented in Figures 10 and 11, respectively. If a 3LP reading on any specimen was not stable, the symbol for the measurement at that time was omitted from the graph.

*AC Impedance*

Values of measured AC impedance at 97.5 Hz include a sum of impedances of concrete and epoxy coating. Since the condition of the coating is of primary interest, all graphs and values refer to the impedance difference, or coating impedance, which is equal to the impedance of the specimen with the ECR, minus the impedance of the control specimen with bare steel. The first set of measurements was performed in the 40th week of the exposure and the last reading was taken in the 117th week of exposure. Coating impedance values for the specimen I-ECR, zero percent area damage, varied from 657,667 ohms to 550,000 ohms. Coating impedance for specimens with various amount of area damaged were significantly lower. The range of coating impedance for the specimen II-T, 0.01 percent area damage, was from 13,500 ohms to 34,083 ohms, while for specimen VI-T, 2 percent area damage, was from 550 ohms to 3633 ohms. The values for specimens III-T, IV-T, and V-T, with 0.2, 0.5, and 1 percent area damage respectively, are between the values for specimens II-T, 0.01 percent area damage, and VI-T, 2 percent area damage. Coating impedances versus percent area damage, for specimens II-T, III-T, IV-T, V-T and VI-T, are presented in Figures 12 and 13, as linear and log relationship, respectively. Figures 14 and 15 present the relationship of coating impedance versus exposure time for specimens with the coating damaged on the top of the bars and bottom of the bars, respectively.

*EIS*

Electrochemical impedance spectroscopy was performed once at the 101st week of exposure. The readings were taken over a frequency range of 5000 Hz - 0.001 Hz. As expected, the specimen I-ECR, zero percent area damage, has the highest impedance at 0.01 Hz frequency, while the specimen I-BS, bare steel, has the lowest. Impedance values for the specimens II, III, IV, V, and VI were always between the limits established by the specimens I-ECR and I-BS. The results for specimens with the coating damage on the top of the bars and the bottom of the bars are presented in Figures 16 and 17, respectively. One might expect that the higher the impedance, the better the coating or the lesser the area damaged. Such behavior was observed with the ECR specimens that had coating damage on top of the bars, with the exception of the specimen II-T, 0.01 percent area damage, which had a lower impedance than the specimen III-T, 0.2 percent area damage (see Figure 16). The interpretation is more complicated for samples with damage on the bottom of the bars (Figure 17). Note that the EIS values, at the 101st week of exposure, at near 100 Hz frequency are very close to the AC impedance values recorded with the AC impedance meter at 99th week of exposure (Figures 16 and 14).

12

# Large Scale Specimens

## *AC Impedance*

LSS were monitored with the AC impedance measurements in the horizontal zone throughout the experiment period. The last two readings were taken after the ponding was discontinued and the specimens were moved outdoors. As shown in Figures 18 to 33, the outdoor impedance measurements are higher than the measurements taken inside the laboratory. The results for the FSC-1 through FSC-5 specimens are presented in Figures 18 to 22; LNE-1 and LNE-2 specimens in Figures 23 and 24; FS-1 and FS-2 specimens in Figures 25 and 26; CGN-1 specimen in Figure 27; CGY-1 specimen in Figure 28; specimens with w/c ratio > 0.7, FSC-51, CGN-11, and CGY-11, in Figures 29 to 31; and two control specimens, BS-1 and BS-2, in Figures 32 and 33.

After ponding was discontinued, additional AC impedance measurements were taken in the immersion and tidal zones on both legs of each specimen. The data are presented in Figures 34, 35, 40, and 41. Once the specimens were moved outdoors, AC impedance readings were taken from all exposure zones; the data are presented in Figures 36 to 39 and 42 to 51. The impedance measurements for May 1996 were recorded prior to moving specimens out of the laboratory. Measurements for August and September of 1996 were recorded outdoors.

None of the specimen parameters--NaCl solution concentration, type of bottom mat reinforcement, or continuity/discontinuity of the reinforcing steel between exposure zones-- influenced the impedance results. Also, ECR type did not appear to influence the AC impedance results. Only two specimens with Canadian bars, CGN-1 in the immersion zone and CGY-1 in the immersion and tidal zones, performed significantly better than the bare steel specimens. However, poor ECR performance (lower impedance) was observed in the vertical zone.

## *Chlorides*

Chloride concentrations were determined for A4 concrete and 6 percent NaCl ponding solution, A4 concrete and 3 percent NaCl ponding solution, and concretes with w/c > 0.7. Concrete powder samples were collected from three depths for all exposure zones, except for the horizontal zone at 1.5 years, for which samples were collected from four depths. Chloride concentrations, for horizontal, vertical, tidal, and immersion zones, versus depth, for A4 concrete and 6 percent NaCl, A4 concrete and 3 percent NaCl, and concrete with w/c > 0.7, are presented in Figures 52-55, 56-59, and 60-63, respectively.

As shown in Figures 52-55, a chloride concentration threshold of 0.71 $kg/m^3$ of concrete, for specimens with A4 concrete and 6 percent NaCl ponding solution, was reached at the 25mm bar depth between 33 weeks and 1 year of ponding, for all exposure zones.[14] The highest concentration of chlorides was observed in the horizontal zone, and the lowest in the tidal zone.

13

For A4 concrete and 3 percent NaCl ponding solution, chloride threshold at the bar depth was reached after 1 year of ponding for the horizontal and vertical zones, Figures 56 and 57, before 1 year of ponding for the immersion zone, Figure 59, and at about 1.5 years of ponding for the tidal zone, Figure 58. The horizontal zone had the highest chloride concentration level, while tidal zone had the lowest.

Chloride threshold level was exceeded before the first sampling, at 33 weeks of exposure, for all exposure zones, in specimens with concrete with w/c > 0.7 and 6 percent NaCl ponding solution. The highest values of chlorides were recorded in vertical and horizontal zones, and the lowest values in immersion and tidal zones (Figures 60-63).

*Corrosion Potentials*

Corrosion potentials were monitored on the control specimens, BS-1 and BS-2, from 18th and 19th week of ponding until the 105th and 106th week of ponding, respectively. As seen in Figures 64 and 65, corrosion potentials in the horizontal zone for the two control specimens were in the range of -170 mV to -278 mV with the exceptions of bar 4 of the BS-1 specimen, and two sets of readings that were taken after the specimens were moved outdoors. Potentials recorded on bar 4, BS-1 specimen, started at -261 mV at 18th week of exposure and stayed in the -242 mV to -269 mV range till the 37th week of exposure. After 37 weeks of ponding, potentials decreased to -305 mV and stayed close to -300 mV. They reached -326 mV after 80 weeks of ponding. Once the specimens were moved outdoors, potentials for the BS-1 specimen increased to a range of -103 mV to -142 mV, after 105 weeks of exposure. For the second control specimen, BS-2, potential values also increased but to a lesser extent. After 98 weeks of exposure, potential values were in the range of -165 mV to -172 mV for bars 1, 2, and 3, and -203 mV for bar 4. After 106 weeks of exposure, potentials for the BS-2 specimen were about -220 mV for all four bars.

As seen in Figures 66 and 67, potential measurements on both legs in the vertical zone of the BS-1 specimen, with an exception of bar 1 in the left leg, ranged from -186 mV to -262 mV for the entire period of the indoor experiment. After the specimen was moved outdoors, potential values ranged from -220 mV to -248 mV after 97 weeks of exposure. Then, after 105 weeks of exposure, the values decreased to a range of -310 mV to -320 mV. Bar 1 in the left leg had significantly lower potentials than two other bars (see Figure 66). After 18 weeks of ponding, the potential value was -305 mV. After 84 weeks of ponding, it decreased to -386 mV. Once the specimen was moved outdoors, after 105 weeks of total exposure, corrosion potential was -424 mV. Potentials in the vertical zone of the BS-2 specimen, as seen in Figures 68 and 69, were in the range from -200 mV to -334 mV. Bar 1 in the left leg had more negative potential values than two other bars, and after moving the specimen outdoors, its potential, after 106 weeks of exposure, decreased to -371 mV. Potential values of two other bars in the left leg were -317 mV and -294 mV. Potential readings taken after 106 weeks of exposure on three bars in the right leg

of the BS-2 specimen were -387 mV, -443 mV, and -445 mV. These potential values were the most negative of all readings, either indoors or outdoors, collected on control specimens.

Potential readings in the immersion and tidal zones were collected three times. The first set of readings was taken after the ponding was discontinued; the other two were taken after the specimens were moved outdoors. Figure 70 presents potential data for the immersion zone. Potentials collected on the left leg of the BS-1 specimen were -154, -223, and -200 mV, and on the right leg were -332, -223, and -231 mV, after 86, 98, and 105 weeks of exposure, respectively. Potentials collected on the left leg of the BS-2 specimen were -283, -292, and -349 mV, and on the right leg were -207, -236, and -308 mV, after 86, 98, and 105 weeks of exposure, respectively. Potential data from the tidal zone is presented in Figure 71. Potentials collected on the left leg of the BS-1 specimen were -284, -180, and -171 mV, and on the right leg were -365, -196, and -216 mV, after 86, 98, and 105 weeks of exposure, respectively. Potentials collected on the left leg of the BS-2 specimen were -372, -225, and -286 mV, and on the right leg were -364, -275, and -342 mV, after 86, 98, and 105 weeks of exposure, respectively.

*Corrosion Rates*

Corrosion rates in the horizontal and vertical zones were collected for BS-1 at 74, 80, 83, 97 and 105 weeks of exposure. The same readings were taken for BS-2 at 75, 81, 84, 98, and 106 weeks of exposure. Corrosion rates in the immersion and tidal zones, for BS-1 and BS-2 specimens, were collected after 83, 97, and 105 weeks of exposure, and 84, 98, and 106 weeks of exposure, respectively. Readings collected after 74, 75, 80, and 81 weeks of exposure were made while the specimens were still indoors and ponding was in progress. Readings after 83 and 84 weeks of exposure were made indoors immediately after ponding was discontinued. Readings at 97th week of exposure and later were taken after the specimens were moved outdoors. The relationship of corrosion rates ($i_{corr}$) versus time for the control specimens with bare steel bars is presented in Figures 72 and 73 for the horizontal zone, Figures 74-77 for the vertical zone, Figures 78-81 for the immersion zone, and Figures 82-85 for the tidal zone.

Corrosion rates in the horizontal zone, Figures 72 and 73, were similar for both control specimens and decreased in time. After 105 weeks of exposure, corrosion rates were slightly above 1 $\mu A/cm^2$ for the BS-1 specimen and slightly below 1 $\mu A/cm^2$ for the BS-2 specimen. In the vertical zone, Figures 74-77, corrosion rates measured on the BS-1 specimen were lower than the ones measured on the BS-2 specimen. As seen in Figures 75 and 76, two bars had significantly higher corrosion rates than the other bars. The corrosion rate for bar 1 in the left leg of the BS-1 specimen was almost 8 $\mu A/cm^2$ after 83 weeks of exposure (immediately after the ponding was discontinued). In bar 1 in the right leg of the BS-2 specimen, it was about 6 $\mu A/cm^2$ after 76 weeks of ponding, decreasing to about 4.5 $\mu A/cm^2$ after 84 weeks of ponding. Once the specimens were moved outdoors, corrosion rates for these two bars decreased to the same level as other bars (in the same specimen, leg, and exposure zone).

15

Corrosion rates in the immersion zone for the two control specimens decreased once the specimens were moved outdoors, as shown in Figures 78-79 and 80-81. Average values of corrosion rates on the right and left legs of the BS-1 specimen were 2.09 and 2.28 $\mu A/cm^2$ after 83 weeks of ponding, 1.36 and 1.46 $\mu A/cm^2$ after 97 weeks of exposure, and 1.08 and 1.06 $\mu A/cm^2$ after 105 weeks of exposure. Average values of corrosion rates on the right and left legs of the BS-2 specimen were 2.32 and 2.53 $\mu A/cm^2$, after 84 weeks of ponding, 1.84 and 2.19 $\mu A/cm^2$, after 98 weeks of exposure, and 0.96 and 1.38 $\mu A/cm^2$, after 106 weeks of exposure, respectively.

Corrosion rates in the tidal zone for the two control specimens were similar to corrosion rates in the immersion zone and also decreased after moving the specimens outdoors, as shown in Figures 82, 83 and 84, 85 for specimens BS-1 and BS-2, respectively. Average values of corrosion rates on the right and left legs of the BS-1 specimen were 2.43 and 2.09 $\mu A/cm^2$, after 83 weeks of ponding, 1.59 and 1.73 $\mu A/cm^2$, after 97 weeks of exposure, and 1.22 and 1.08 $\mu A/cm^2$, after 105 weeks of exposure, respectively. Average values of corrosion rates on the right and left legs of the BS-2 specimen were 2.93 and 3.36 $\mu A/cm^2$, after 84 weeks of ponding, 2.58 and 2.54 $\mu A/cm^2$, after 98 weeks of exposure, and 1.07 and 1.58 $\mu A/cm^2$, after 106 weeks of exposure, respectively.

*Rapid Concrete Chloride Permeability*

Rapid permeability was measured on cylinders of all concrete batches used for specimen fabrication according to ASTM C-1202.[13] Measurements were taken after 28 days (Figure 86) and 1 year (Figure 87) of wet curing.

*Visual Observations*

A crack survey was performed after approximately four months of outdoor exposure. Visually observed cracks and rust stains in the control specimens, BS-1 and BS-2, as well as in the specimens with epoxy-coated steel, FSC-2, FSC-3, FSC-5, LNE-2, FS-1, FS-2, CGY-1, FSC-51, CGN-11, and CGY-11, are presented in Figures 88-99. Since neither cracks nor rust stains were observed in the FSC-1, FSC-4, LNE-1, and CGN-1 specimens, these are not presented.

Figures 88 and 89 present visually observed cracks and rust stains in the BS-1 and BS-2 specimens after approximately four months of outdoor exposure. Most cracking occurred in the horizontal and vertical zones and over the bars that were not included in the corrosion condition assessment. For the BS-1 specimen, one crack in the horizontal zone was found (Figure 88). A crack with a rust spot was first observed after 54 weeks of exposure over bar 4a, between points 4 and 8. Five smaller cracks were found in the vertical zone, four of which were on the left leg and one on the right leg Figure 88). For the four cracks on the left leg, one was associated with

16

the deck bars that are in the leg face and three were from the left leg bars. The crack from the deck bar was at the location of the top mat in the leg face. The three cracks from the left leg bars were in the vertical zone. Two cracks were observed over bar 1a and one crack appeared over bar 1. In addition to the two cracks over bar 1a, relatively large rust stains were also observed. The crack in the right leg was observed in the upper right corner. It was the only crack progressing vertically and was the shortest of all cracks found in the BS-1 specimen. As shown in Figure 89, several cracks were found in the horizontal zone, as well as in the legs of the BS-2 specimen. The two cracks in the horizontal zone were found over side bars 1a and 4a. Bar 1a also caused cracking in the right leg, and bar 4a in the left leg. These cracks appeared in the upper parts of the specimen's legs. Some cracks were also found over bar 1 in the tidal zone. In addition, two structural cracks were found in specimen's left and right legs. The structural crack in the left leg occurred in the vicinity of bar 1a, while the other crack occurred in the face of the right leg and was close to the bottom mat of the deck reinforcement. It should be noted that structural cracks also formed while the specimen was being removed from the steel forms. These cracks progressed through the whole length and thickness of each leg.

Out of all ECR specimens, FSC-1, FSC-4, LNE-1, and CGN-1 had no visible cracks. The FSC-2 specimen had a structural crack in the left leg and two cracks in the horizontal zone (see Figure 90). The structural crack occurred just above bar 1a in the vertical zone. The two cracks in the horizontal zone were both found over bar 1. The FSC-3 specimen had only a structural crack that occurred in the right leg face, below the bottom mat of deck's reinforcement (Figure 91). Two cracks were observed in the FSC-5 specimen (see Figure 92). A structural crack occurred in the left leg, below the bottom mat of deck's reinforcement, while the other crack occurred in the horizontal zone over bar 1. The LNE-2, FS-1, FS-2, and CGY-1 specimens had one structural crack each (Figures 93-96), respectively. The location of these cracks in the four specimens was the same - the left leg, below the bottom mat of deck's reinforcement. One crack in the right leg and nine cracks in the deck were found in the FSC-51 specimen, see Figure 97. The crack in the right leg was structurally related and was found below the bottom mat of deck's reinforcement. All other cracks were found in the horizontal zone over bars 1a, 1, 2, 2a, 3a, and 4. Two structural cracks were observed in the legs of the CGN-11 specimen (see Figure 98). The crack in the left leg occurred above bar 1a in the vertical zone. The crack in the right leg occurred below the bottom mat of deck's reinforcement. Three cracks were found in the CGY-11 specimen (Figure 99). Two cracks found in the legs were structurally related and both of them were located below the bottom mat of deck's reinforcement. The third crack was found in the horizontal zone above bar 4a.

Before exposure to sodium chloride solution, all structural cracks were filled with silicone and covered with duct tape to minimize the influence of these cracks to corrosion development. The observed structural cracks appeared to have no influence on the corrosion development on the bars in the vicinity of these cracks. It was concluded that the silicone and duct tape protection was adequate.

17

# DISCUSSION

## Small Scale Specimens

### *Corrosion Rates*

Based on the results presented in Figures 5, 6 and 7, it is apparent that the corrosion rates for coated bars, regardless of the amount of coating damage, are significantly lower than those for bare steel. The values are so low that if measured on bare steel reinforcement, they would certainly be neglected and classified as "no corrosion." Since the area of coating damage is known, true corrosion current density can be calculated by dividing the values of the corrosion rates by the percent area damage (presented in Figures 10 and 11, for the specimens with the damage on the top of the bars and on the bottom of the bars, respectively). The values for the bars with the top areas damaged are more similar than for the bars with the bottom of the bars damaged. Only the values for the specimen II-B and II-T, 0.01 percent area damage, and V-T, 1.0 percent area damage, are about one magnitude higher than others.

Based on the 3LP results, Figure 10, it is apparent that, in the case where the top of the bar is damaged, measured corrosion rates of the ECR are very similar to bare steel. This result indicates that steel corrodes at the same rate regardless of the area of coating damage, or if the bar is epoxy-coated or not. The difference is in the area that is affected by the corrosion process. The data are more variable for the bars with the damage on the bottom of the bars. A possible explanation is that either the polarization of the bottom half of the reinforcing bar is not as effective as of the top half of the bar, or the oxygen content at the top half of the bar is higher than at the bottom half.

### *AC Impedance*

As previously mentioned, the coating impedance is the difference between the impedance of the specimen with the ECR and the impedance of the control specimen with bare steel. As seen in Figures 12 and 13, a majority of readings were very close to each other, with the exception of two sets of measurements taken at 67th and 77th week of exposure. Based on Figure 13, a logarithmic relationship between the coating impedance and the percent area damage was observed. It was very difficult, if not impossible, to distinguish between specimens with 2, 1, 0.5, and even 0.2 percent area damage, despite the fact that the lower the area damage, the higher the impedance (Figures 14 and 15). The bar must be in almost perfect condition, 0.01 percent area damage or less, in order for impedance measurements to differentiate between bar damage conditions of less than and greater than 0.01 percent area damage. Thus, this test can tell the researcher only whether a particular bar has a perfect coating.

18

Based on the limited EIS results, it was possible to distinguish the bars with varying percent area damage, but only for samples with damage on the top of the bars. However, if one had only the EIS graph with no data on the bar condition, it would be difficult, if not impossible to identify the damage area. The bar, or rather the coating, must be in almost perfect condition to be distinguished as a perfect bar when employing the EIS technique.

## Large Scale Specimens

### *Impedance*

The AC impedance measurement results for the horizontal zone, as shown in Figures 18 to 33, indicated that after the initial ponding and impedance decrease, there was almost no difference between specimens with ECR and BS, regardless of the ECR manufacturer and specimen configuration. The impedance values recorded on FSC specimens are very similar to each other regardless of concentration of the ponding solution or type of bottom mat reinforcement (Figures 18-22). As shown in Figures 23-26, AC impedance data for LNE and FS specimens demonstrate the same results as FSC specimens. When compared to controls, 360 - 1360 ohms range, only specimens with Canadian bars had higher impedance values, 1600 to 3400 ohms for CGN-1 and 5000 to 7800 ohms for CGY-1. The researchers derived this result by comparing Figures 27, 28, 32, and 33.

It appears that the decrease in impedance occurring in the initial stage of ponding is attributable to concrete and coating saturation. It is best illustrated on specimens with Canadian bars, Figures 27 to 30. After the specimens were moved outdoors, an increase in impedance was observed for all specimens. The impedance values for control specimens BS-1 and BS-2 while indoors were in the range of 360 - 1360 ohms, and increased to almost 3300 ohms after ponding was discontinued. This increase was observed on all specimens, with the highest gain for the specimen CGN-1, from the 1600 to 3400 ohms range to 21100 ohms. It is believed that these higher impedance results, recorded outdoors and compared to indoor data, can be attributed to drier conditions of outdoor exposure.

### *Corrosion Potentials*

Corrosion potentials observed in the horizontal zone of BS-1 and BS-2 specimens suggest the possibility of an active corrosion process development during indoor exposure. Potentials measured for the left and right legs in the vertical zone of the BS-1 specimen stayed in an uncertain region of the corrosion process, with the exception of bar 1 in the left leg (see Figures 66 and 67). For bar 1, observed potentials were always more negative than -300 mV, with a higher probability of active corrosion after 37 weeks of exposure. After moving

specimens outdoors, measured potentials on the bar 1 in the left leg of the BS-1 specimen increased at first, but then decreased significantly (Figure 66). Potentials for all other bars in both legs also decreased significantly (Figures 66 and 67). Potentials measured on the left leg in the vertical zone of the BS-2 specimen were in an uncertain region of corrosion throughout the indoor exposure period. Only bar 1 had more negative potentials than other samples, but not negative enough to suggest an active corrosion occurring on this bar (Figure 68). Potentials measured on the right leg were more negative than for the left leg, indicating an active corrosion stage (see Figure 69). Corrosion potential values measured after the specimens were moved outdoors show a significant decrease, especially for the right leg, where the potentials were the most negative of all readings collected on the BS-1 and BS-2 specimens.

As for the immersion and tidal zones, potential data presented in Figure 70 demonstrate no significant difference between specimens BS-1 and BS-2 during the first two sets of readings. The last reading, however, indicates macro-cell action on the BS-2 specimen since potential values on both legs are more negative than the potential on the BS-1 specimen. Similar behavior can be observed in the tidal zone (Figure 71). In this case, both readings taken outdoors show more negative potentials on the BS-2 specimen than on the BS-1 specimen, indicating influence of macro-cell corrosion.

*Corrosion Rates*

The corrosion rates results indicate that control specimens were in an active region of corrosion when they were kept indoors, since the corrosion rates measured outdoors were lower than indoors (Figures 72-85). The data from the horizontal zone agree with potential data, indicating lesser corrosion activity when the specimens were kept outdoors than occurred when the specimens were indoors. In the vertical zone, the highest corrosion rates were observed in the same place where the most negative potentials were observed, the right leg of BS-2 specimen (Figures 74-77). Macro-cell action is a probable explanation of differences in corrosion rates in the immersion and tidal zones between specimens BS-1, legs reinforcement not connected, and BS-2, legs reinforcement connected.

*Visual Observations*

Cracking, other than structural cracking, appeared to be related to reinforcing steel corrosion in the BS-1 and BS-2 samples. Bars 1a and 4a in the horizontal zone were expected to corrode first since they were exposed to more severe conditions than any other bar. The chlorides diffused from the top to 25 mm of the cover depth in the horizontal zone, and from the side to 25 mm cover depth in the leg. This behavior was clearly observed in both control specimens, BS-1 and BS-2. It is believed that the cracks and rust stain in the tidal zone of the BS-2 specimen resulted from the corrosion of the steel ties that must have changed their positions during concrete placement and vibration, resulting in a shallower cover depth than 25 mm.

20

The ECR LSS specimens performed significantly better than the bare steel controls in this short laboratory exposure period. Most of the specimens had no cracks that were caused by the corrosion of the reinforcing steel. The only specimens with corrosion-related cracks were FSC-2, FSC-5, FSC-51, and CGY-11 with two, one, nine, and one cracks, respectively; these cracks all appeared in the horizontal zone. It should be noted that the FSC-51 and CGY-11 specimens were cast with concrete with w/c ratios of 0.71 and 0.74 respectively, so that the amount of chloride ions at the bar level was much larger than in other specimens.

## CONCLUSIONS

1. Corrosion rate readings were much higher for bare bars than for coated bars but when the area of corrosion is taken into account, corrosion rates are for the coated and bare bars were the same.

2. Neither 3LP measurements nor AC impedance measurements provide a good indication of corrosion area damage on coated bars.

3. AC impedance measurements can indicate that a bar has a perfect coating.

4. The SSS with bare steel (I-BS) cracked after 9 months of exposure. No cracks were observed on the ECR specimens during the two-year exposure period. However, the coating was well adhered, a test condition that is not representative of most of the ECR in bridges in Virginia after 4 years in service.

5. The LSS constructed for this study have sufficient chlorides present at the bar level for corrosion to occur, coatings and/or concrete are fully saturated, and the corrosion process has already started. However, it is not in an advanced stage since none of the LSS with ECR have cracked to date.

6. None of the non-destructive techniques used in this study were determined to be appropriate for determining the condition of ECR. Direct examination of the bar and coating condition is the best method for evaluating the performance of ECR.

7. The ECR LSS specimens performed significantly better than controls in this short laboratory exposure period. However, the ECR in the LSS was well adhered.

21

# RECOMMENDATIONS

Annual monitoring of the SSS and LSS specimens should be continued until cracking has occurred in all specimens in order to better estimate the service extension provided by ECR. Specimens already exposed to the 3 percent sodium chloride solution should be taken to the Hampton Road North Tunnel Island and placed in the water to a depth of the immersion zone at low tide for further exposure to chloride. The specimens exposed to the 6 percent sodium chloride solution should remain in an outdoor exposure in Southwest Virginia, such as that at the Civil Engineering Materials Research Laboratory in Blacksburg, Virginia.

# ACKNOWLEDGMENTS

# REFERENCES

1.    Weyers, R.E. et al. (November 1995). *Protocol for in-service evaluation of bridges with epoxy-coated reinforcing steel*, NCHRP 10-37B, Final Report, p. 110.

2.    Clear, K.C. (December 1992). *Effectiveness of epoxy-coated reinforcing steel: Final report*. Canadian Strategic Highway Research Program, Ottawa, Ontario, p. 128.

3.    Sagues, A.A., et al. (May 1994). *Corrosion of epoxy-coated rebar in Florida bridges.* College of Engineering, University of South Florida, p. 70.

4.    Weyers, R.E., et al. (October 1997). *Field investigation of the corrosion protection performance of bridge decks and piles constructed with epoxy-coated reinforcing steel in Virginia*, VTRC 98-R4, Virginia Transportation Research Council, Charlottesville, Virginia, p. 34.

5.    Krauss, P.D., D.B. McDonald, and M.R. Sherman (June 1996). *Corrosion investigation of four bridges built between 1973 and 1978 containing epoxy-coated reinforcing steel.* MN/RC - 96/25. Minnesota Department of Transportation, St. Paul, p. 163.

6.    ASTM C 876-80. *Standard test method for half-cell potentials of reinforcing steel in concrete.*

7. Malesheski, G., D. Maurer, D. Mellott, and J. Arellano, *Bridge deck protective systems*, Report FHWA-PA-88-001 + 85-17, Pennsylvania Department of Transportation, Harrisburg, 1989.

8. Newhouse, Charles D., *Corrosion rates and the time to cracking of chloride contaminated reinforced concrete bridge components*, Master's Thesis, Virginia Polytechnic University, Blacksburg, December, 1993.

9. SHRP-S/FR-92-110, *Condition evaluation of concrete bridges relative to reinforcement corrosion.* Volume 8: Procedure Manual, 1992.

10. ASTM C 114-88. *Standard test methods for chemical analysis of hydraulic cement, section 19: chloride (reference test method).*

11. NCHRP Report 370, *Performance of epoxy-coated reinforcing steel in highway bridges.* TRB, National Research Council, 1995.

12. Jones, D.A., *Principles and prevention of corrosion.* 1992, p. 109.

13. ASTM C 1202, *Standard test method for electrical indication of concrete's ability to resist chloride ion penetration.*

14. Weyers, R.E., Cady, P.D., Deterioration of concrete bridge decks from corrosion of reinforcing steel, *Concrete International*, Vol. 9, No. 1, January, 1987, pp. 15-20.

15. Clear, K.C., NCHRP 10-37, *Performance of epoxy-coated reinforcing steel in highway bridges.* Final Report, July 29, 1994.

# TABLES

Table 1. Epoxy-Coated Reinforcing Steel Used in the Study

| Symbol | ECR Manufacturer | Coating | Construction Site Location | Comments |
|---|---|---|---|---|
| FSC | Free State Coaters | (information not available) | Norfolk, VA | green |
| LNE | Lane Enterprises | 3M Scotchcote Brand 413 FBEC | Danville, VA | green |
| FS | Florida Steel | (information not available) | Coeburn, VA | green |
| CGN | Harris Rebar, Canada | Resicoat 500607 (flexible) | n/a (directly from manufacturer) | proprietary chromate pretreatment; green |
| CGY | Harris Rebar, Canada | Resicoat 500711 (semi-flexible) | n/a (directly from manufacturer) | type (?) pretreatment; grey |

Table 2. Small Scale Specimens - Configuration.

| Specimen | Bar Symbol | % Area Damaged | # of Damaged Areas | Notes |
|---|---|---|---|---|
| I | BS | 100 | n/a | I BS = Specimen I, bare steel bar |
| | ECR | 0 | 0 | I ECR = Specimen I, epoxy-coated bar with no area damage |
| II | T | 0.01 | 1 | |
| | B | 0.01 | 1 | T = area damaged on the top of the bar |
| III | T | 0.2 | 1 | |
| | B | 0.2 | 1 | B = area damaged on the bottom of the bar |
| IV | T | 0.5 | 6 | |
| | B | 0.5 | 6 | example: |
| V | T | 1 | 12 | IV T = Specimen IV, epoxy-coated bar with 0.5% area damage on the top of the bar |
| | B | 1 | 12 | |
| VI | T | 2 | 23 | |
| | B | 2 | 23 | |

Table 3. Concrete Mixture Proportions for Small Scale Specimens.

| Ingredient | kg/m³ of concrete |
|---|---|
| Cement, Type I/II | 377 |
| Coarse Aggregate (crushed limestone, 13 mm max size) | 867 |
| Fine Aggregate (natural sand) | 864 |
| Water | 170 |
| Air Entraining Admixture | 198 |
| Sodium Chloride | 7.48 |

Table 4. Large Scale Specimens - Configuration.

| Specimen Legs' Reinforcement | ECR Manufacturer | | | | | Controls Bare Steel | Solution [% NaCl] |
| --- | --- | --- | --- | --- | --- | --- | --- |
| | FSC | | LNE | FS | CGN & CGY | | |
| | with BS bottom mat | with FSC bottom mat | | | | | |
| Type I | FSC-3 | FSC-1 | LNE-1 | FS-1 | | BS-1 | 6 |
| | FSC-4 | FSC-2 | LNE-2 | FS-2 | | | 3 |
| Type II | | FSC-5 | | | | BS-2 | 6 |
| | | FSC-51 | | | | | |
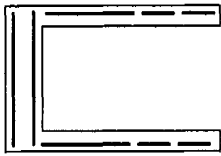
Type
III

CGN-1
CGY-1
CGN-11
CGY-11

3

Table 5. ASTM C-876 Interpretation of Potential Readings.

| Voltmeter Reading | Interpretation |
|---|---|
| greater than -200 mV | 90% probability of no corrosion |
| from -200 mV to -350 mV | uncertain |
| less than -350 mV | 90% probability of active corrosion |

Table 6. Manufacturer's Data Interpretation for 3LP Device.

| $i_{corr}$ | Interpretation |
|---|---|
| < 0.2 μA/cm² | no damage expected |
| 0.2 - 1.0 μA/cm² | damage possible in 10-15 years |
| 1.0 - 10.0 μA/cm² | damage possible in 2-10 years |
| > 10.0 μA/cm² | damage possible in less than 2 years |

Table 7. Recommended Action for Chloride Content Measurements [8].

| Chloride Concentration | Recommendation |
|---|---|
| $< 0.59$ kg/m$^3$ | leave intact |
| $0.59 - 1.19$ kg/m$^3$ | questionable area |
| $> 1.19$ kg/m$^3$ | remove concrete below bar level or replace entire section |

Table 8. Interpretation of the EIS Measurements at about 0.01 Hz [11].

| Overall Impedance [$ohm/cm^2$] | Coating Corrosion Resistance |
|---|---|
| greater than $10^8$ | Excellent |
| from $10^6$ to $10^8$ | Intermediate |
| less than $10^6$ | Poor |

Table 9. Physical and Chemical Properties of Bare Steel.

Physical Properties:

| | |
|---|---|
| Yield Point [MPa] | 425 - 473 |
| Tensile Strength [MPa] | 645 - 703 |
| % Elongation [200 mm] | 10 |

Chemical Properties:

| | |
|---|---|
| C [%] | 0.38 - 0.43 |
| Mn [%] | 0.83 - 1.00 |
| P [%] | 0.01 |
| S [%] | 0.03 - 0.05 |

Table 10. A4 Concrete Mixture.

| Ingredients | kg/m$^3$ |
| --- | --- |
| Cement (Type I/II) | 377 |
| #78 Coarse Aggregate (crushed limestone, 13 mm max. size) | 867 |
| Fine Aggregate (natural sand) | 864 |
| Water | 170 |

| Admixtures | ml/100 kg of cement |
| --- | --- |
| HRWR: WRDA-19 | 522 - 1232 |
| AEA: Daravair-M | 54 - 72 |

Table 11. Test Data on Type I/II Cement (as Provided by the Manufacturer).

| Chemical Test Data | | Physical Test Data | |
|---|---|---|---|
| $SiO_2$ | 22.1 | Fineness - Blaine | 3760 |
| $Al_2O_3$ | 4.29 | Fineness - Wagner | 2212 |
| $Fe_2O_3$ | 2.83 | Autoclave Expansion | 0.05 |
| CaO | 63.4 | Initial Set (H:min.) | 2:25 |
| MgO | 2.86 | Final Set (H:min.) | 3:35 |
| $SO_3$ | 2.23 | Vicat (min.) | 95 |
| Total Alkalies | 0.62 | Air Content (Mortar) | 6.6 |
| Insoluble Residue | --- | Compressive Strength [MPa] | |
| Ignition Loss | 1.1 | 1 day | 15.0 |
| $C_3S$ | 51.3 | 3 day | 27.4 |
| $C_3A$ | 6.58 | 7 day | 35.5 |

Table 12. Fresh Concrete Properties.

| Specimen | w/c ratio | Slump [mm] | Air [%] | Temperature [C] | Density [g/cm$^3$] |
|---|---|---|---|---|---|
| FSC-1, BS-1 | 0.46 | 191 | 6.2 | 25 | 2.34 |
| LNE-2, FS-2 | 0.45 | 140 | 6.2 | 24 | 2.35 |
| FSC-2 | 0.45 | 114 | 5 | 24 | 2.38 |
| BS-2, LNE-1 | 0.44 | 203 | 5.5 | 26 | 2.34 |
| FSC-3, FSC-4 | 0.45 | 140 | 3.8 | 26 | 2.4 |
| FS-1 | 0.45 | 102 | 6.8 | 25 | 2.28 |
| CGN-11, CGY-11 | 0.74 | 203 | 12 | 21 | 2.14 |
| FSC-51 | 0.71 | 152 | 7.4 | 22 | 2.25 |
| FSC-5 | 0.44 | 203 | 8 | 18 | 2.29 |
| CGN-1, CGY-1 | 0.44 | 140 | 6.4 | 22 | 2.31 |

Table 13.  Compressive Strengths.

| Specimen | Average Compressive Strength (MPa) | | | | |
|---|---|---|---|---|---|
| | 3 days | 7 days | 28 days | 56 days | 1 year |
| FSC-1, BS-1 | 39 | 48 | 58 | 62 | 72 |
| LNE-2, FS-2 | 39 | 46 | 55 | 61 | 71 |
| FSC-2 | 39 | 46 | 55 | 61 | 71 |
| BS-2, LNE-1 | 35 | 40 | 48 | 54 | 63 |
| FSC-3, FSC-4 | 40 | 48 | 54 | 57 | 74 |
| FS-1 | 27 | 30 | 40 | 44 | 49 |
| CGN-11, CGY-11 | 8 | 9 | 12 | 13 | 14 |
| FSC-51 | 11 | 15 | 21 | 21 | 22 |
| FSC-5 | 36 | 39 | 44 | 50 | 59 |
| CGN-1, CGY-1 | 22 | 27 | 34 | 38 | 47 |

Table 14. Rapid Concrete Chloride Permeability.

| Specimen | w/c ratio | Charge Passed [Coulomb] | |
|---|---|---|---|
| | | 28 days | 1 year |
| FSC-1, BS-1 | 0.46 | 3049 | 1816 |
| LNE-2, FS-2 | 0.45 | 2600 | 1548 |
| FSC-2 | 0.45 | 2923 | 1751 |
| BS-2, LNE-1 | 0.44 | 3120 | 2048 |
| FSC-3, FSC-4 | 0.45 | 2340 | 1438 |
| FS-1 | 0.45 | 4501 | 2924 |
| CGN-11, CGY-11 | 0.74 | 8341 | 5081 |
| FSC-51 | 0.71 | 8818 | 4999 |
| FSC-5 | 0.44 | 2958 | 1209 |
| CGN-1, CGY-1 | 0.44 | 3515 | 2502 |

# FIGURES

Dimensions: mm

25

305

102

152

305
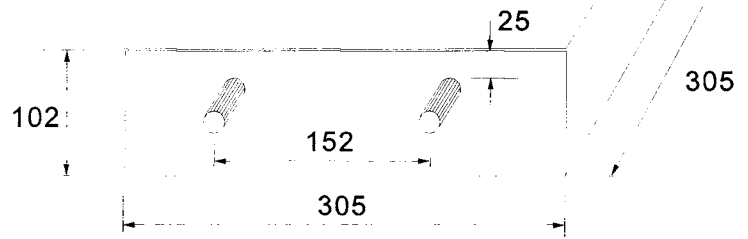
Figure 1.  Small Scale Specimen - Typical Configuration.
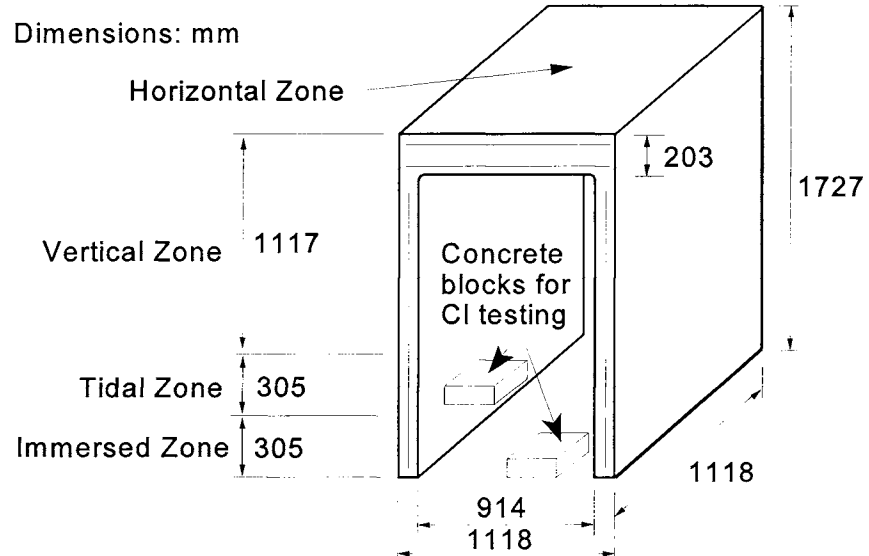
Figure 2. Large Scale Specimen - Typical Configuration.

Figure 3. Measurement Plan.
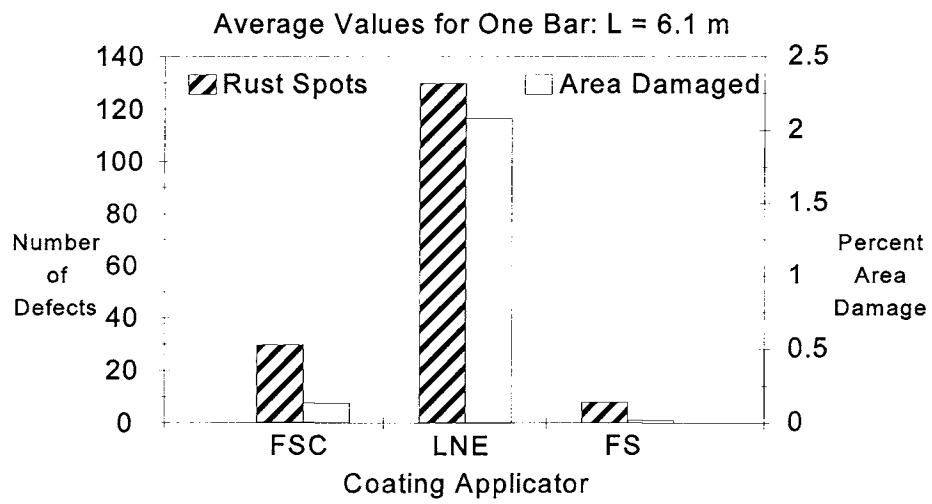
Figure 4. Epoxy-Coated Bars from the US Manufacturers - Visual Observations.

**ECR - small scale specimens**
(Control Specimen - Bare Steel)
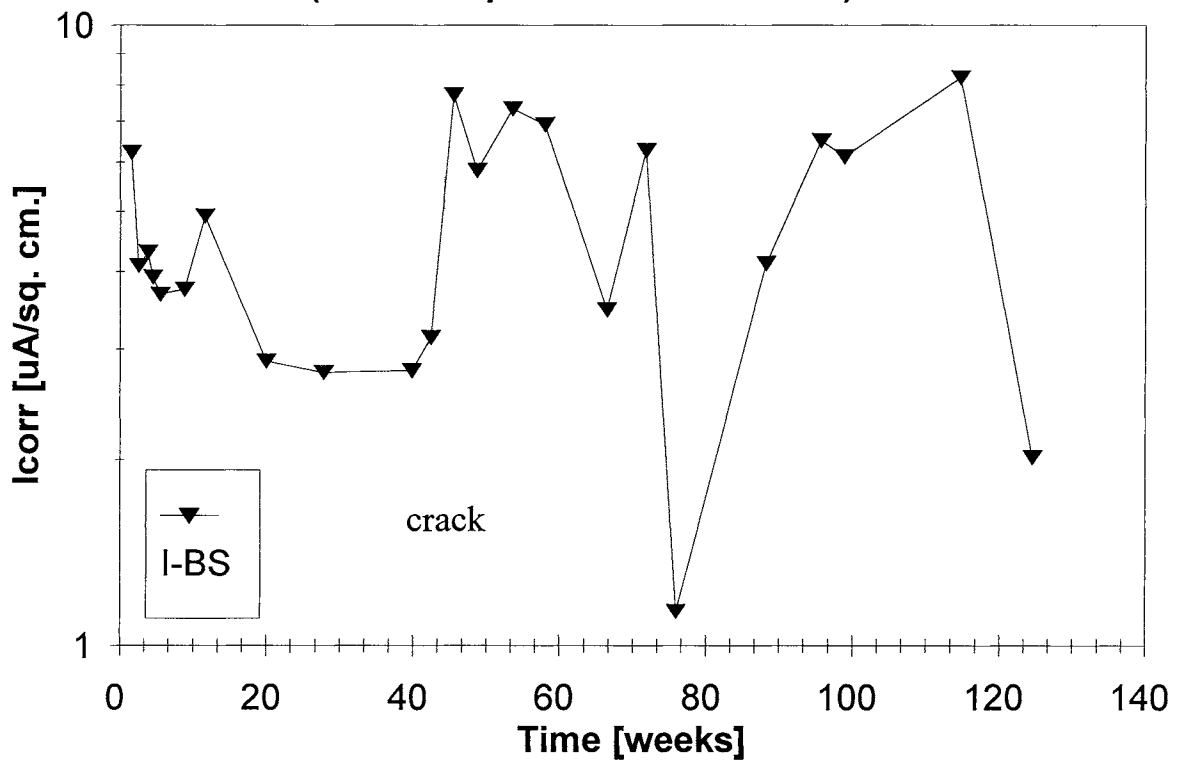
Figure 5.   Corrosion Rates - Small Scale Specimens: Control Specimen, I-BS.
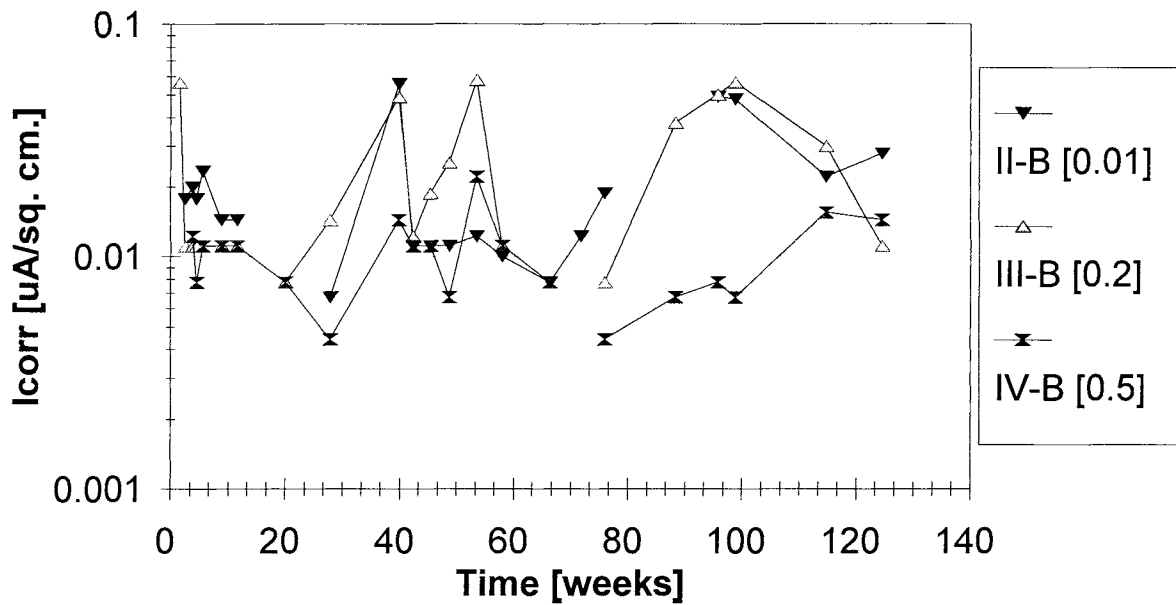
Figure 6.  Corrosion Rates - Small Scale Specimens, Specimens with Bottom of the Bars
Damaged: II-B (0.01% Area Damage), III-B (0.2% Area Damage), IV-B (0.5% Area
Damage).

# ECR - small scale specimens
## (Bottom of the bars damaged)
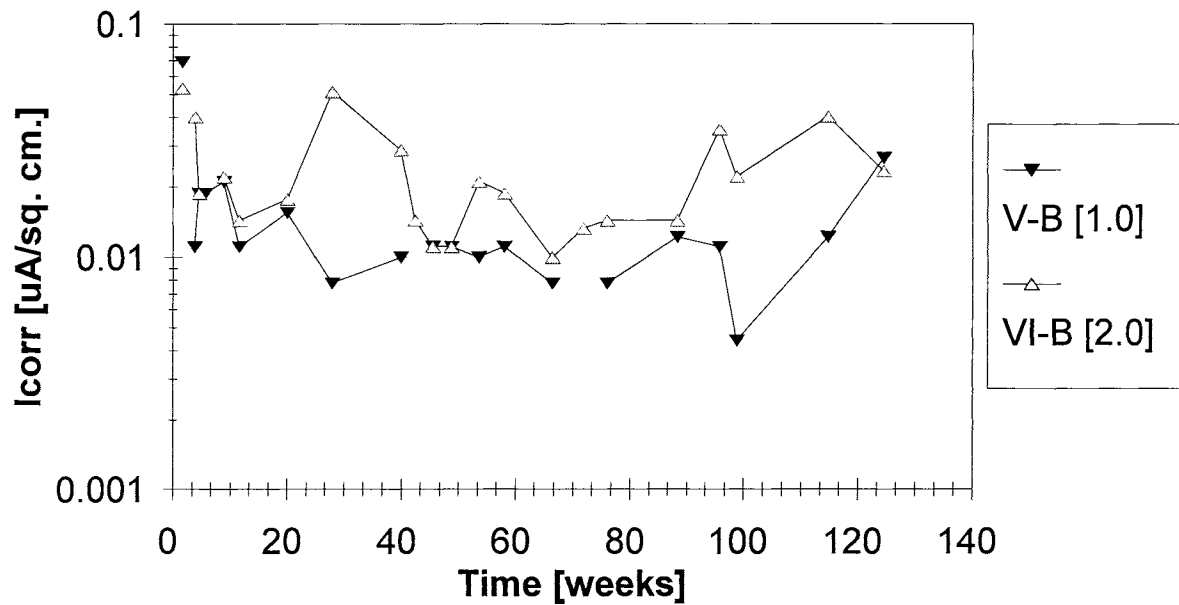


Figure 7.   Corrosion Rates - Small Scale Specimens, Specimens with Bottom of the Bars
Damaged: V-B (1.0% Area Damage), VI-B (2.0% Area Damage).

**ECR - small scale specimens**
**(Top of the bars damaged)**
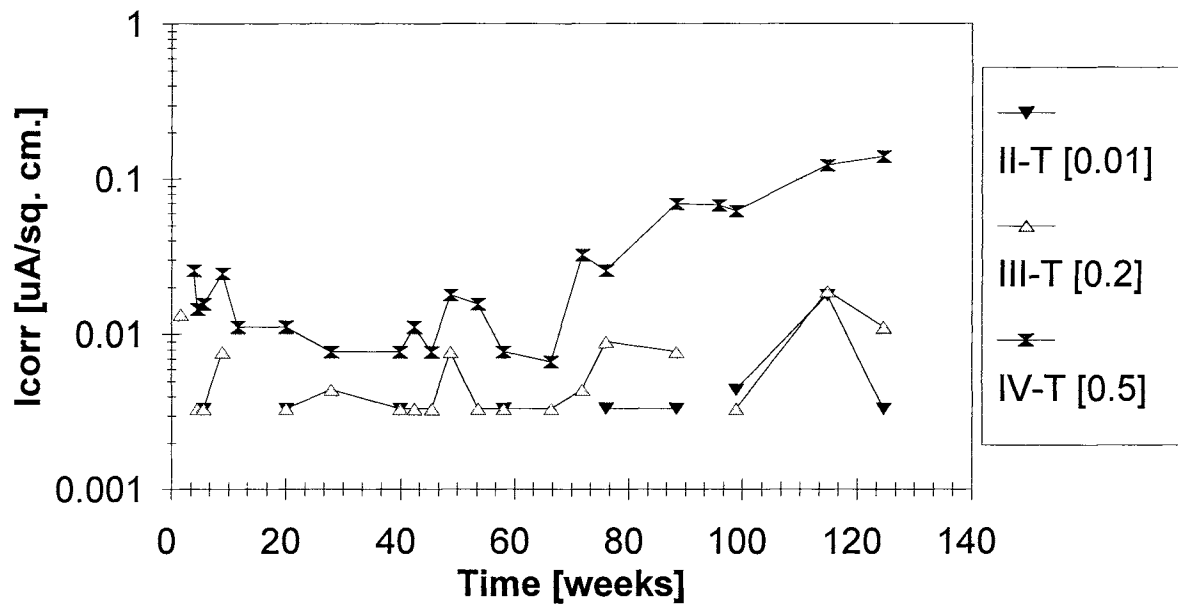
Figure 8.   Corrosion Rates - Small Scale Specimens, Specimens with Top of the Bars Damaged:
II-T (0.01% Area Damage), III-T (0.2% Area Damage), IV-T (0.5% Area Damage).

**ECR - small scale specimens**
**(Top of the bars damaged)**
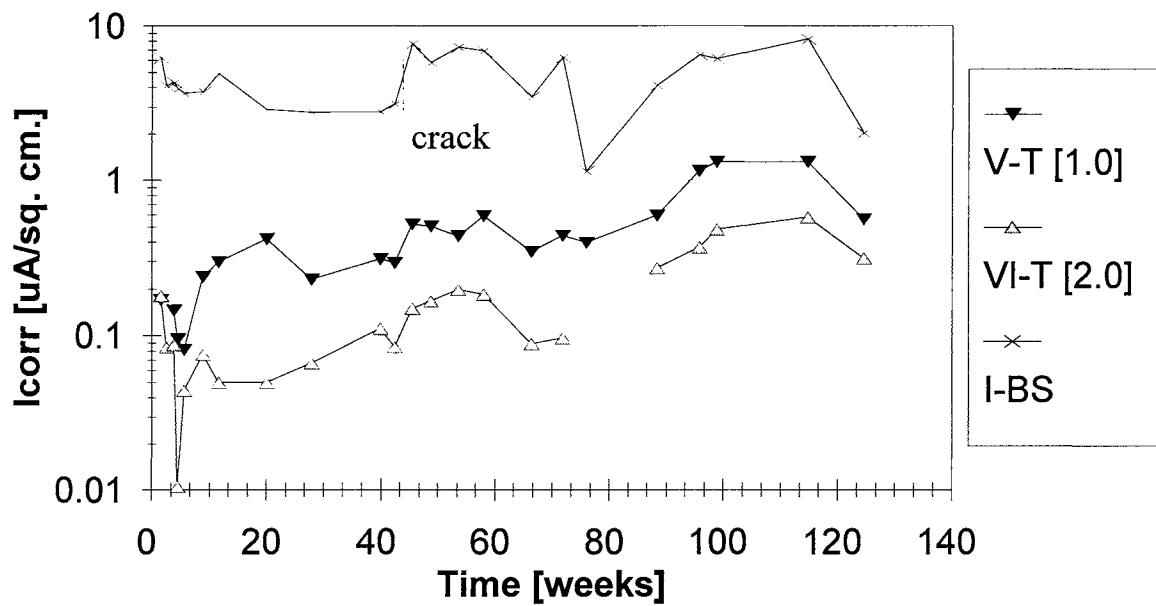
Figure 9.   Corrosion Rates - Small Scale Specimens, Specimens with Top of the Bars Damaged:
V-T (1.0% Area Damage), VI-T (2.0% Area Damage), and Control Specimen, I-BS.
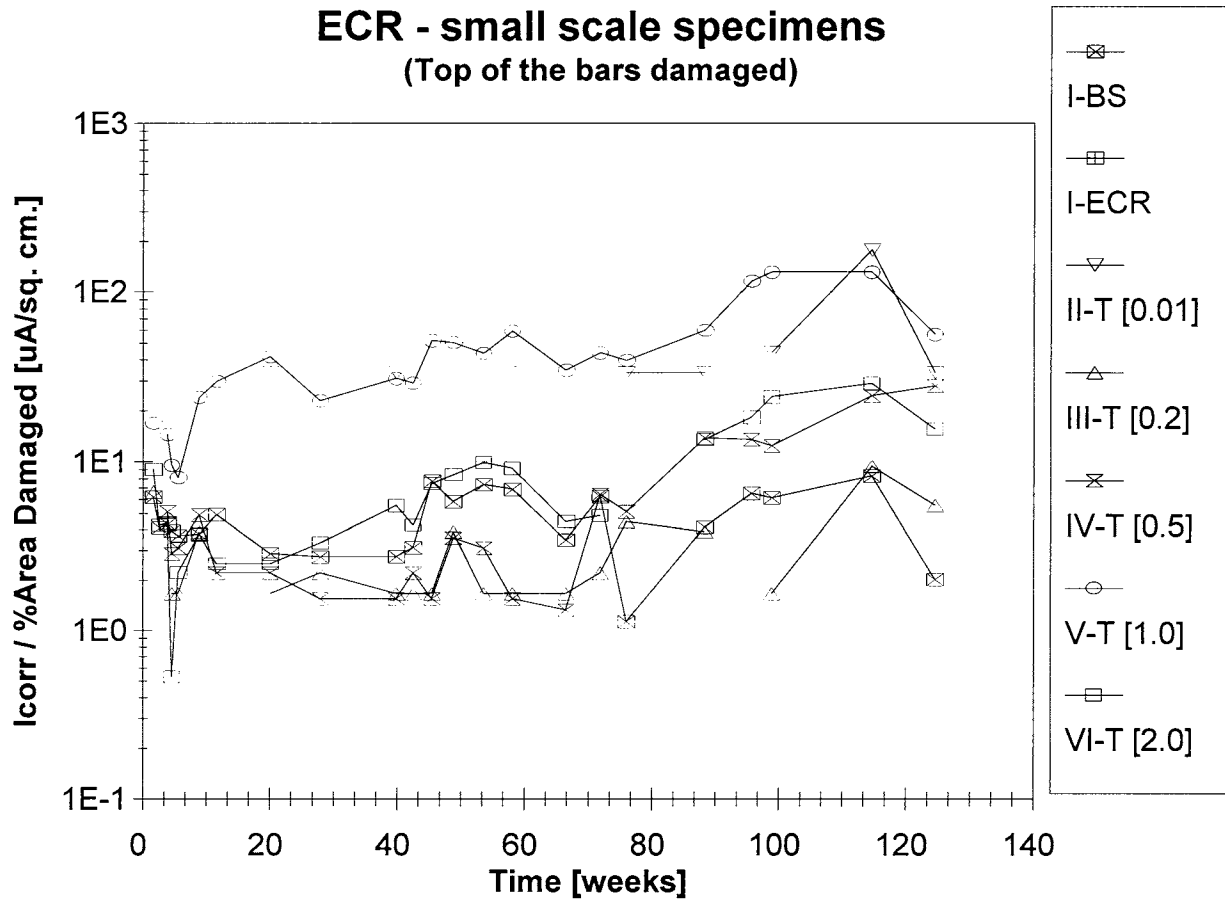
Figure 10. Corrosion Rates - Small Scale Specimens, Specimens with Top of the Bars Damaged.

**ECR - small scale specimens**
**(Bottom of the bars damaged)**

Legend:
- I-BS
- I-ECR
- II-B [0.01]
- III-B [0.2]
- IV-B [0.5]
- V-B [1.0]
- VI-B [2.0]

Y-axis: Icorr / %Area Damaged [mA/sq. ft.]
X-axis: Time [weeks]
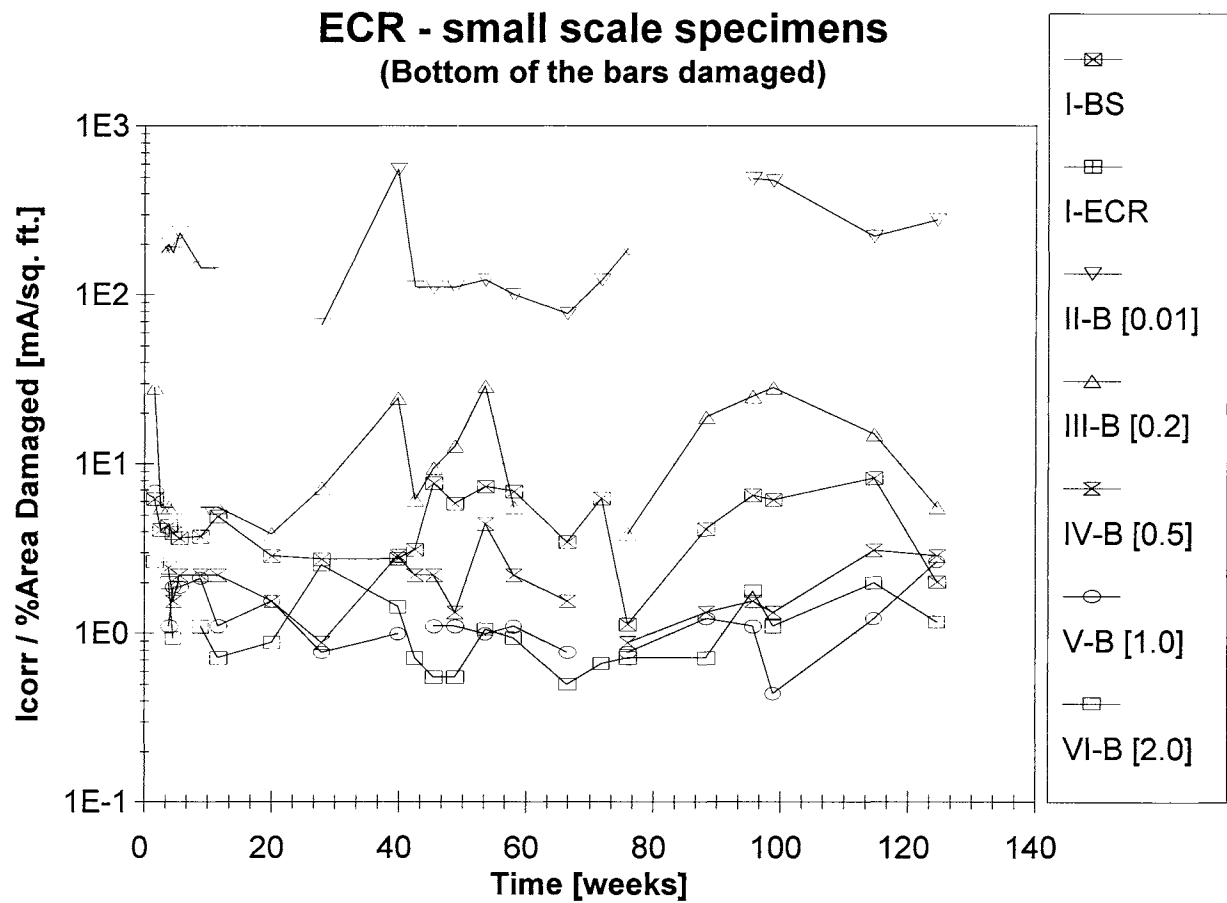
Figure 11. Corrosion Rates - Small Scale Specimens, Specimens with Bottom of the Bars
Damaged.

# Small Scale Specimens
## Top of the Bars Damaged
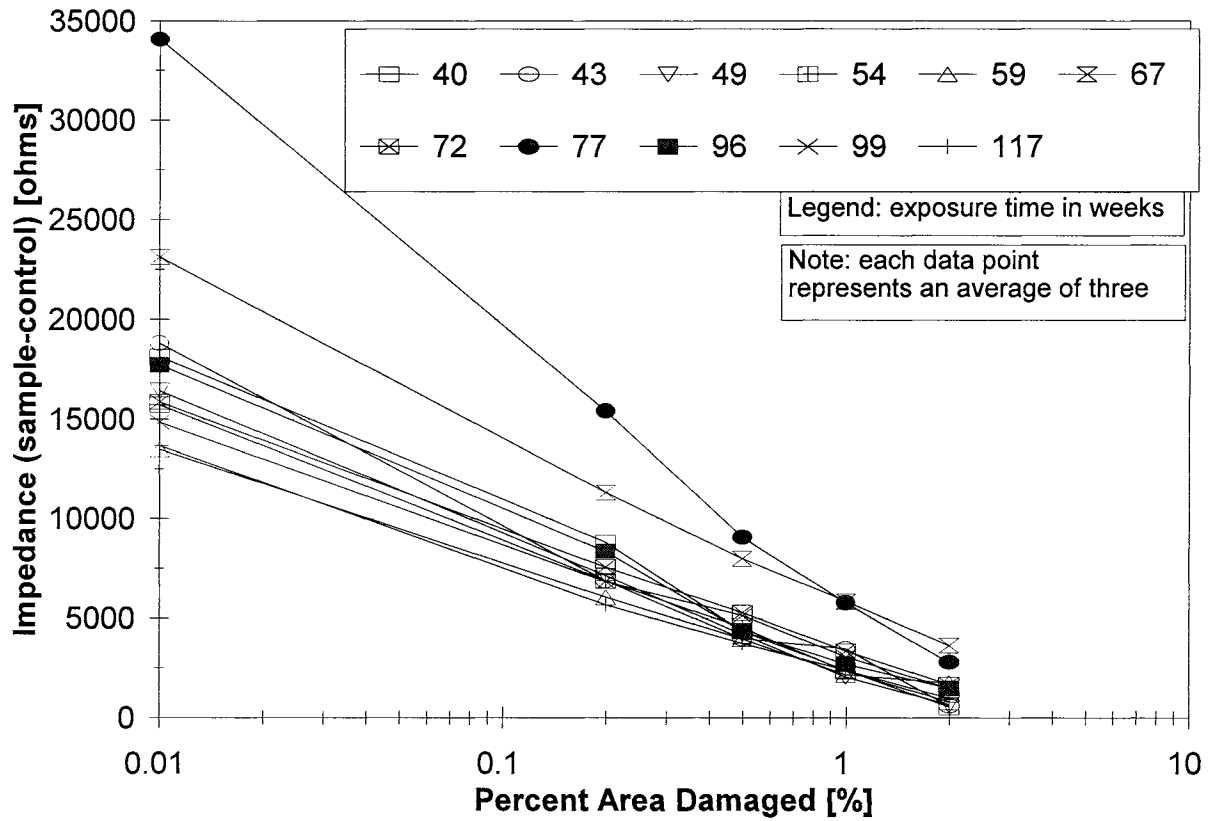


Figure 12. AC Impedance at 97.4 Hz vs. Log (Percent Area Damage) - Small Scale Specimens with Top of the Bars Damaged.

# Small Scale Specimens
## Top of the Bars Damaged



Legend: exposure time in weeks

Note: each data point represents an average of three
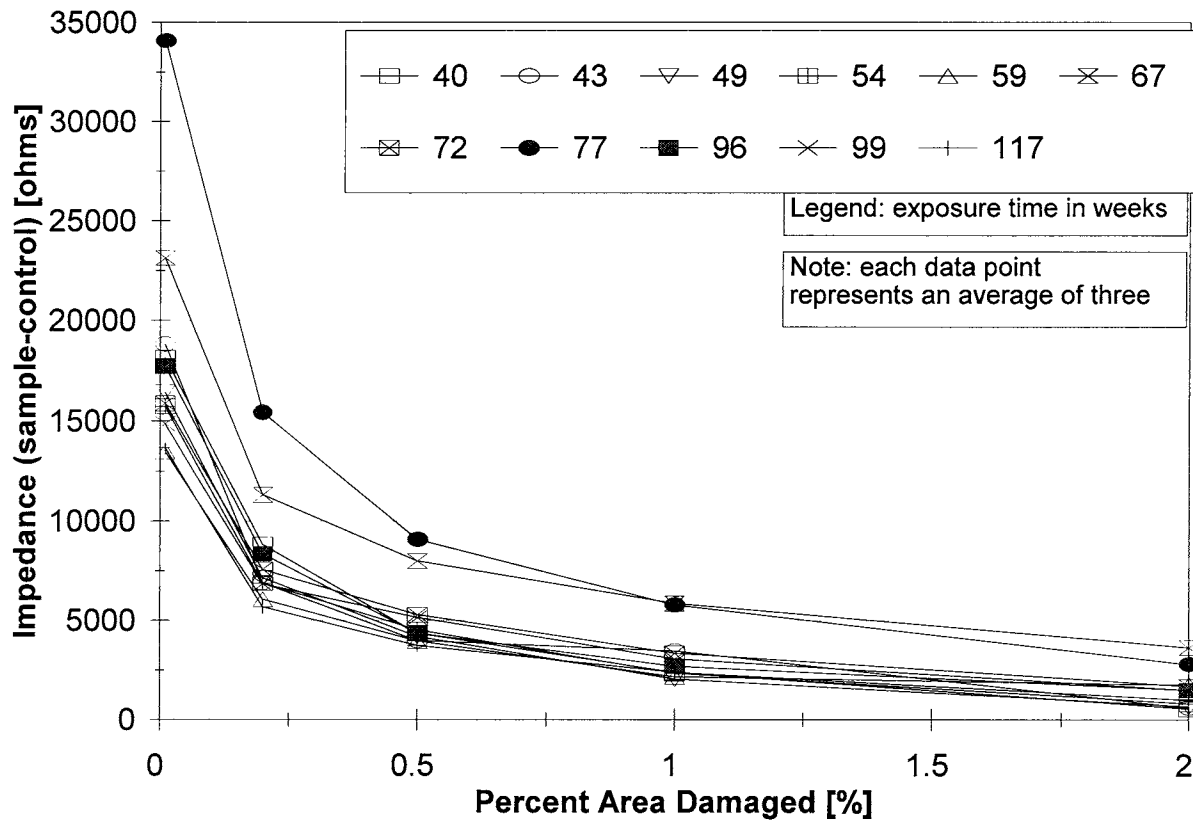
Figure 13. AC Impedance at 97.4 Hz vs. Percent Area Damage - Small Scale Specimens with Top of the Bars Damaged.

**Small Scale Specimens**

Varying % Damage [top areas]

Note: each data point
represents an average of three

Legend: 0, 0.01, 0.2, 0.5, 1, 2
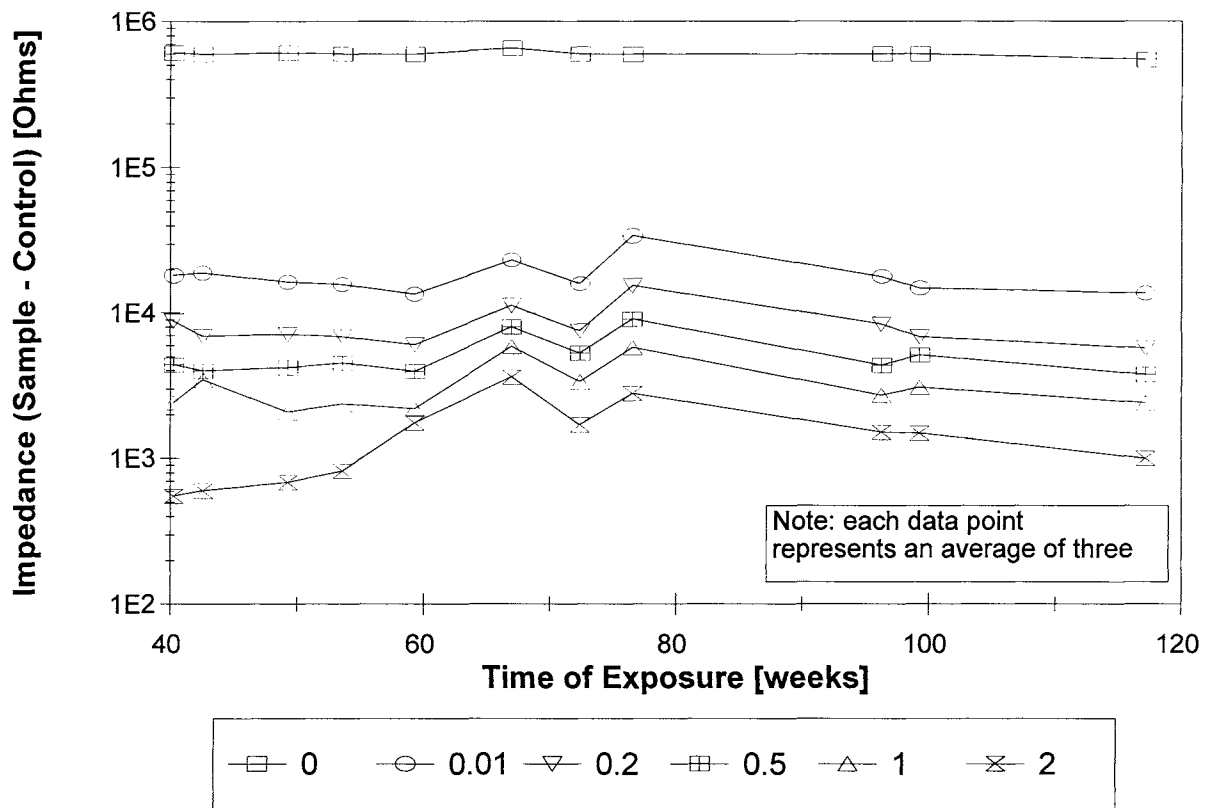
Figure 14. AC Impedance at 97.4 Hz vs. Time - Small Scale Specimens with Top of the Bars
Damaged.
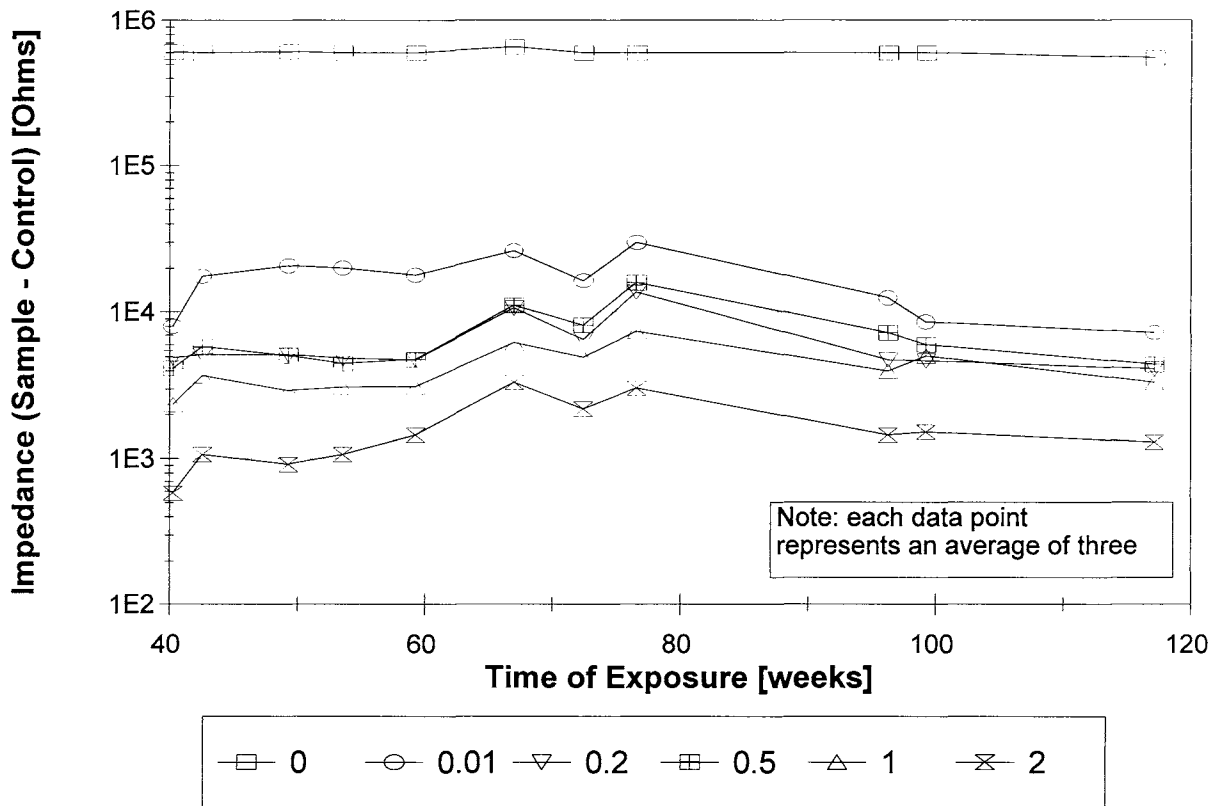
Figure 15. AC Impedance at 97.4 Hz vs. Time - Small Scale Specimens with Bottom of the Bars Damaged.

Figure 16. EIS - Small Scale Specimens with Top of the Bars Damaged at 101 Weeks.

**Small Scale Specimens - EIS Results**

Bottom of the Bars Damaged

Legend:specimen, percent area damage

I-BS, 100%

I-ECR, 0%

II-B, 0.01%

III-B, 0.2%

IV-B, 0.5%

V-B, 1.0%

VI-B, 2.0%
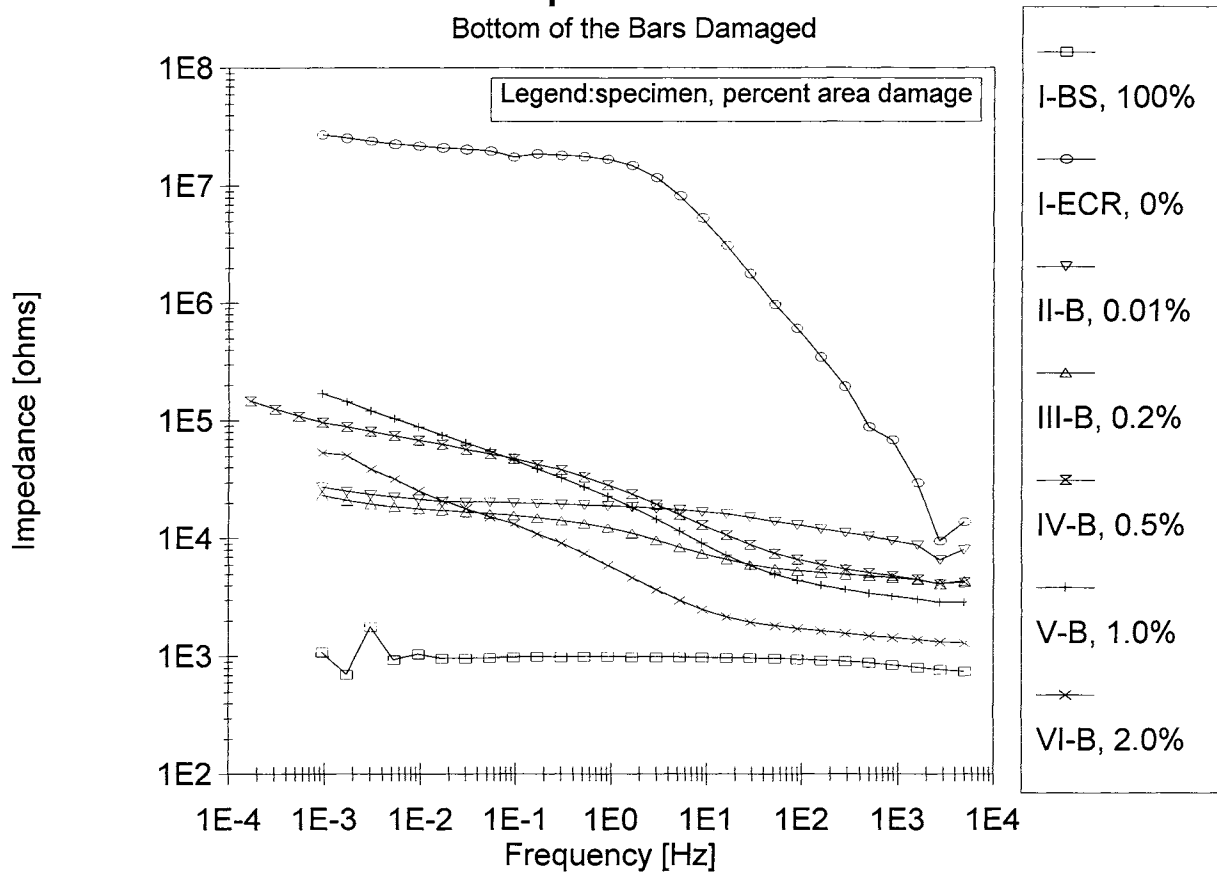
Figure 17. EIS - Small Scale Specimens with Bottom of the Bars Damaged at 101 Weeks.

**FSC-1 Specimen**
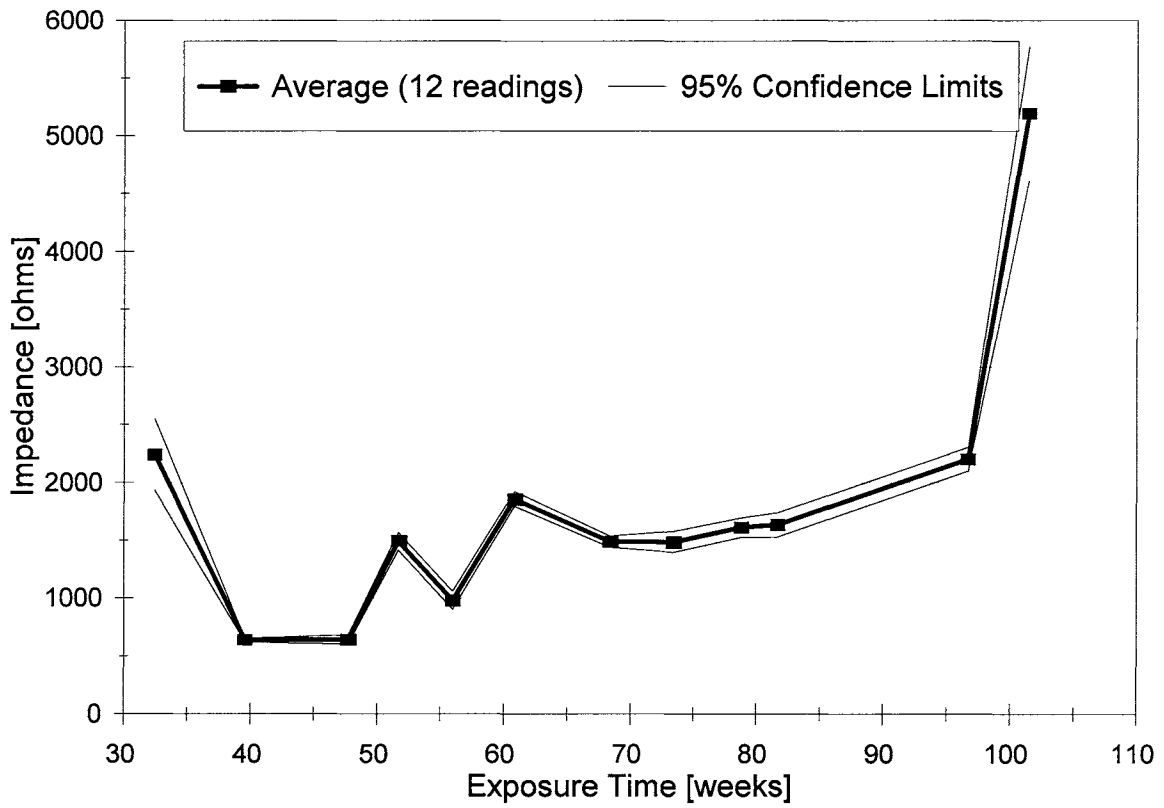


Figure 18. AC Impedance at 97.4 Hz - Large Scale Specimens: FSC-1 Specimen.

**FSC-2 Specimen**
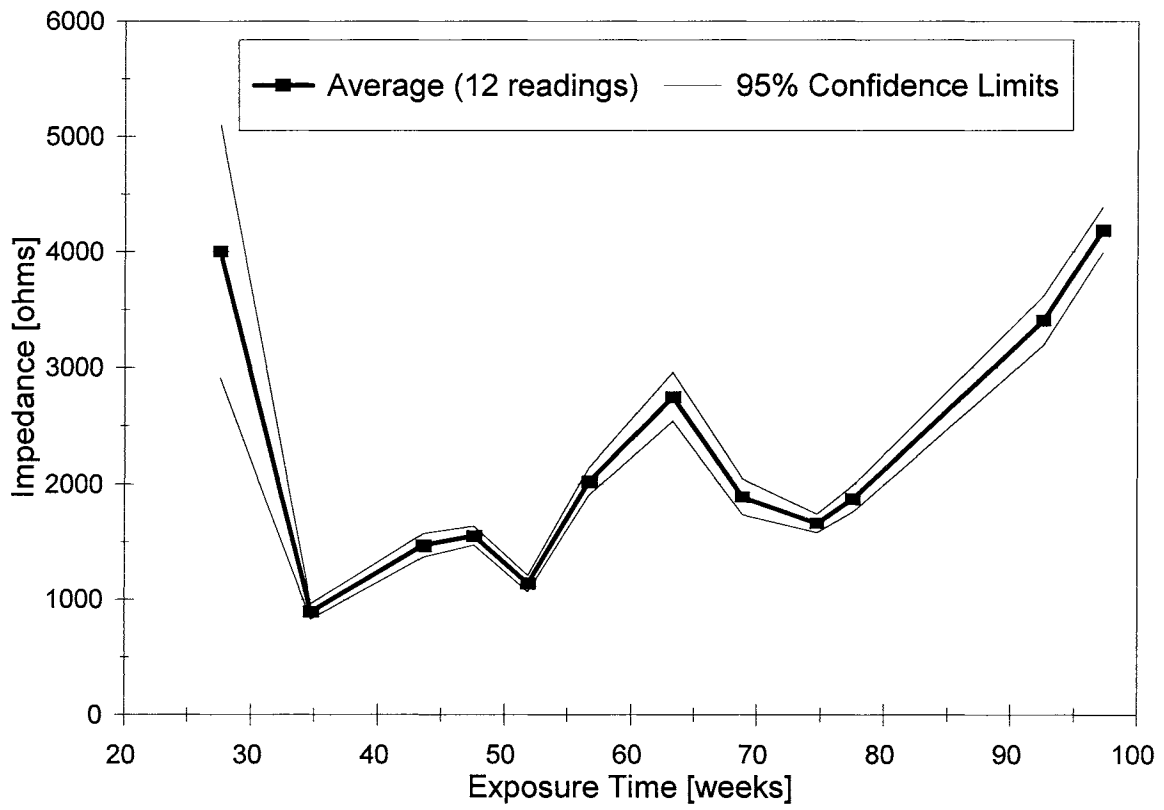
Figure 19. AC Impedance at 97.4 Hz - Large Scale Specimens: FSC-2 Specimen.

**FSC-3 Specimen**
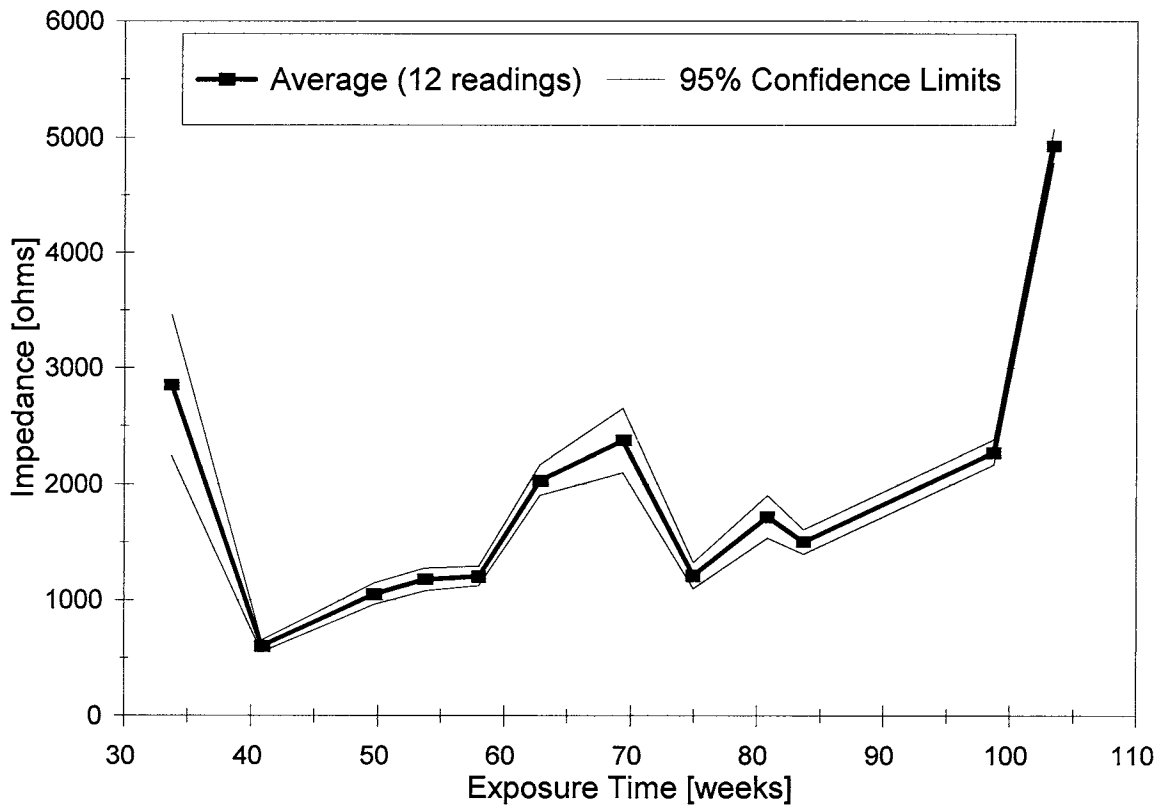


Figure 20. AC Impedance at 97.4 Hz - Large Scale Specimens: FSC-3 Specimen.

**FSC-4 Specimen**
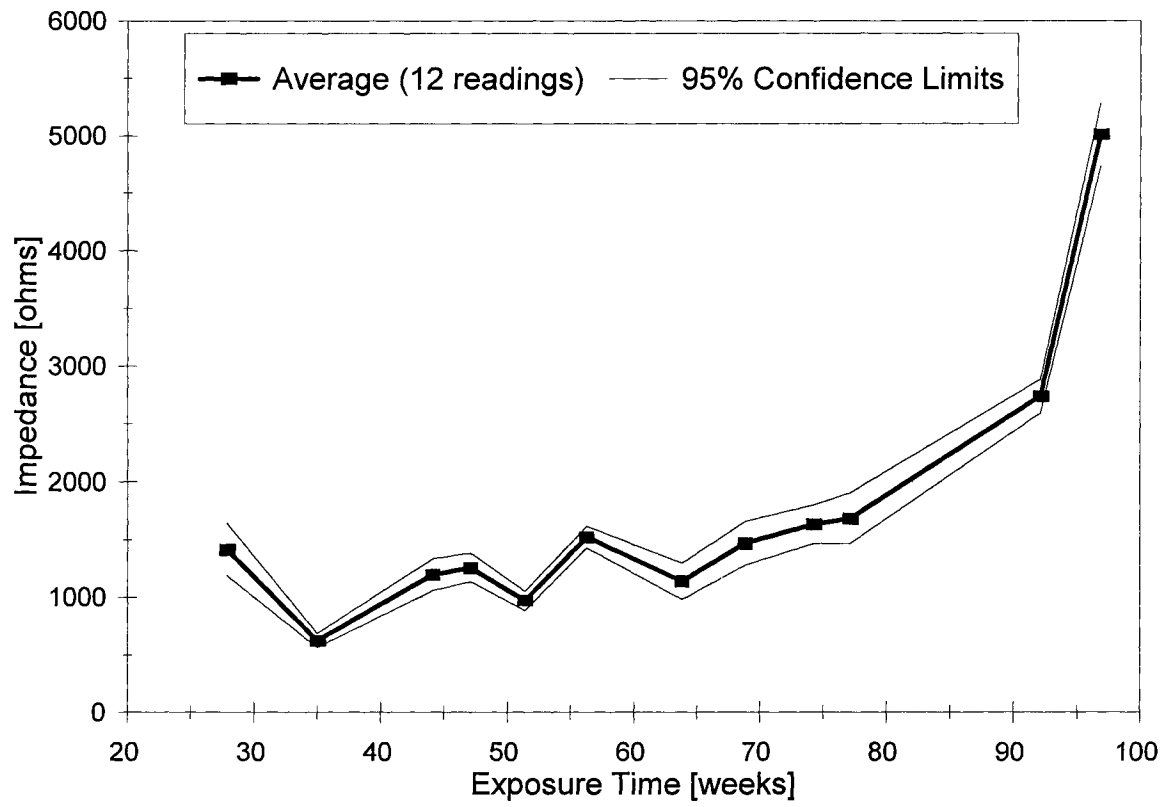


Figure 21. AC Impedance at 97.4 Hz - Large Scale Specimens: FSC-4 Specimen.

# FSC-5 Specimen
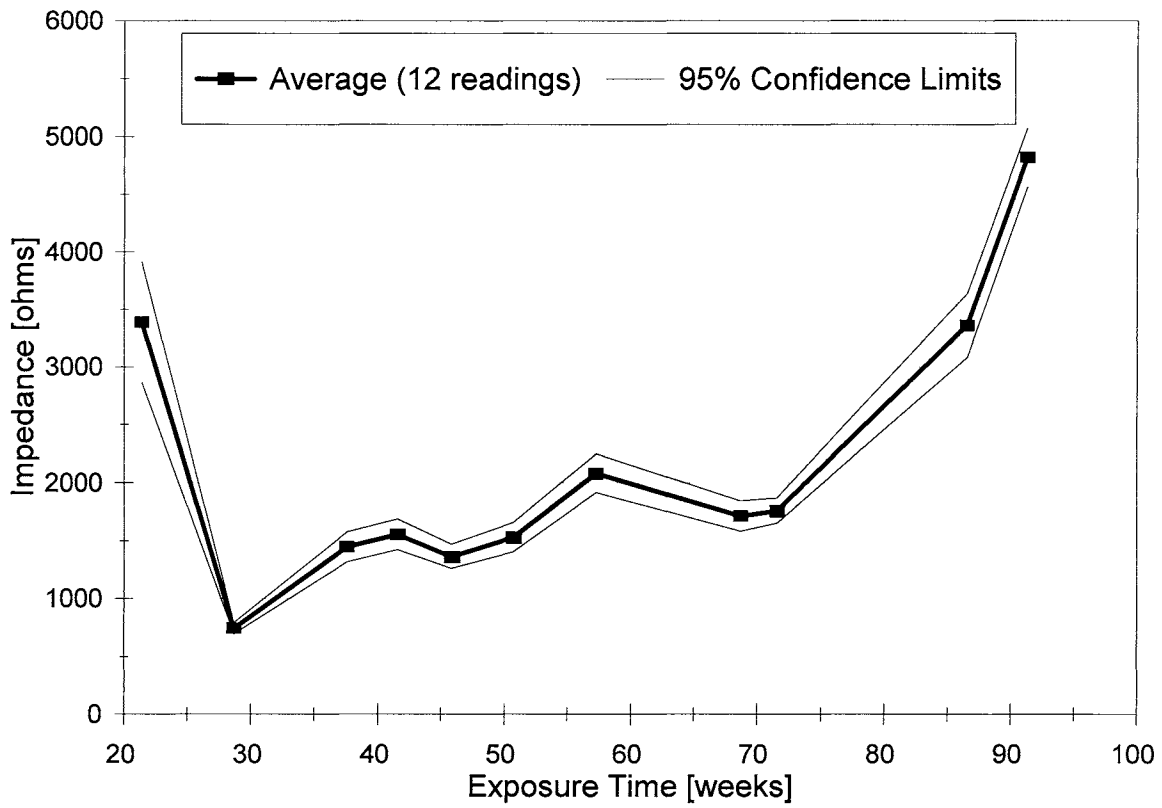


Figure 22. AC Impedance at 97.4 Hz - Large Scale Specimens: FSC-5 Specimen.

# LNE-1 Specimen
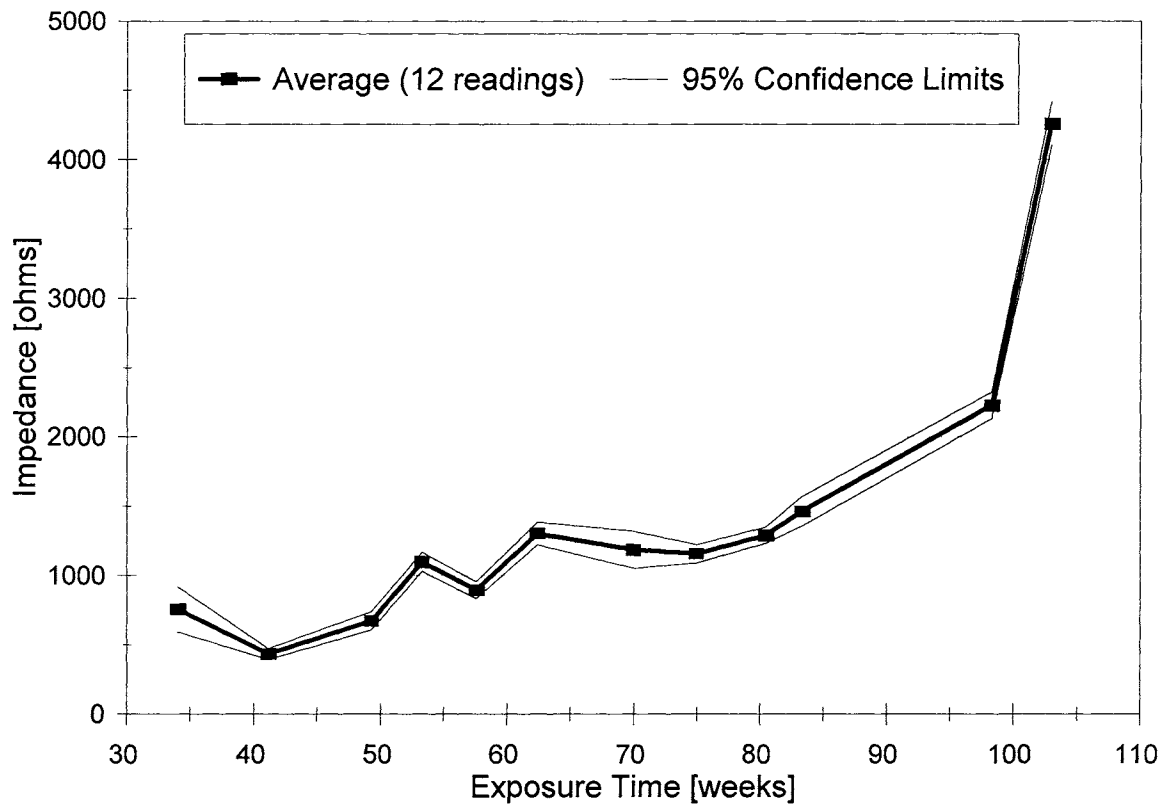


Figure 23. AC Impedance at 97.4 Hz - Large Scale Specimens: LNE-1 Specimen.

## LNE-2 Specimen
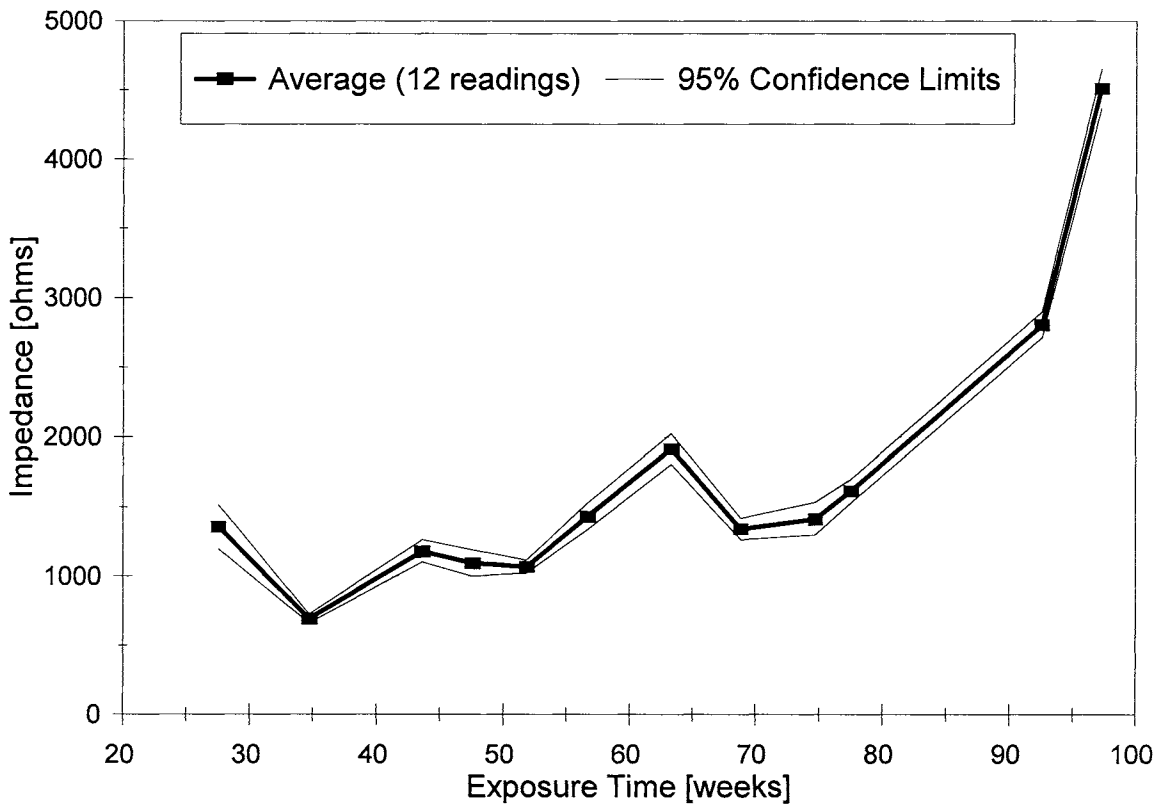


Figure 24. AC Impedance at 97.4 Hz - Large Scale Specimens: LNE-2 Specimen.

**FS-1 Specimen**
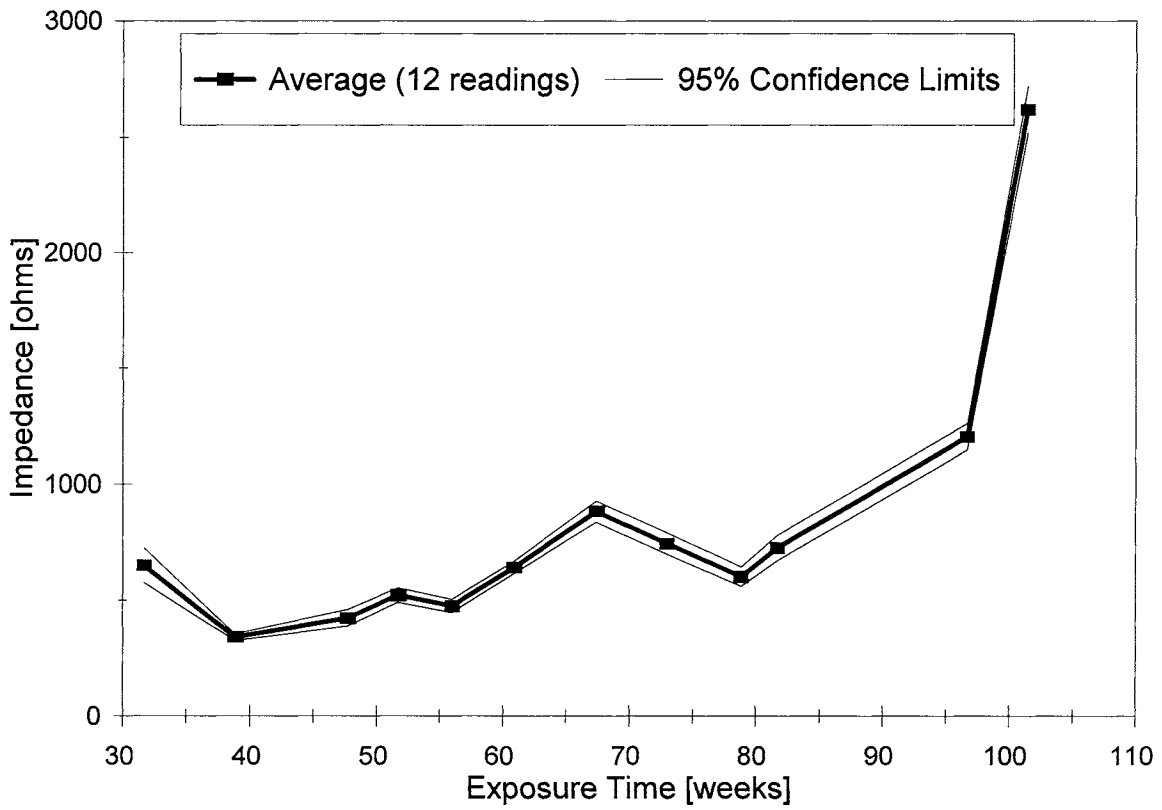


Figure 25. AC Impedance at 97.4 Hz - Large Scale Specimens: FS-1 Specimen.
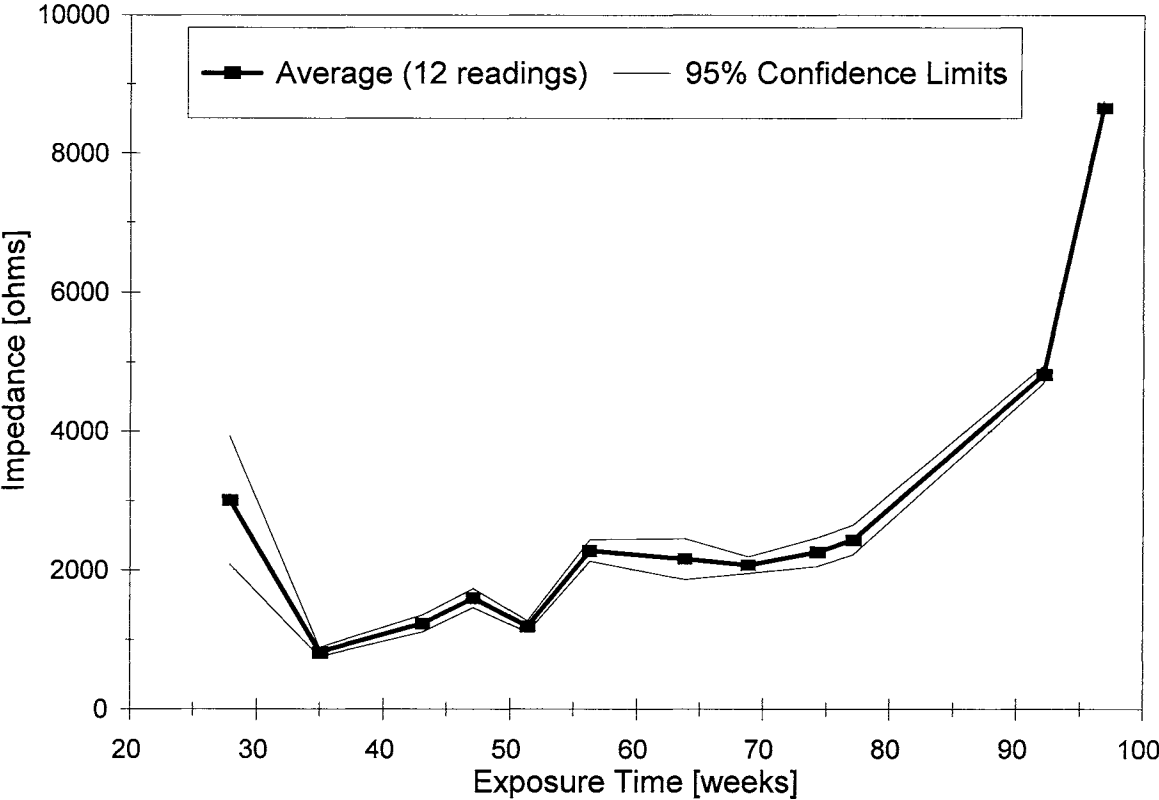
Figure 26. AC Impedance at 97.4 Hz - Large Scale Specimens: FS-2 Specimen.

# CGN-1 Specimen
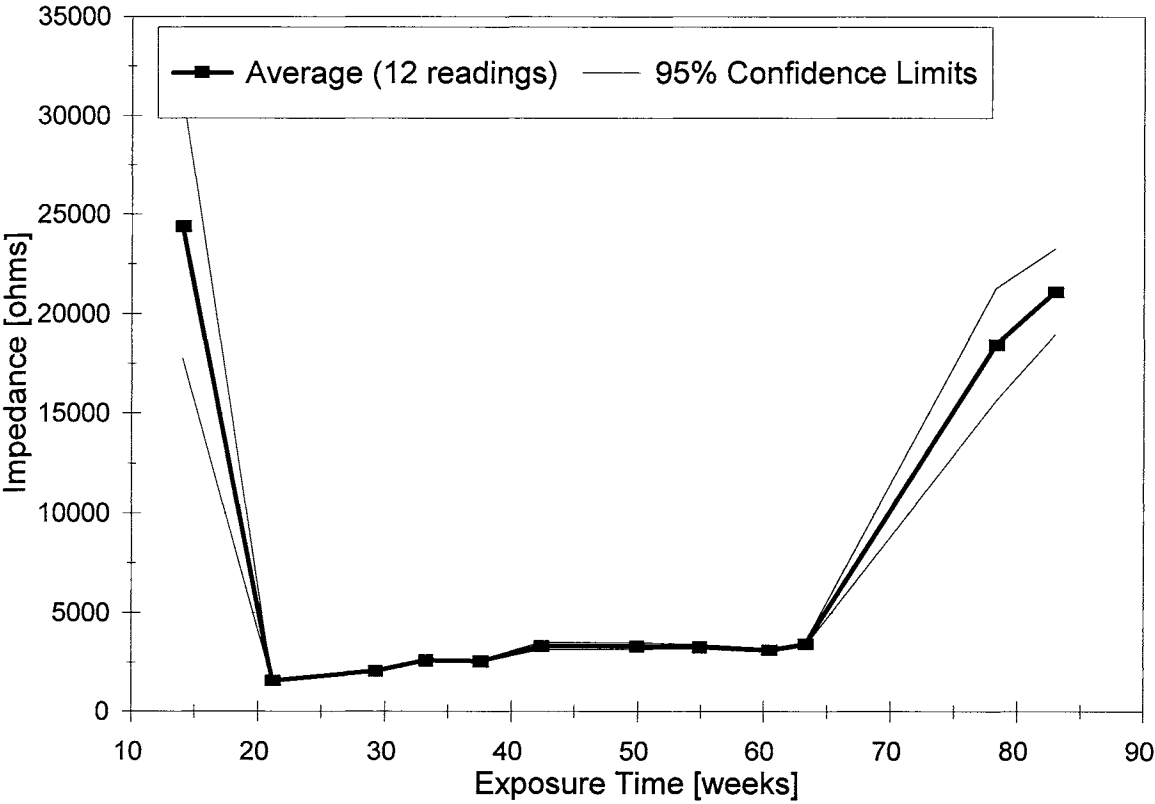


Figure 27. AC Impedance at 97.4 Hz - Large Scale Specimens: CGN-1 Specimen.

# CGY-1 Specimen
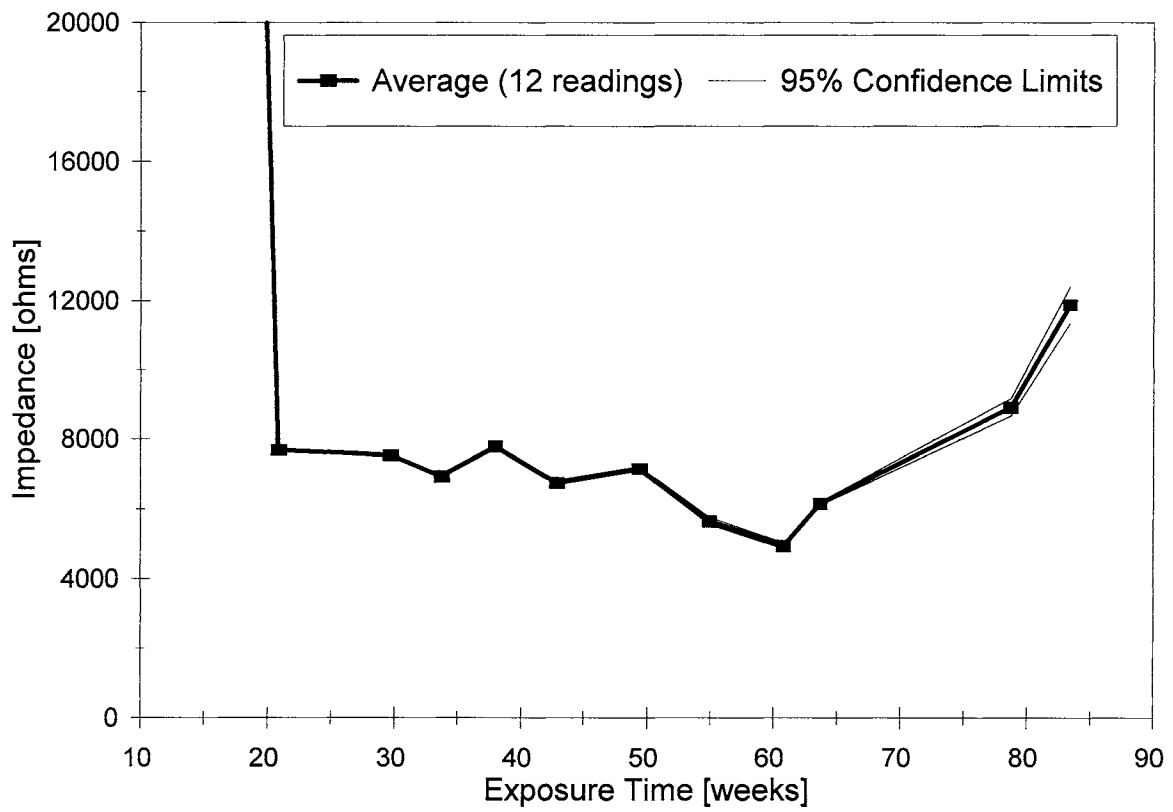


Figure 28. AC Impedance at 97.4 Hz - Large Scale Specimens: CGY-1 Specimen.

**CGN-11 Specimen**
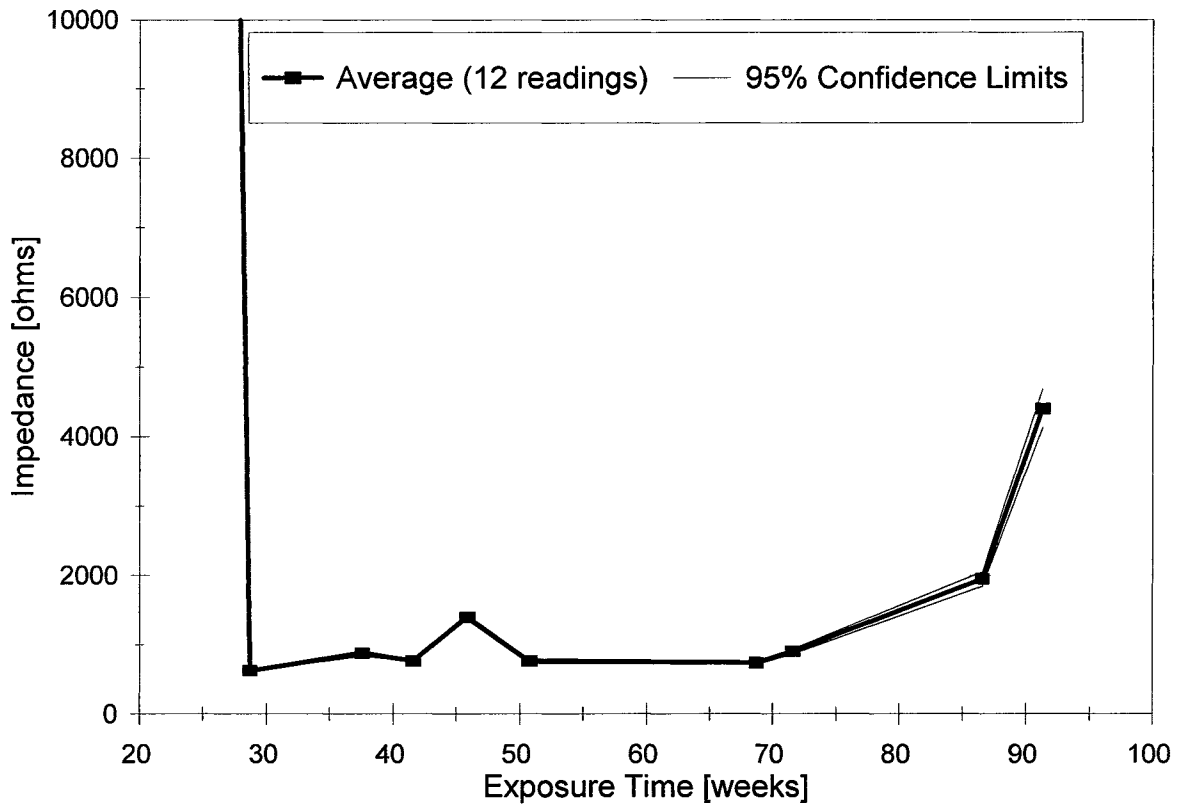


Figure 29. AC Impedance at 97.4 Hz - Large Scale Specimens: CGN-11 Specimen.

## CGY-11 Specimen
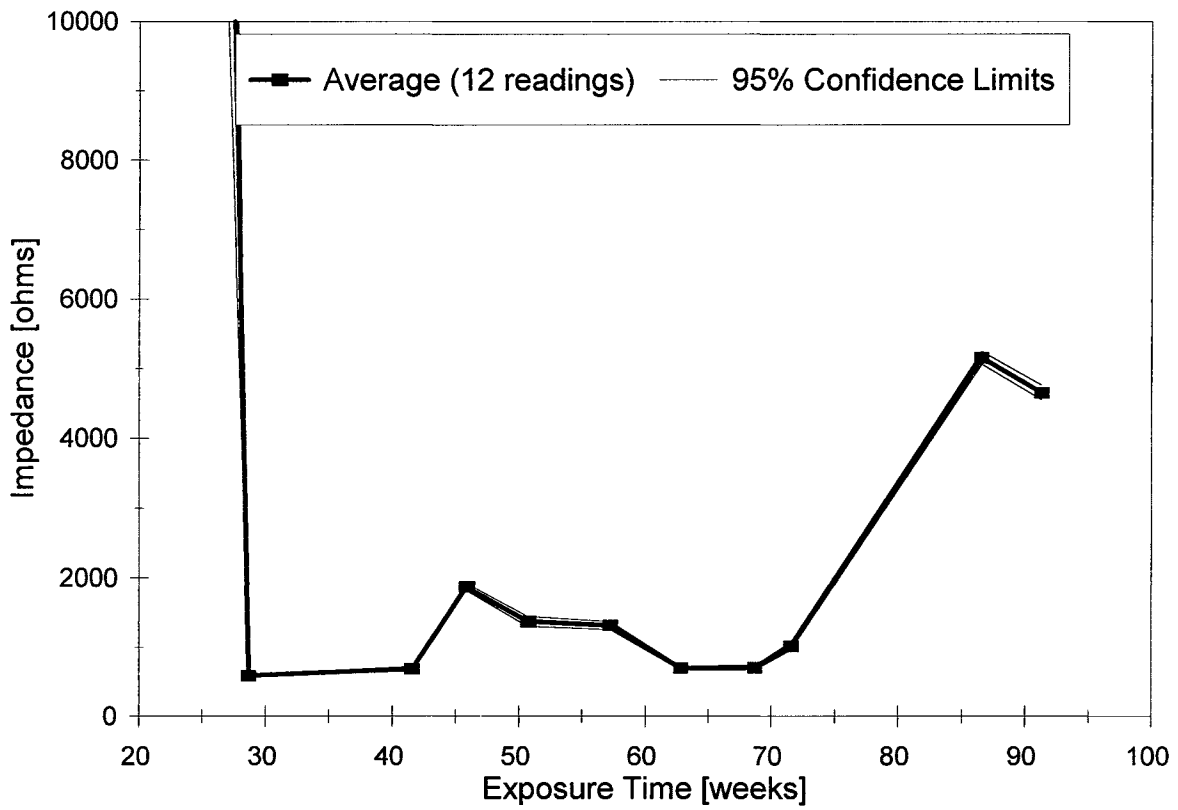


Figure 30.  AC Impedance at 97.4 Hz - Large Scale Specimens: CGY-11 Specimen.

# FSC-51 Specimen
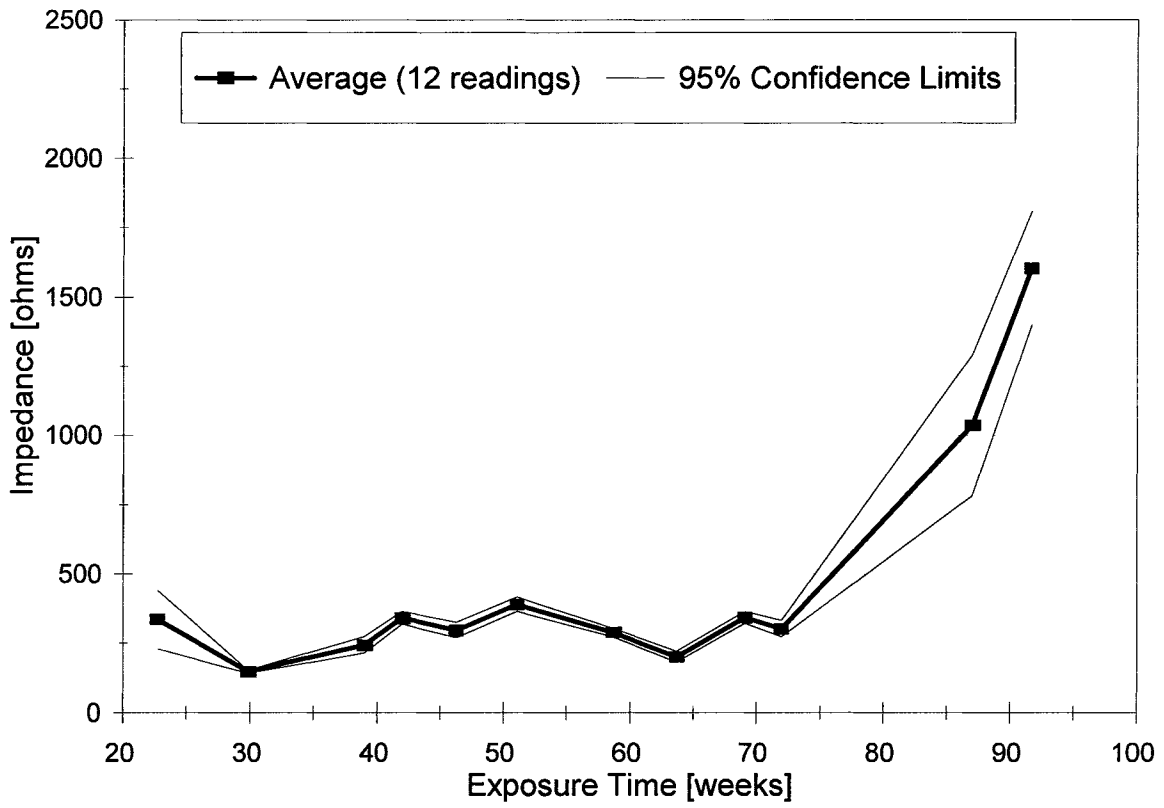


Figure 31. AC Impedance at 97.4 Hz - Large Scale Specimens: FSC-51 Specimen.

# BS-1 Specimen
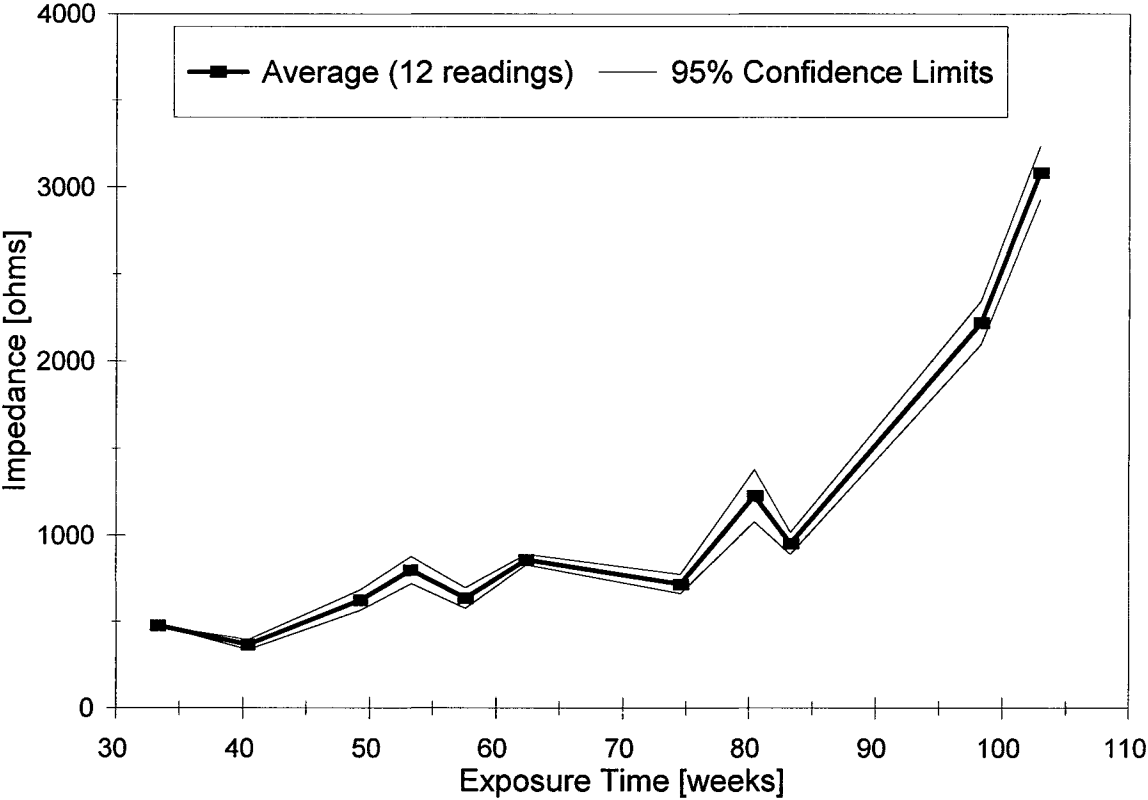


Figure 32. AC Impedance at 97.4 Hz - Large Scale Specimens: BS-1 Specimen.

**BS-2 Specimen**
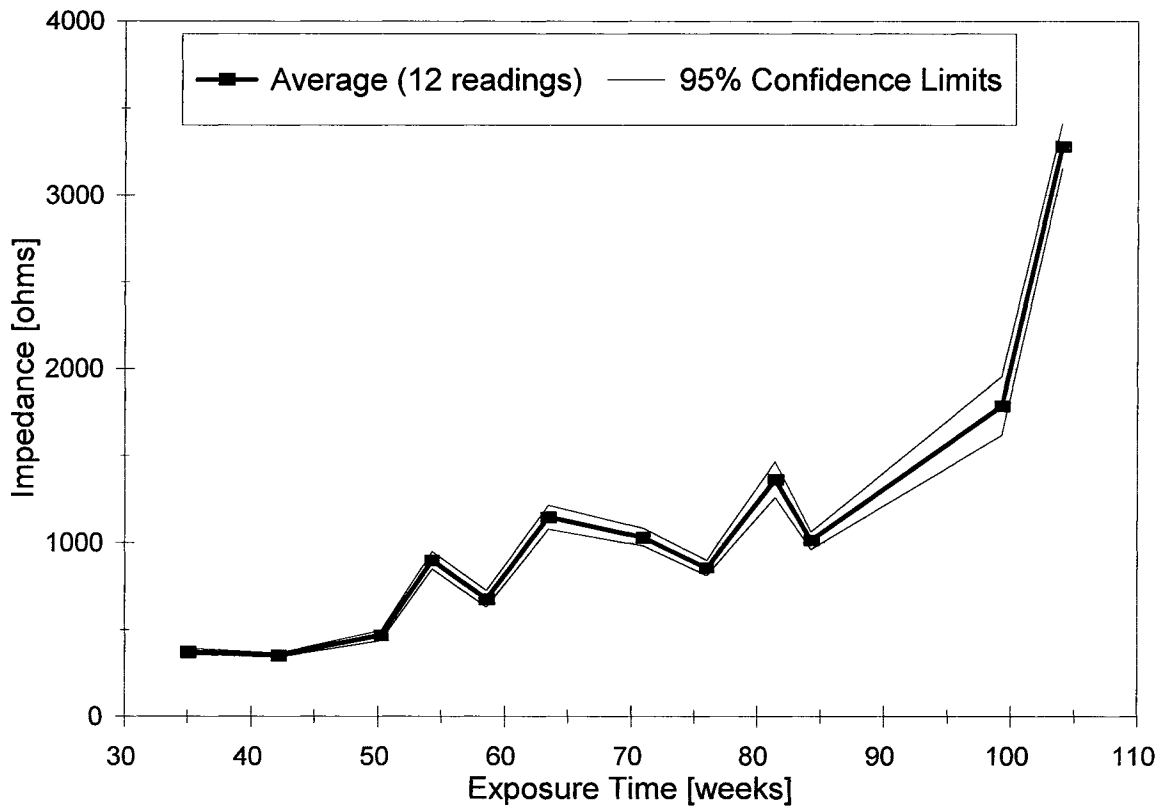
Figure 33. AC Impedance at 97.4 Hz - Large Scale Specimens: BS-2 Specimen.
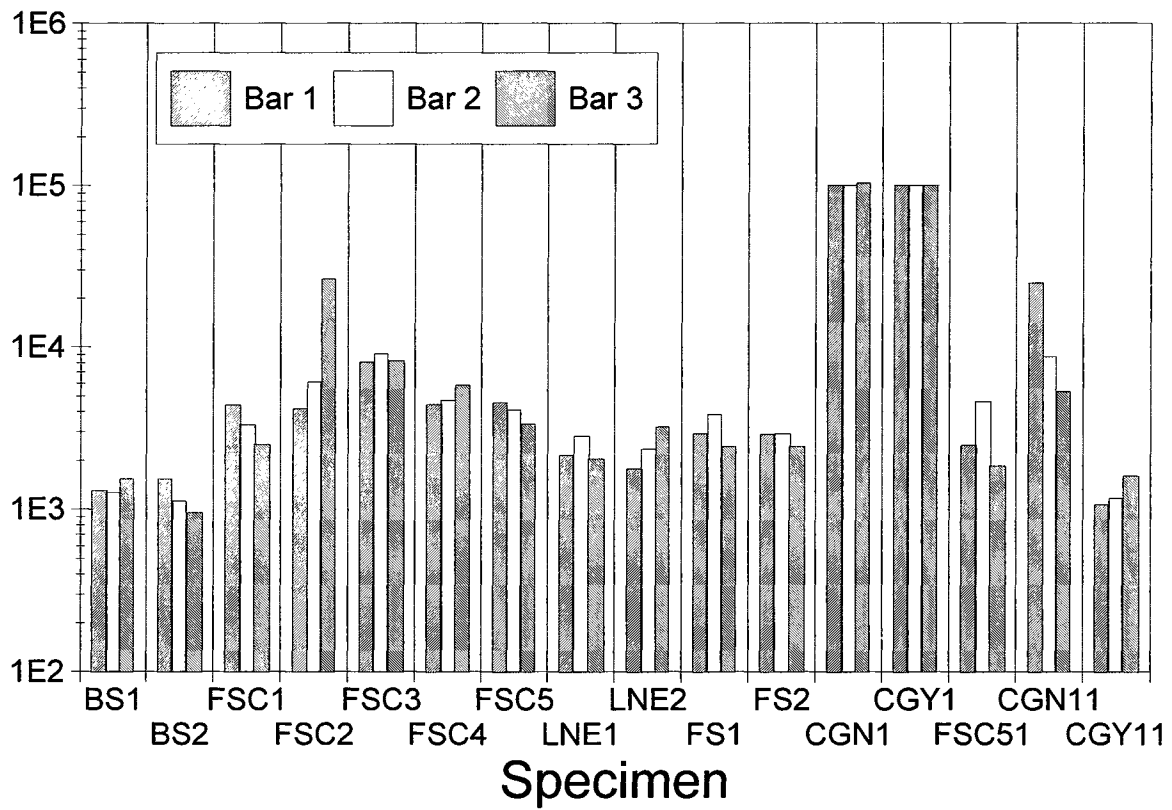
Figure 34. AC Impedance at 97.4 Hz - Large Scale Specimens, Immersed Zone, Left Leg, End of Ponding at about 76 Weeks (63-84 Weeks).
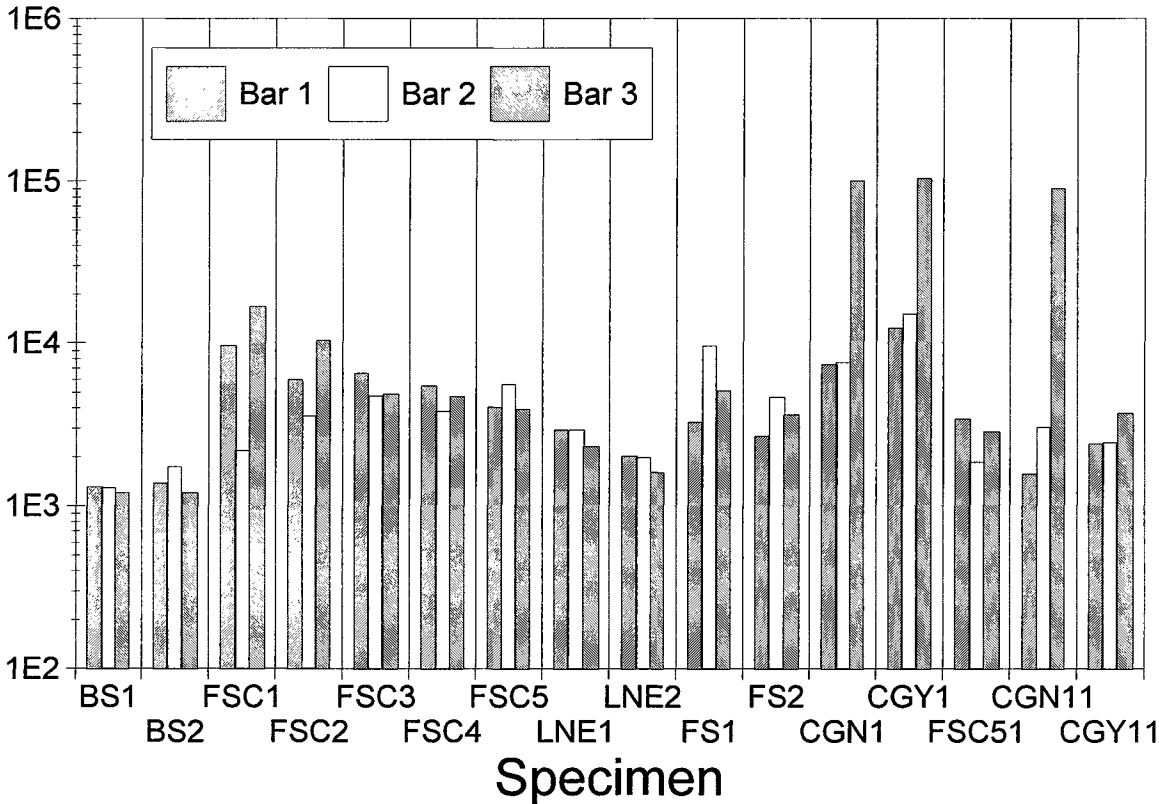
Figure 35. AC Impedance at 97.4 Hz - Large Scale Specimens, Immersed Zone, Right Leg, End of Ponding at about 76 Weeks (63-84 Weeks).
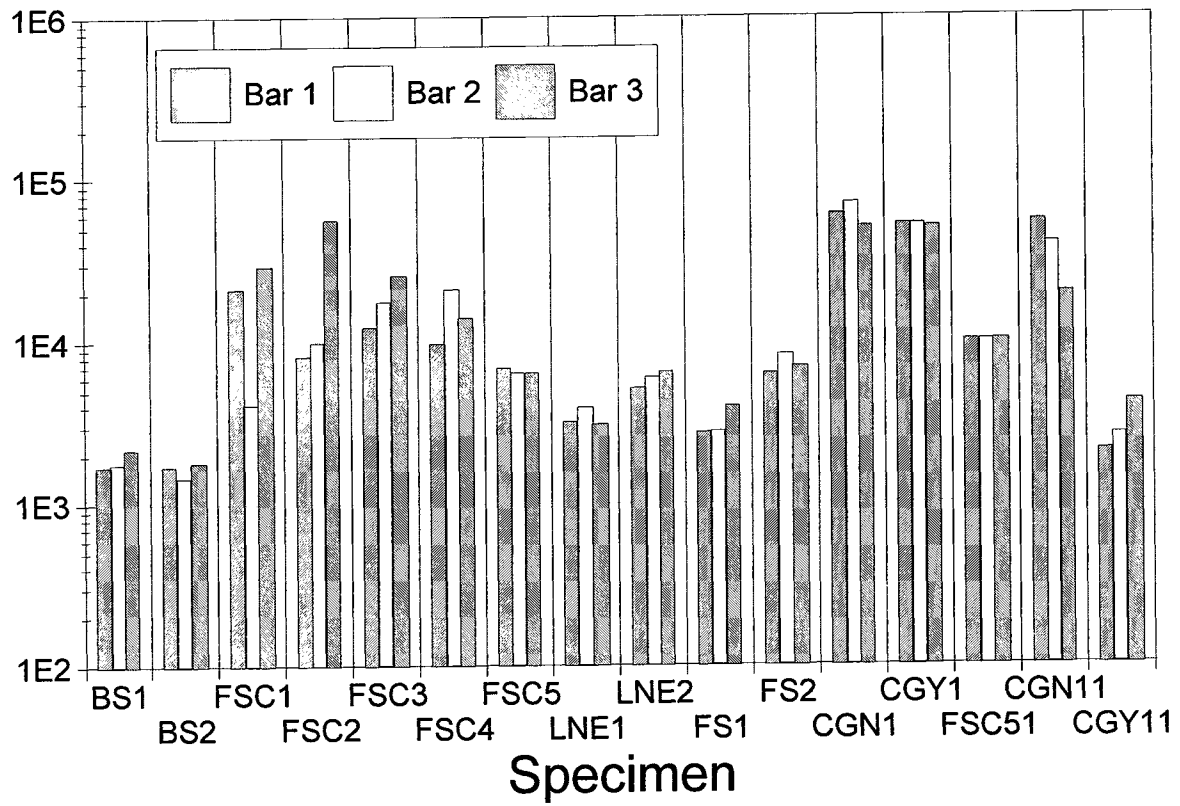
Figure 36. AC Impedance at 97.4 Hz - Large Scale Specimens, Immersed Zone, Left Leg, 1st Measurement Outdoors at about 91 Weeks (78-99 Weeks).
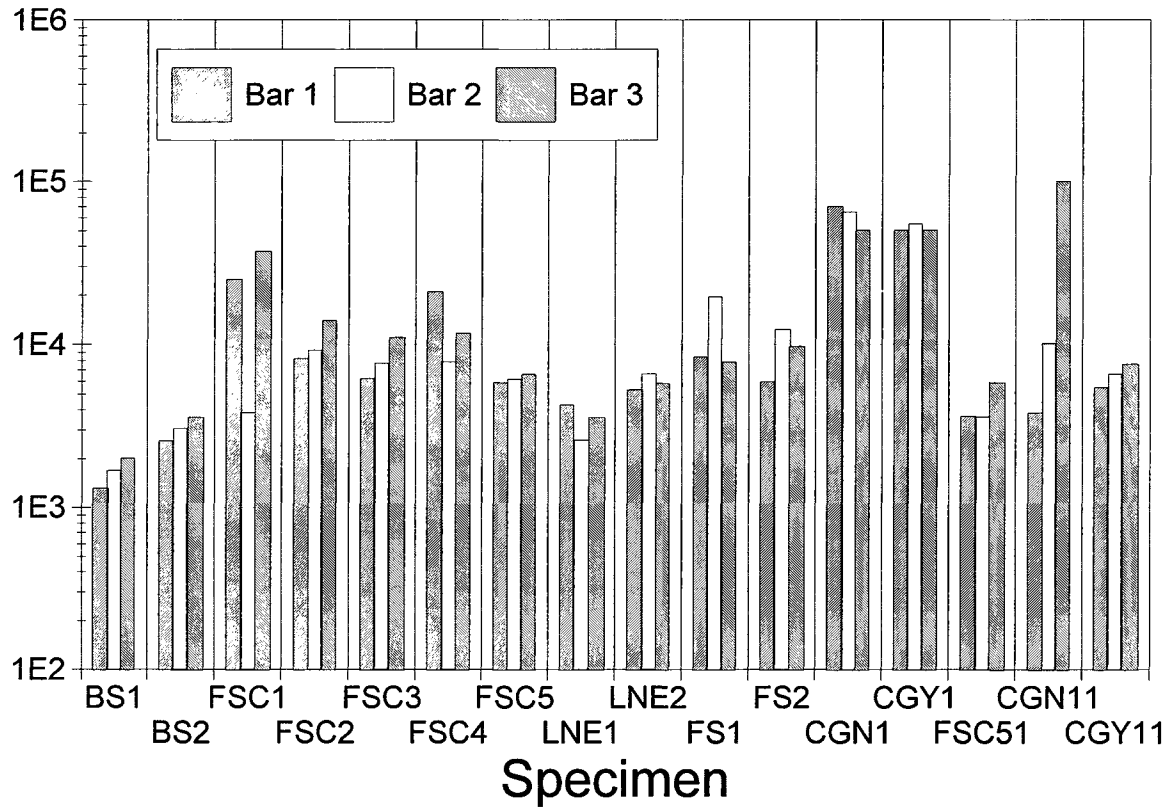
Figure 37. AC Impedance at 97.4 Hz - Large Scale Specimens, Immersed Zone, Right Leg, 1st Measurement Outdoors at about 91 Weeks (78-99 Weeks).
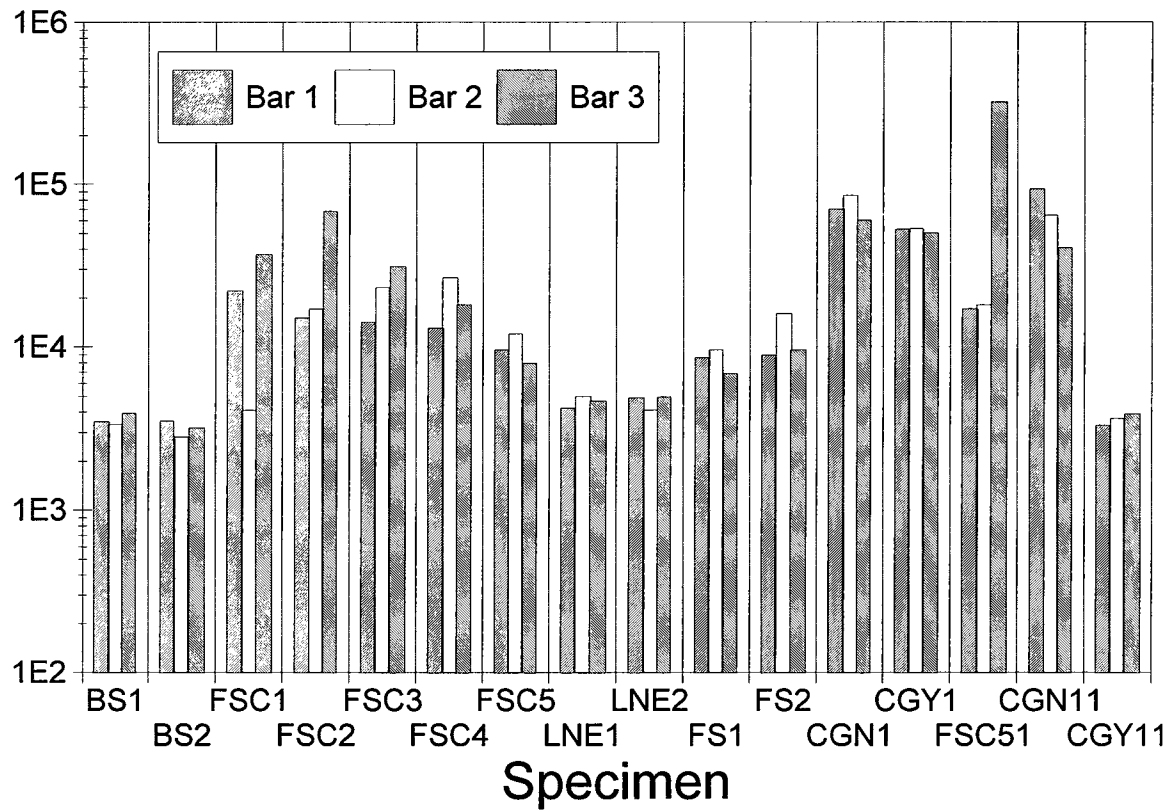
Figure 38. AC Impedance at 97.4 Hz - Large Scale Specimens, Immersed Zone, Left Leg, $2^{nd}$ Measurement Outdoors at about 96 Weeks (83-104 Weeks).
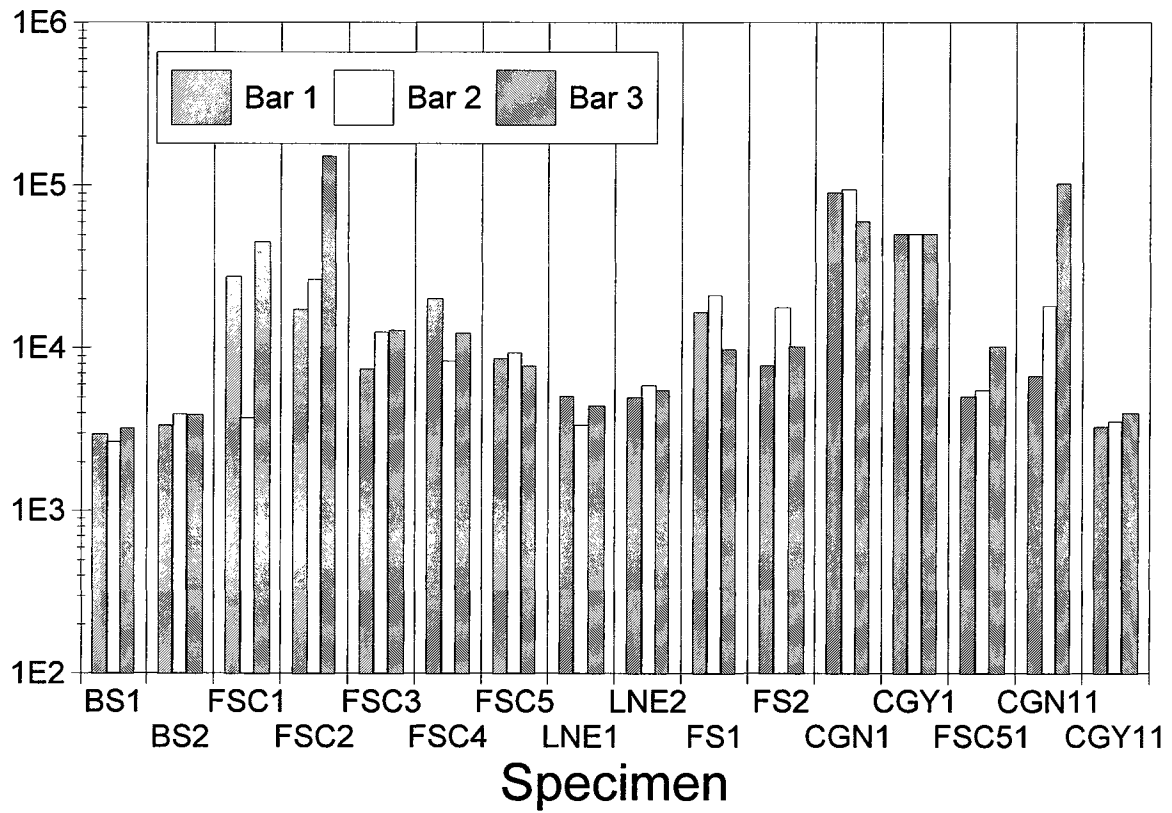
Figure 39. AC Impedance at 97.4 Hz - Large Scale Specimens, Immersed Zone, Right Leg, 2nd
Measurement Outdoors at about 96 Weeks (83-104 Weeks).
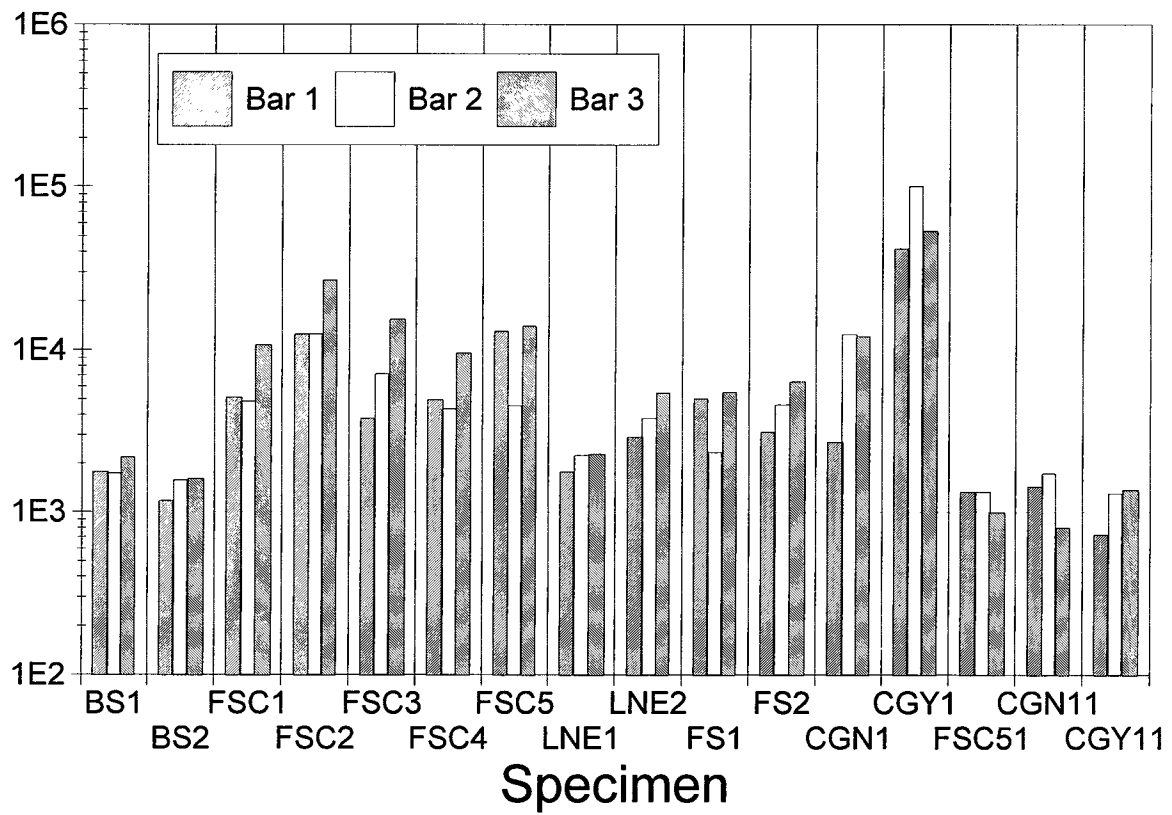
Figure 40. AC Impedance at 97.4 Hz - Large Scale Specimens, Tidal Zone, Left Leg, End of Ponding at about 76 Weeks (63-84 Weeks).
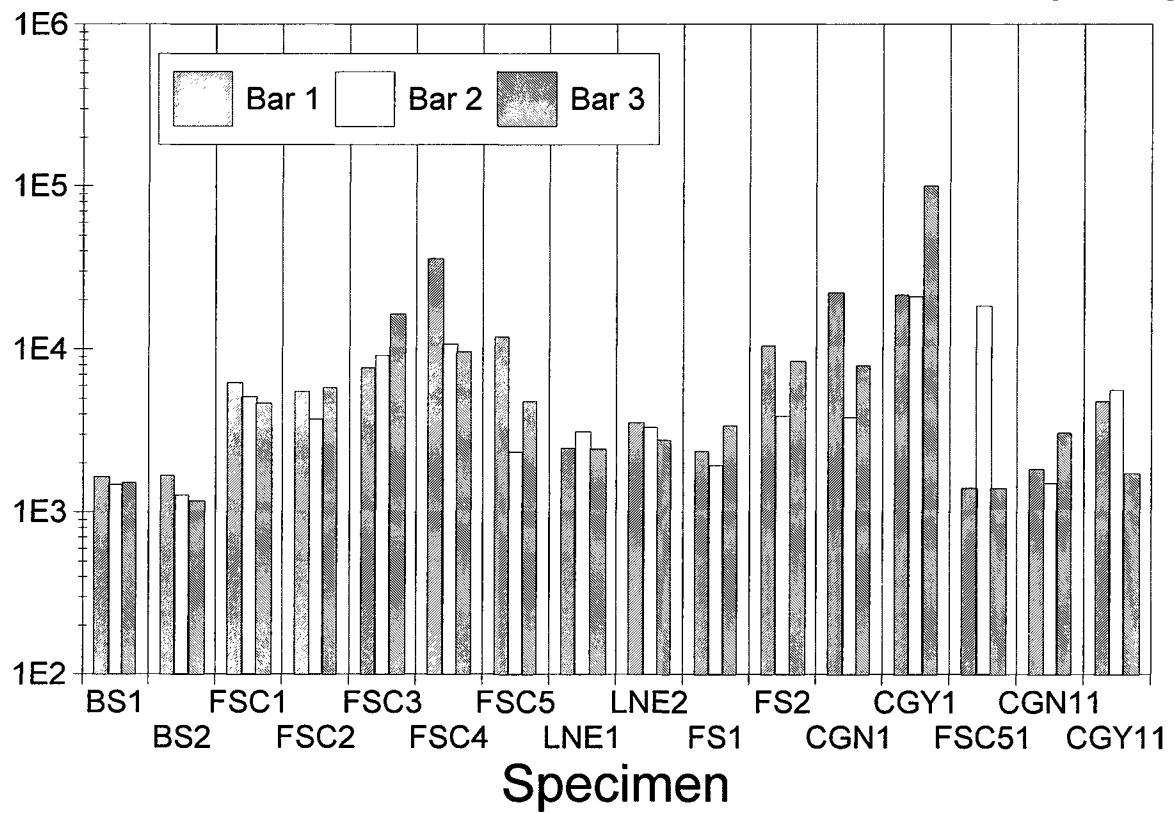
Figure 41. AC Impedance at 97.4 Hz - Large Scale Specimens, Tidal Zone, Right Leg, End of Ponding at about 76 Weeks (63-84 Weeks).
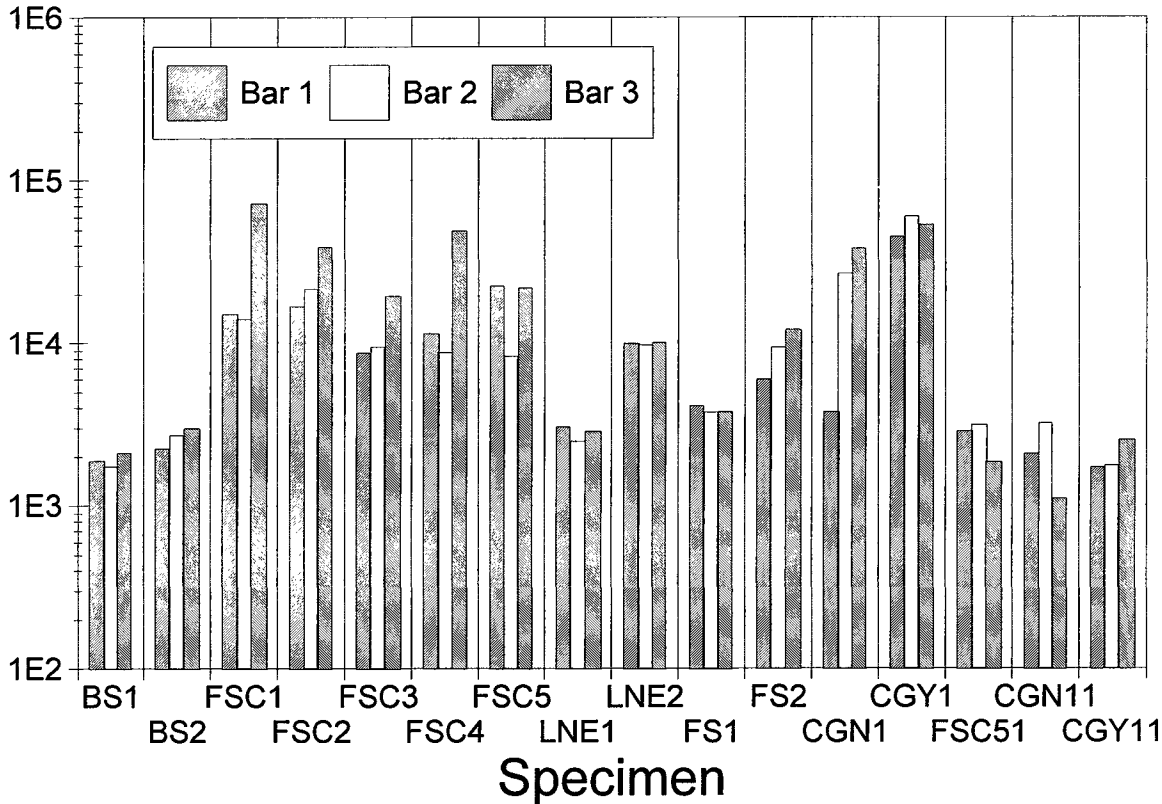
Figure 42. AC Impedance at 97.4 Hz - Large Scale Specimens, Tidal Zone, Left Leg, 1st Measurement Outdoors at about 91 Weeks (78-99 Weeks).
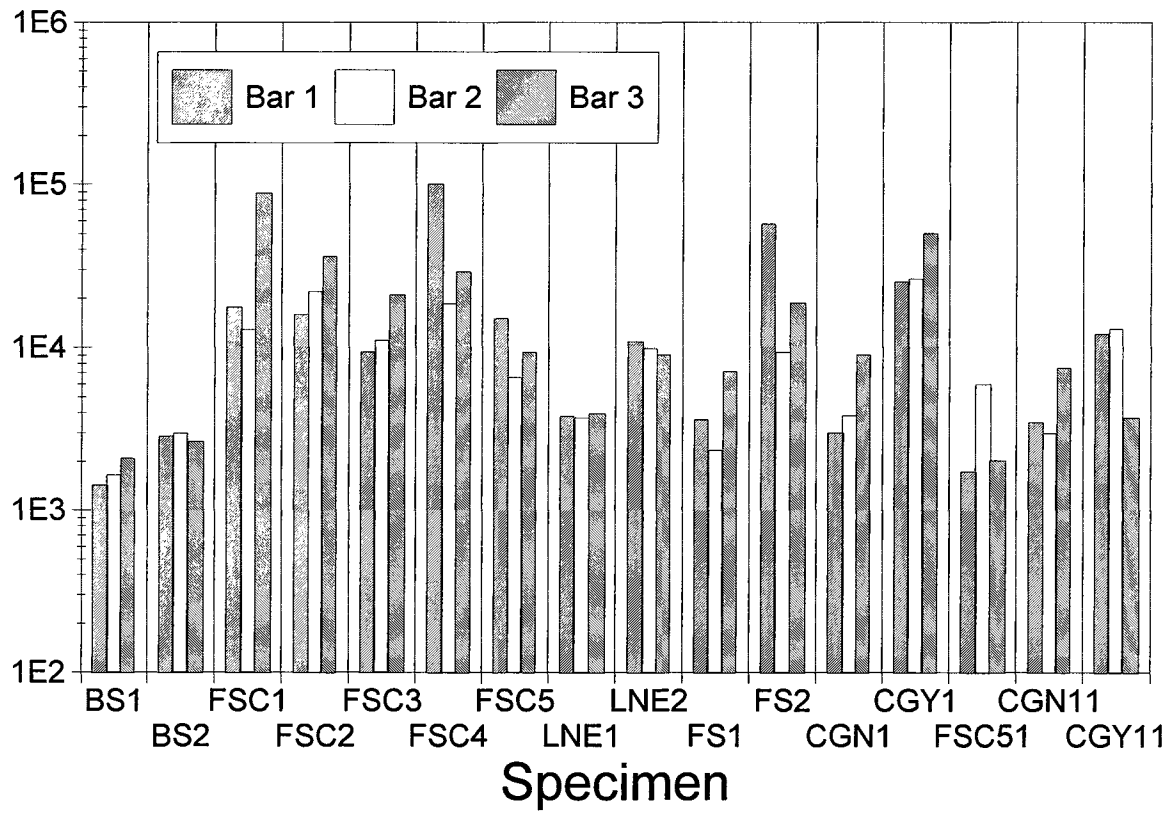
Figure 43. AC Impedance at 97.4 Hz - Large Scale Specimens, Tidal Zone, Right Leg, 1st Measurement Outdoors at about 91 Weeks (78-99 Weeks).
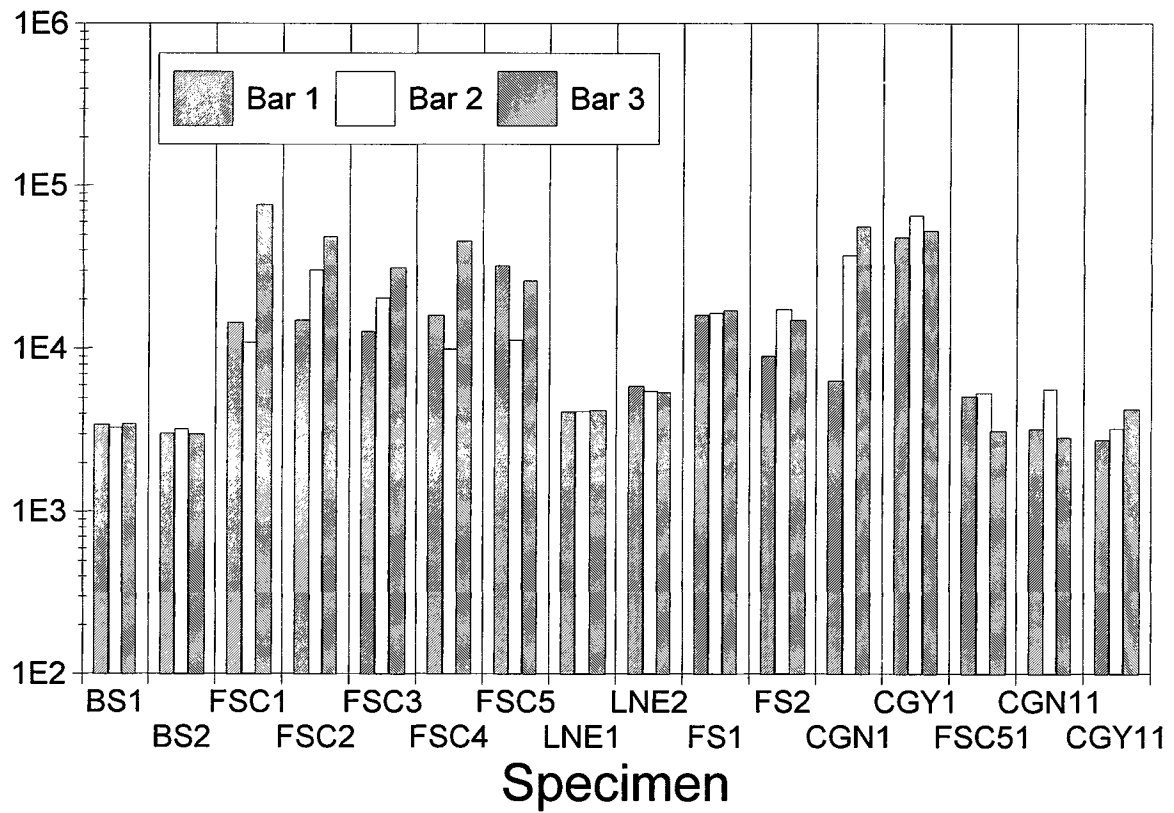
Figure 44.  AC Impedance at 97.4 Hz - Large Scale Specimens, Tidal Zone, Left Leg, 2nd
Measurement Outdoors at about 96 Weeks (83-104 Weeks).
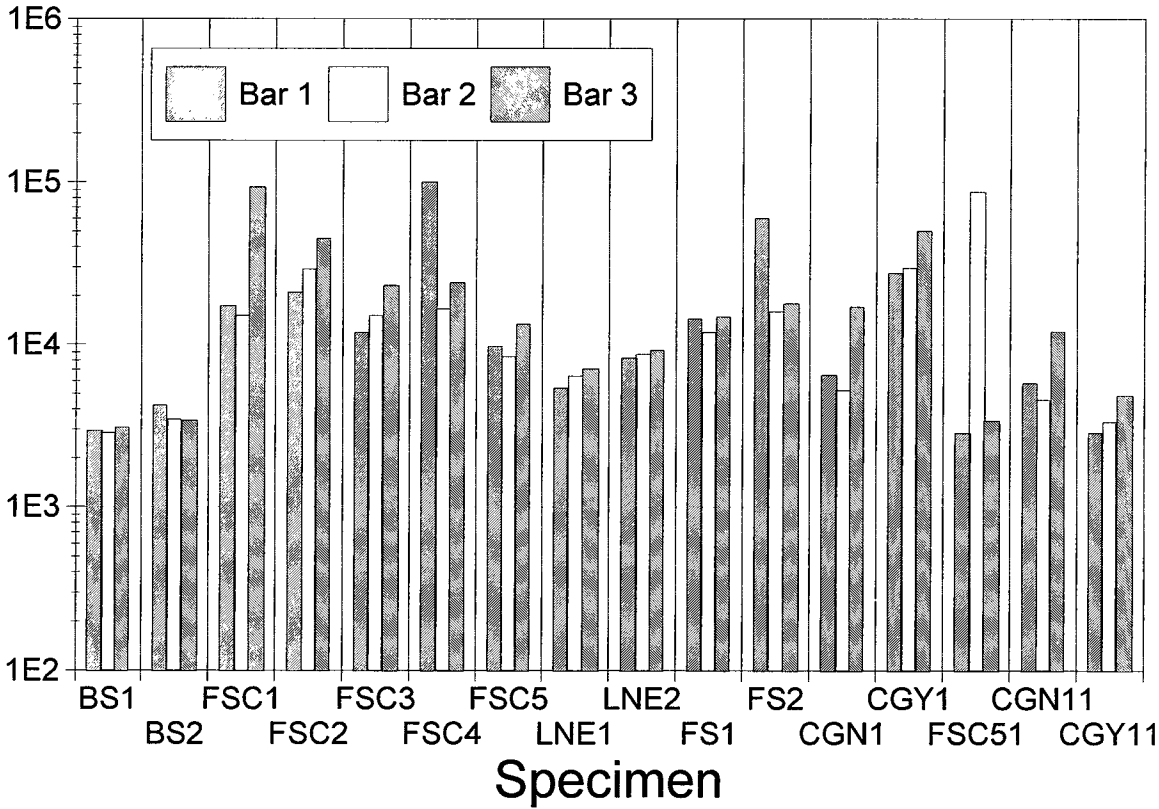
Figure 45. AC Impedance at 97.4 Hz - Large Scale Specimens, Tidal Zone, Right Leg, 2nd Measurement Outdoors at about 96 Weeks (83-104 Weeks).
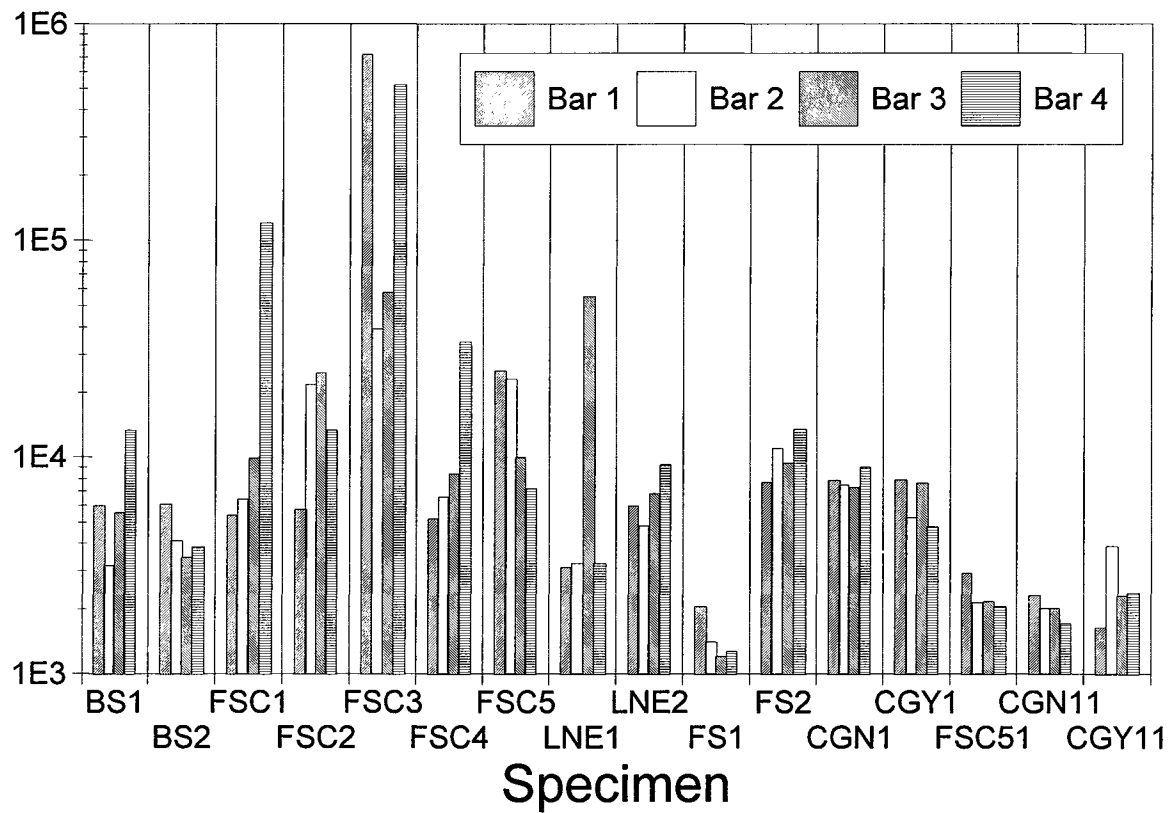
Figure 46. AC Impedance at 97.4 Hz - Large Scale Specimens, Vertical Zone, Left Leg, 1st Measurement Outdoors at about 91 Weeks (78-99 Weeks).
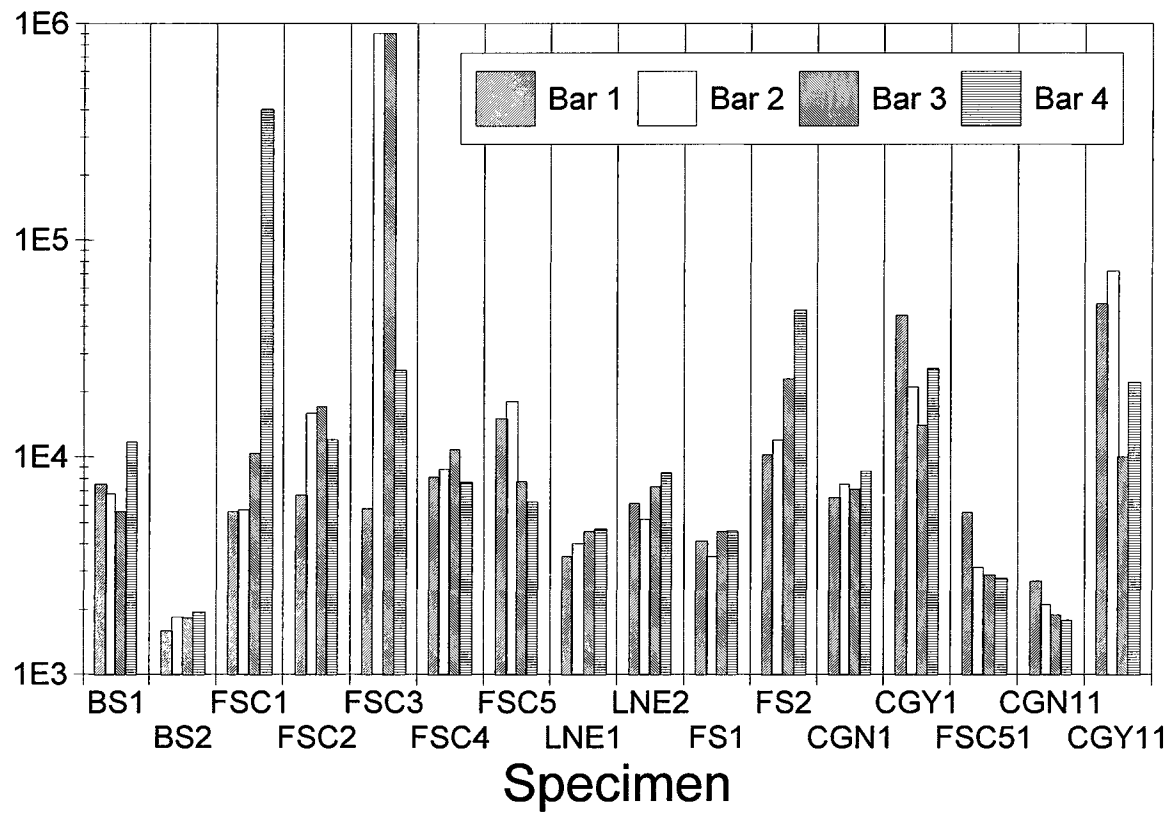
Figure 47. AC Impedance at 97.4 Hz - Large Scale Specimens, Vertical Zone, Right Leg, 1st Measurement Outdoors at about 91 Weeks (78-99 Weeks).
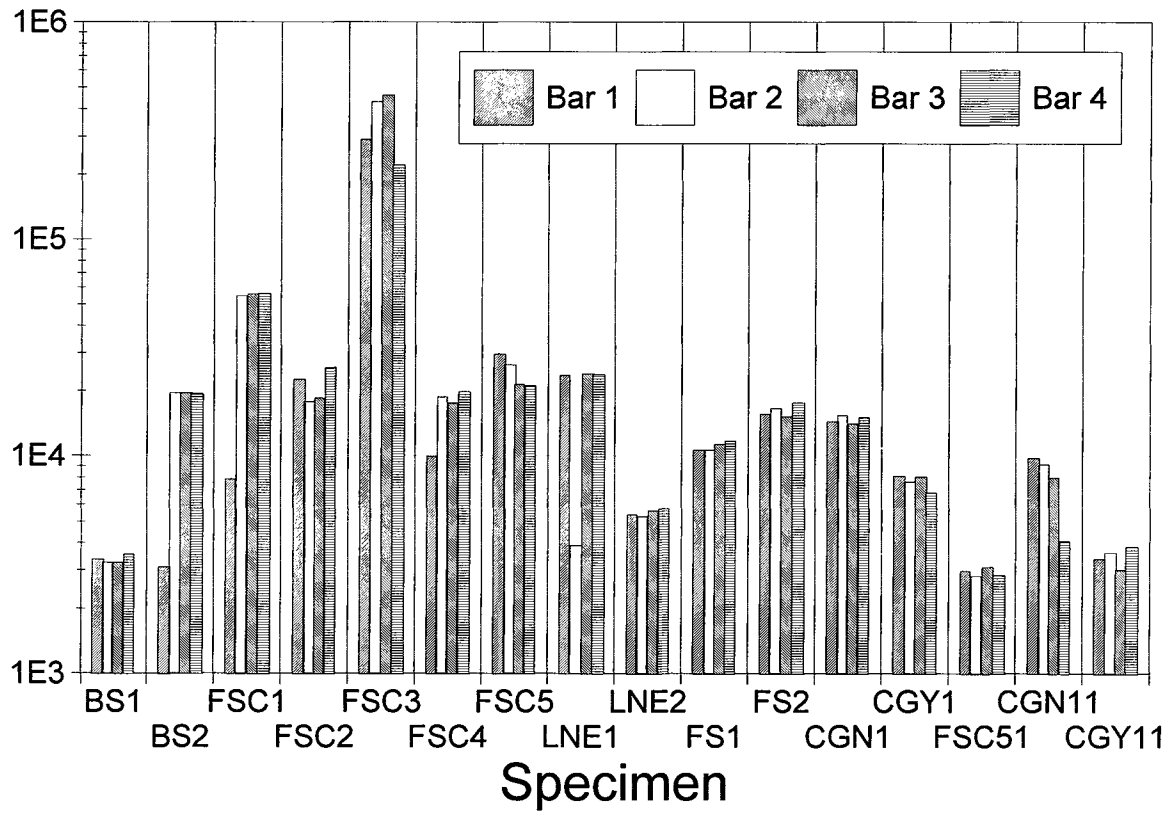
Figure 48. AC Impedance at 97.4 Hz - Large Scale Specimens, Vertical Zone, Left Leg, 2nd Measurement Outdoors at about 96 Weeks (83-104 Weeks).
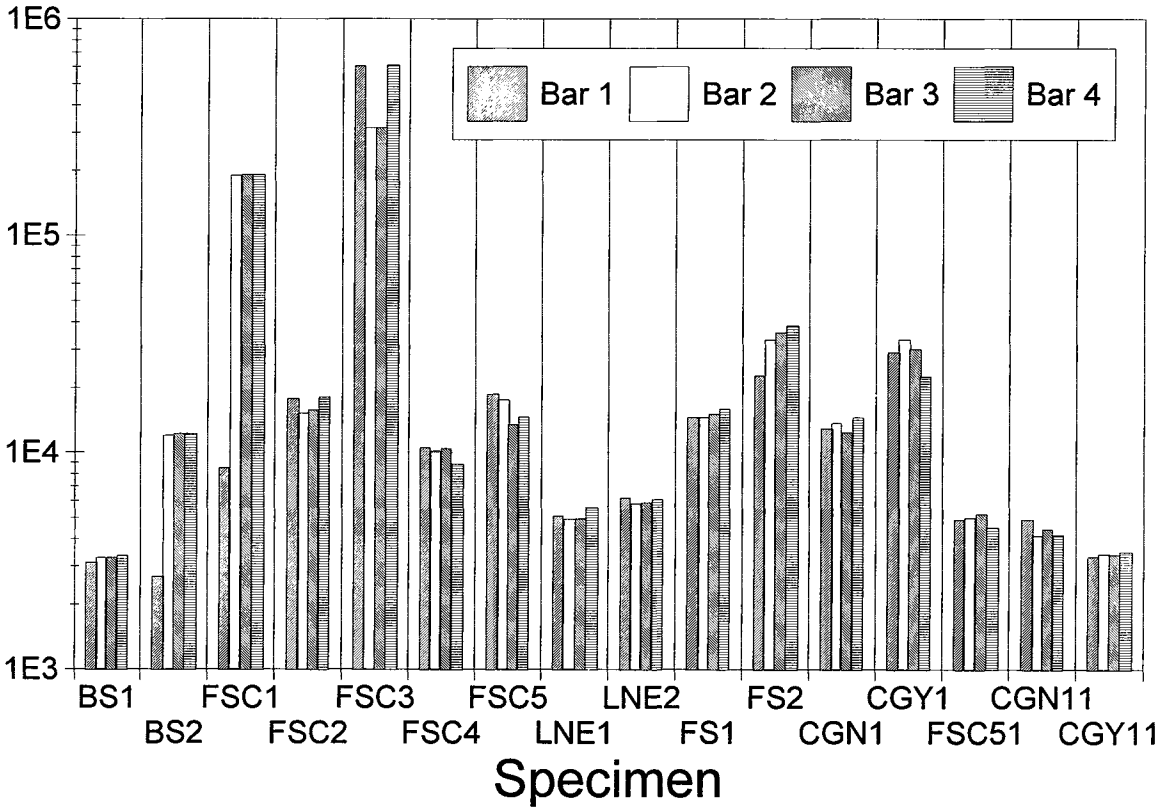
Figure 49. AC Impedance at 97.4 Hz - Large Scale Specimens, Vertical Zone, Right Leg, 2nd Measurement Outdoors at about 96 Weeks (83-104 Weeks).
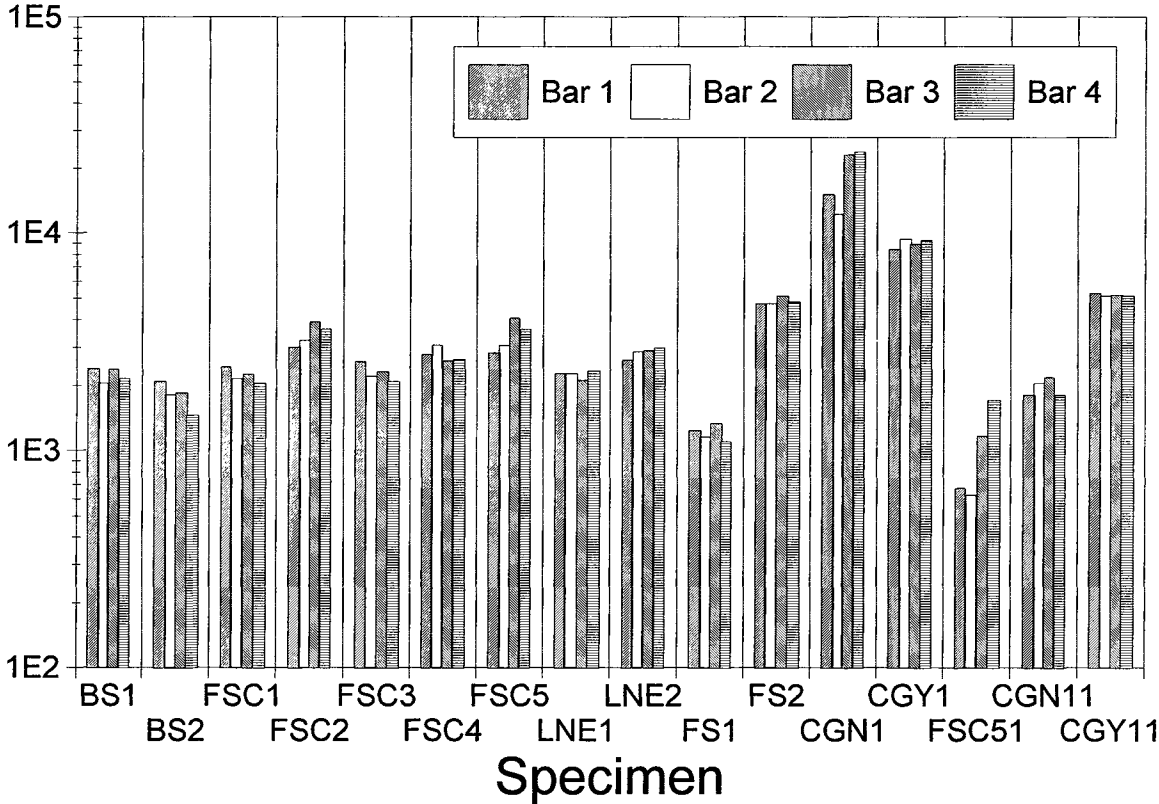
Figure 50. AC Impedance at 97.4 Hz - Large Scale Specimens, Horizontal Zone, 1st Measurement Outdoors at about 91 Weeks (78-99 Weeks).
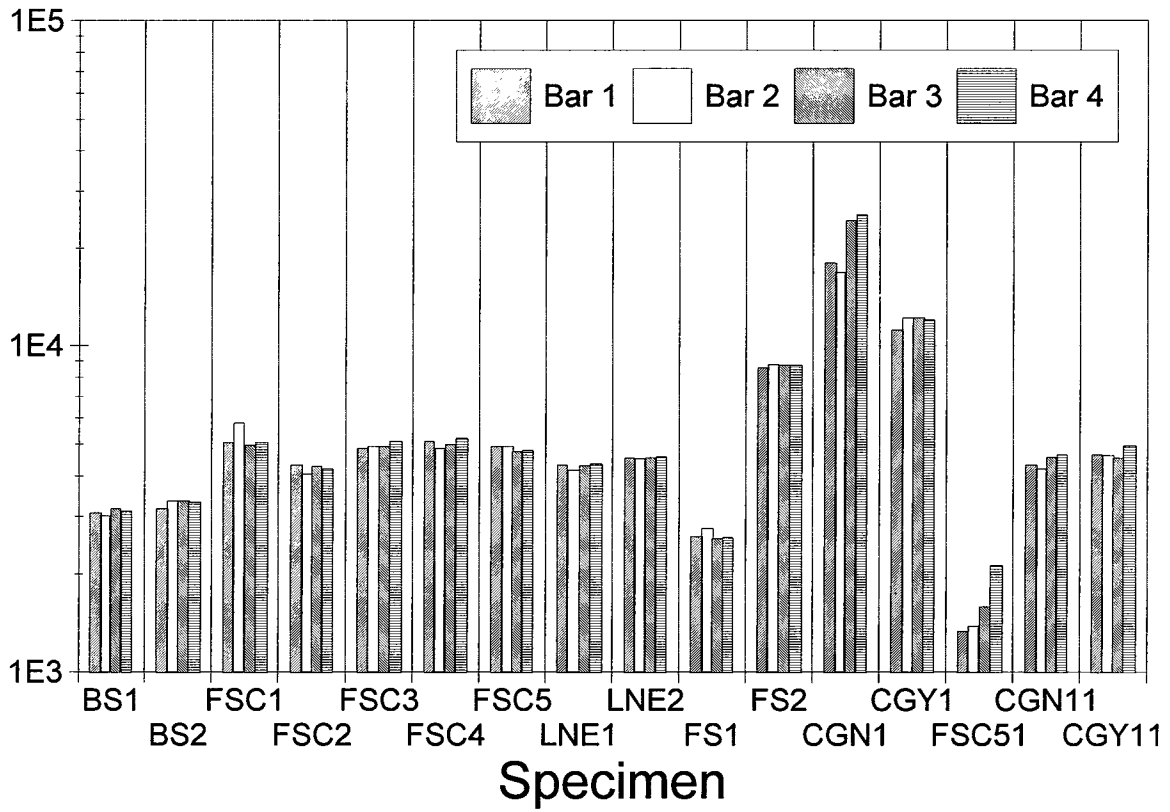
Figure 51. AC Impedance at 97.4 Hz - Large Scale Specimens, Horizontal Zone, 2nd
Measurement Outdoors at about 96 Weeks (83-104 Weeks).

# Chloride Concentrations: Horizontal Zone A4 Concrete, 6 % NaCl

Chloride Concentration (kg/m^3)
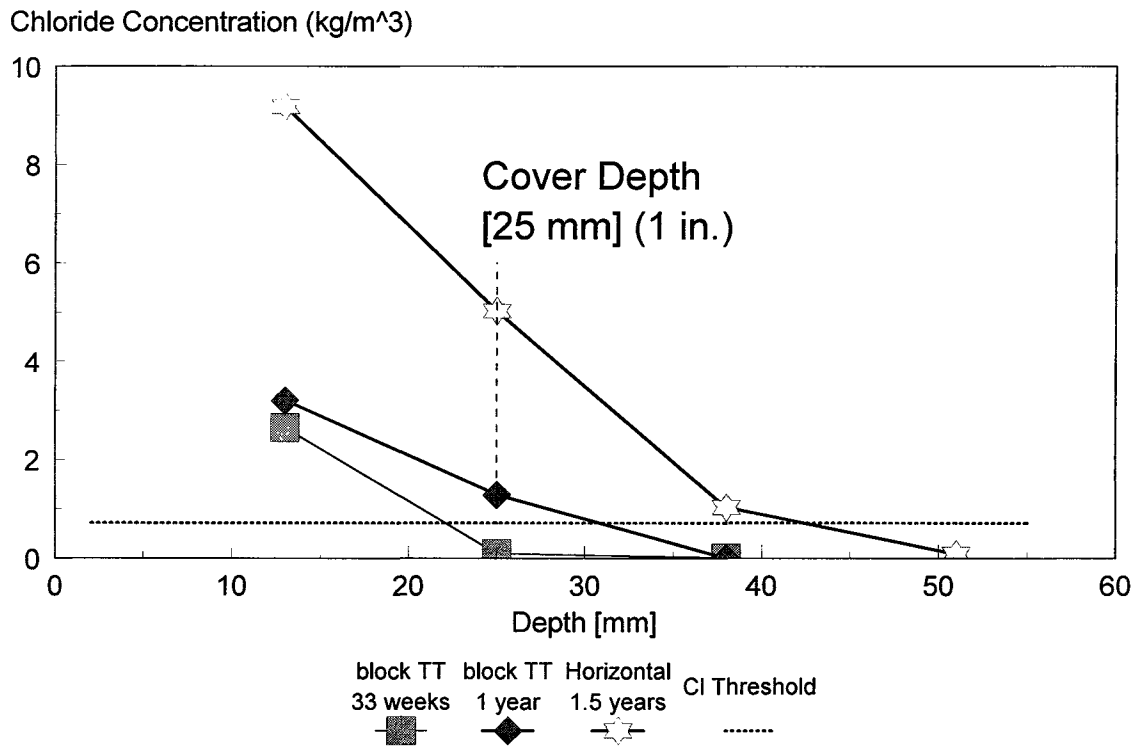


Figure 52. Chloride Concentrations, Horizontal Zone, A4 Concrete, 6% NaCl Solution.

# Chloride Concentrations: Vertical Zone A4 concrete, 6 % NaCl

**Chloride Concentration (kg/m^3)**



Cover Depth
[25 mm] (1 in.)

block TT 33 weeks   block TT 1 year   Vertical 1.5 years   Cl Threshold
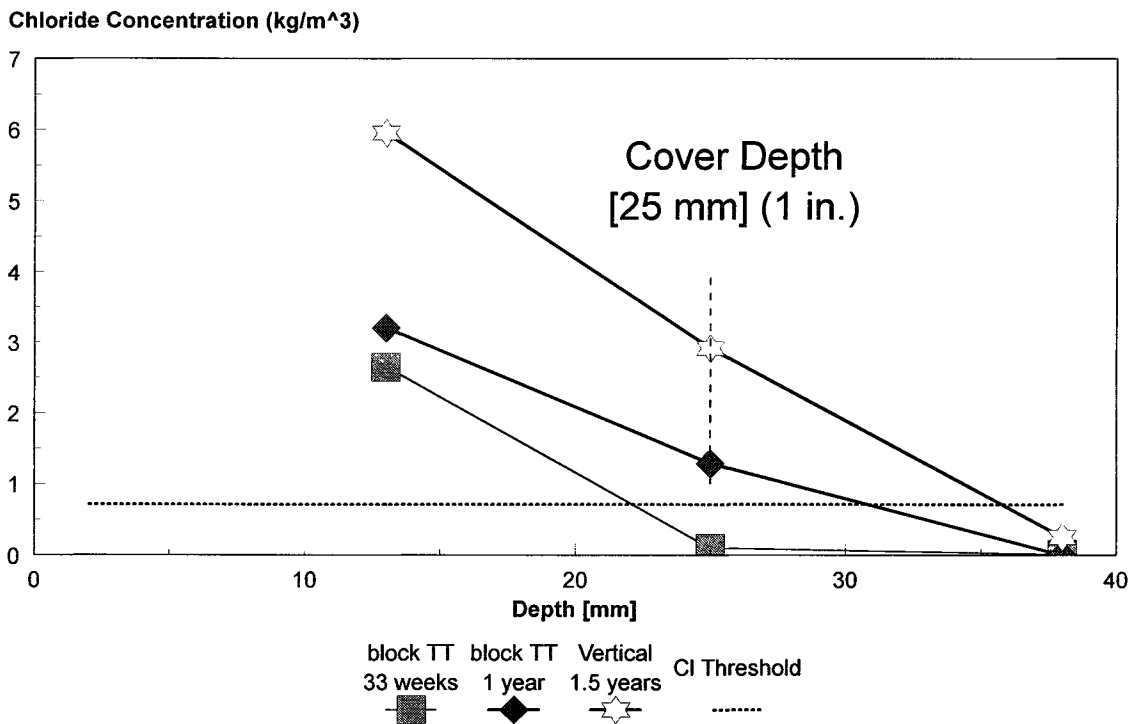
Figure 53. Chloride Concentrations, Vertical Zone, A4 Concrete, 6% NaCl Solution.

# Chloride Concentrations: Tidal Zone
## A4 concrete, 6 % NaCl
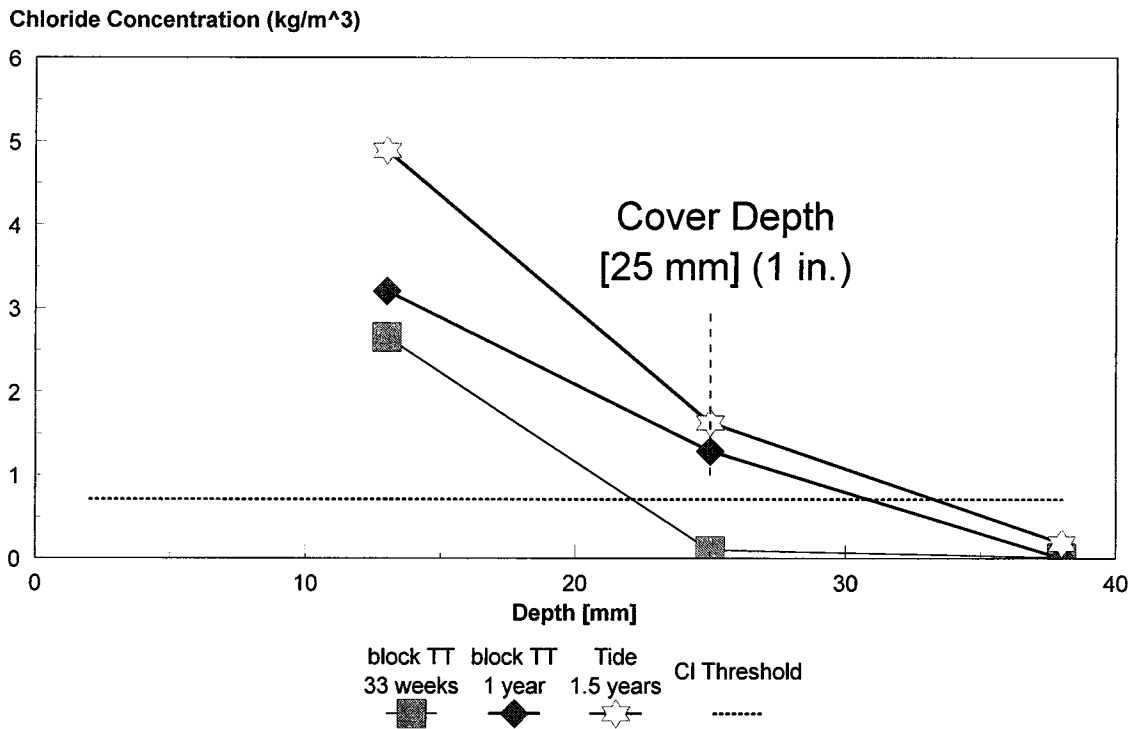


Figure 54. Chloride Concentrations, Tidal Zone, A4 Concrete, 6% NaCl Solution.

# Chloride Concentrations: Immersed Zone
## A4 concrete, 6 % NaCl

**Chloride Concentration (kg/m^3)**
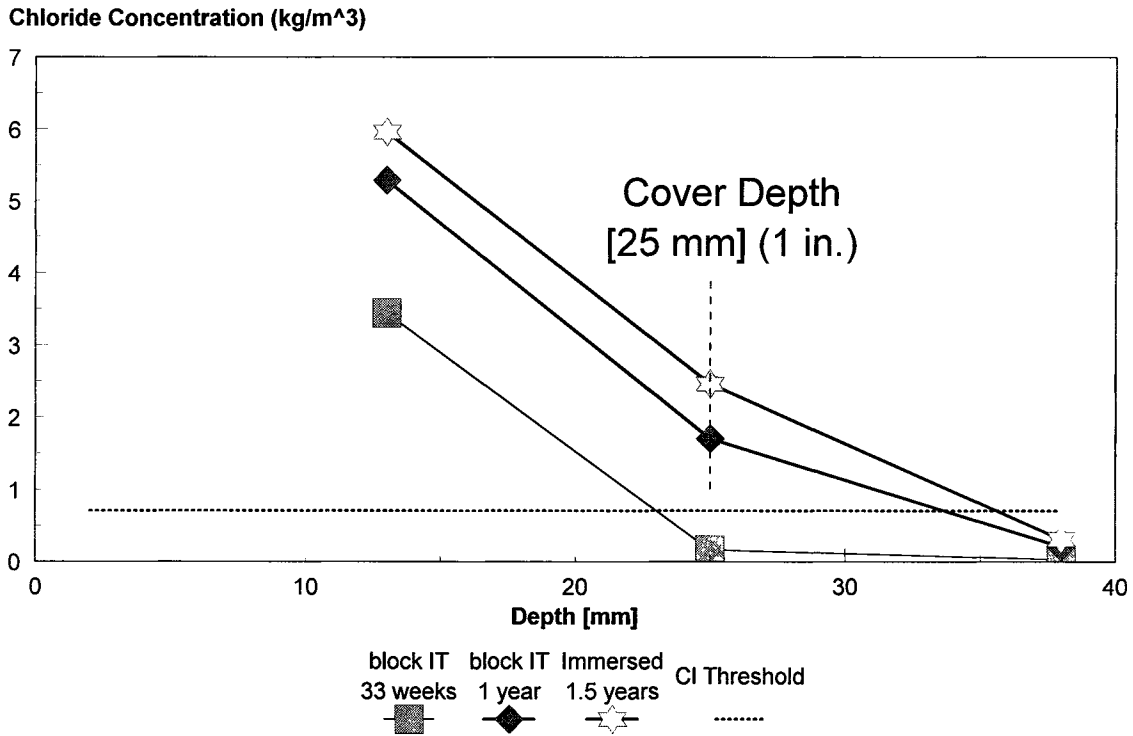


Figure 55. Chloride Concentrations, Immersed Zone, A4 Concrete, 6% NaCl Solution.

# Chloride Concentrations: Horizontal Zone
# A4 Concrete, 3 % NaCl
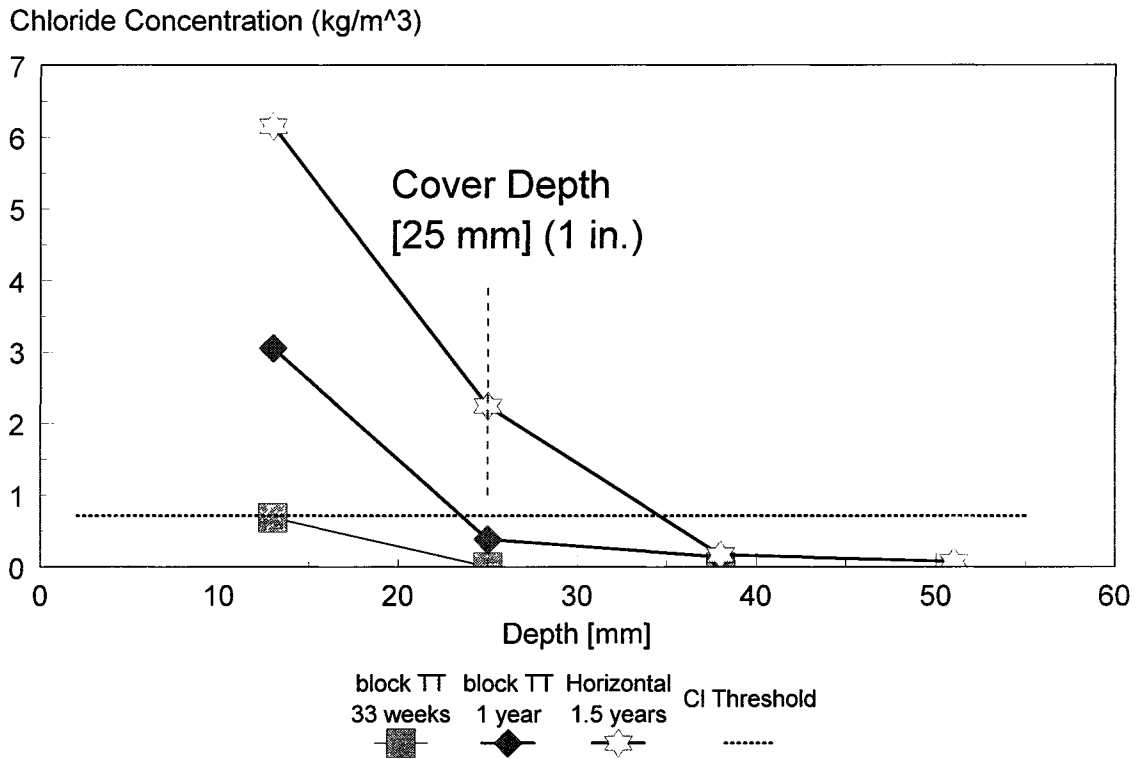


Figure 56. Chloride Concentrations, Horizontal Zone, A4 Concrete, 3% NaCl Solution.

# Chloride Concentrations: Vertical Zone
# A4 concrete, 3 % NaCl

**Chloride Concentration (kg/m^3)**
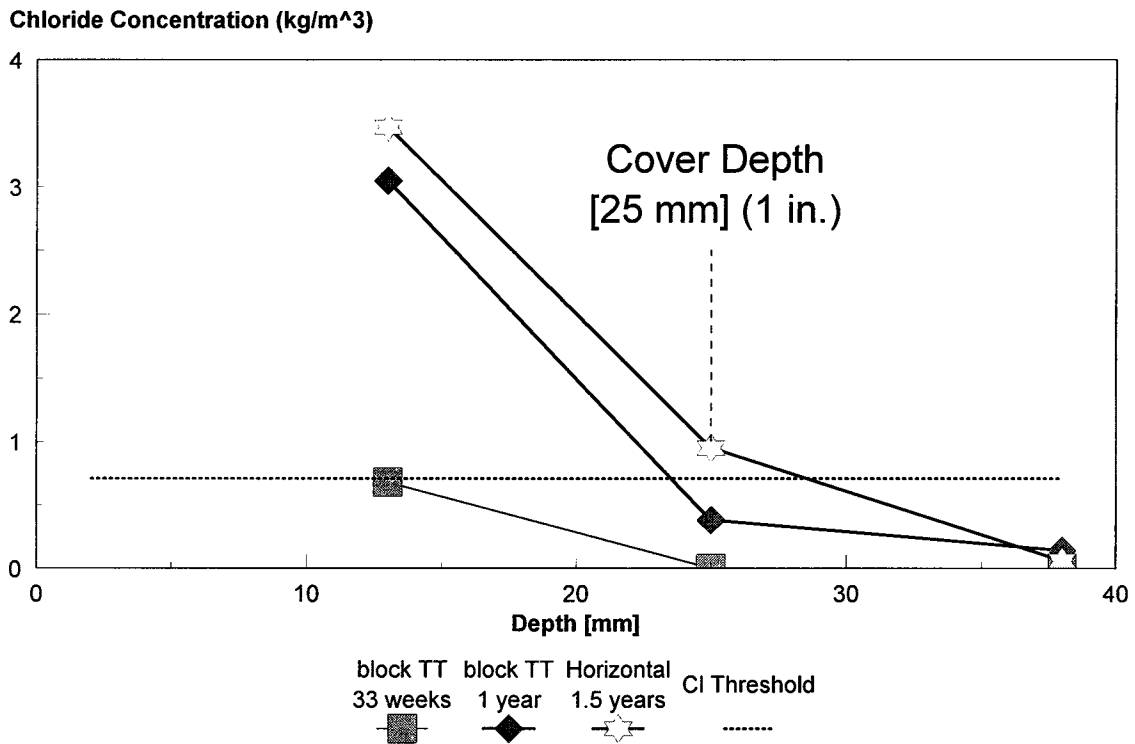


Figure 57. Chloride Concentrations, Vertical Zone, A4 Concrete, 3% NaCl Solution.

# Chloride Concentrations: Tidal Zone
# A4 concrete, 3 % NaCl

**Chloride Concentration (kg/m^3)**
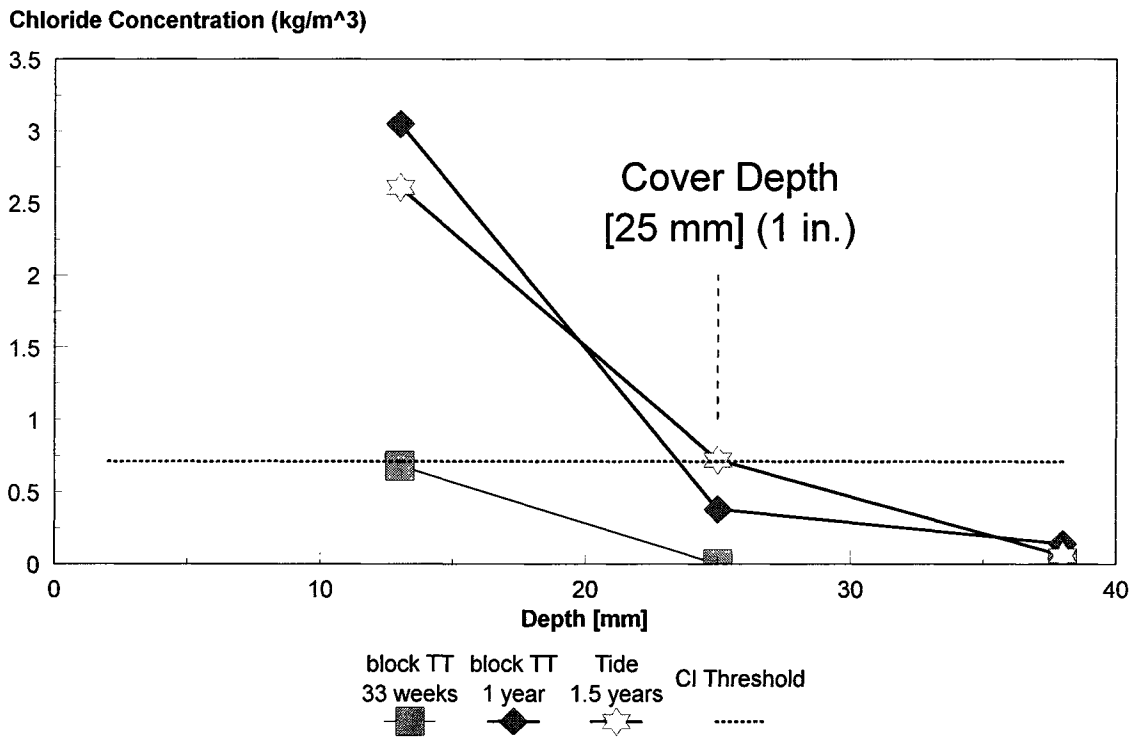


Figure 58. Chloride Concentrations, Tidal Zone, A4 Concrete, 3% NaCl Solution.

# Chloride Concentrations: Immersed Zone
## A4 concrete, 3 % NaCl

**Chloride Concentration (kg/m^3)**
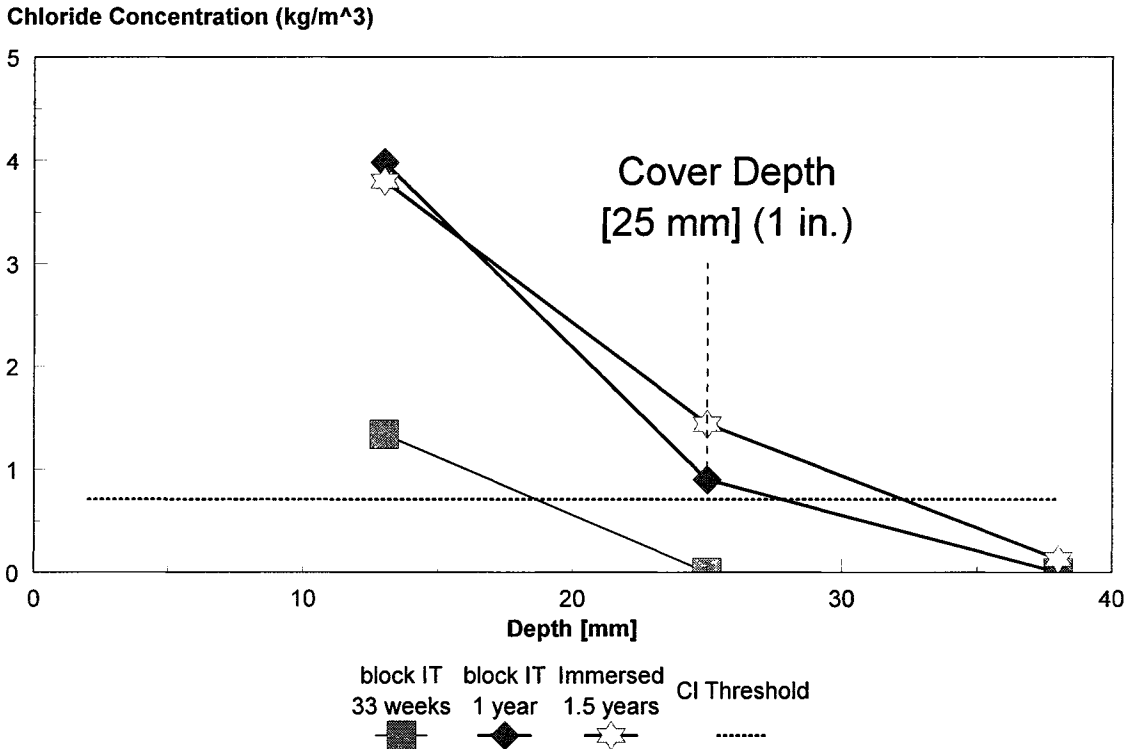


Figure 59. Chloride Concentrations, Immersed Zone, A4 Concrete, 3% NaCl Solution.

# Chloride Concentrations: Horizontal Zone Concrete with w/c > 0.7, 6 % NaCl

Chloride Concentration (kg/m^3)
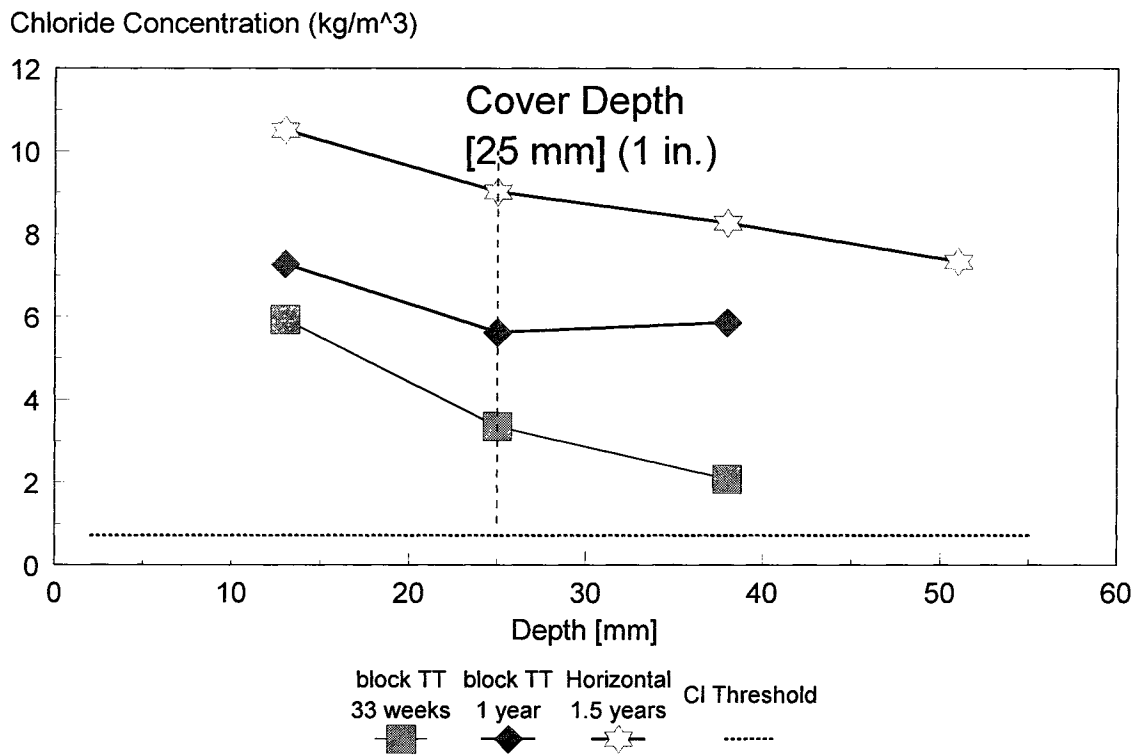


Figure 60. Chloride Concentrations, Horizontal Zone, Concrete with w/c > 0.7, 6% NaCl Solution.

# Chloride Concentrations: Vertical Zone Concrete with w/c > 0.7, 6 % NaCl

**Chloride Concentration (kg/m^3)**
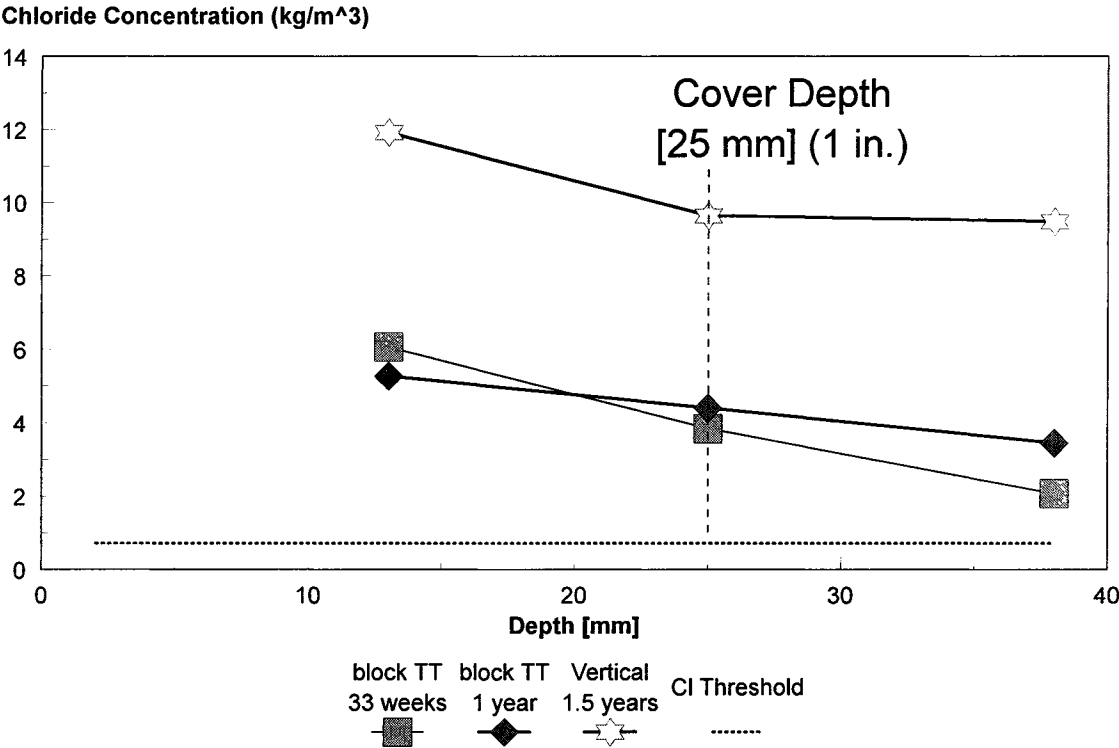


Figure 61. Chloride Concentrations, Vertical Zone, Concrete with w/c > 0.7, 6% NaCl Solution.

# Chloride Concentrations: Tidal Zone Concrete with w/c > 0.7, 6 % NaCl

**Chloride Concentration (kg/m^3)**
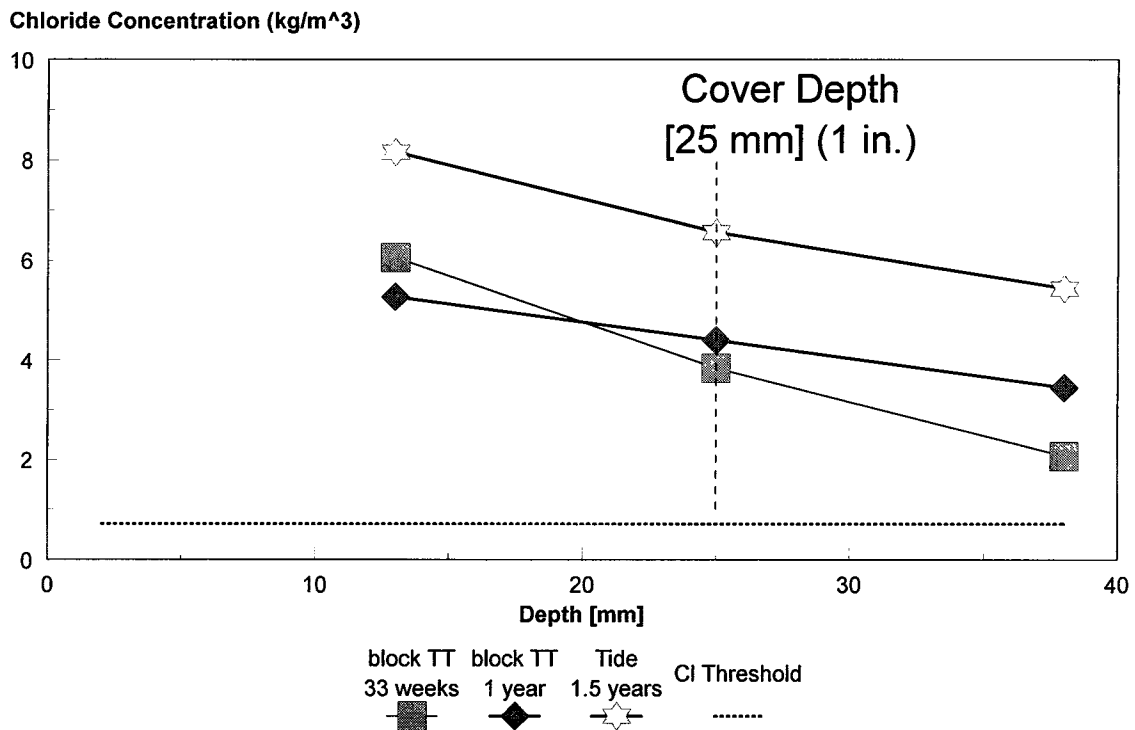


Figure 62. Chloride Concentrations, Tidal Zone, Concrete with w/c > 0.7, 6% NaCl Solution.

# Chloride Concentrations: Immersed Zone Concrete with w/c > 0.7, 6 % NaCl

**Chloride Concentration (kg/m^3)**
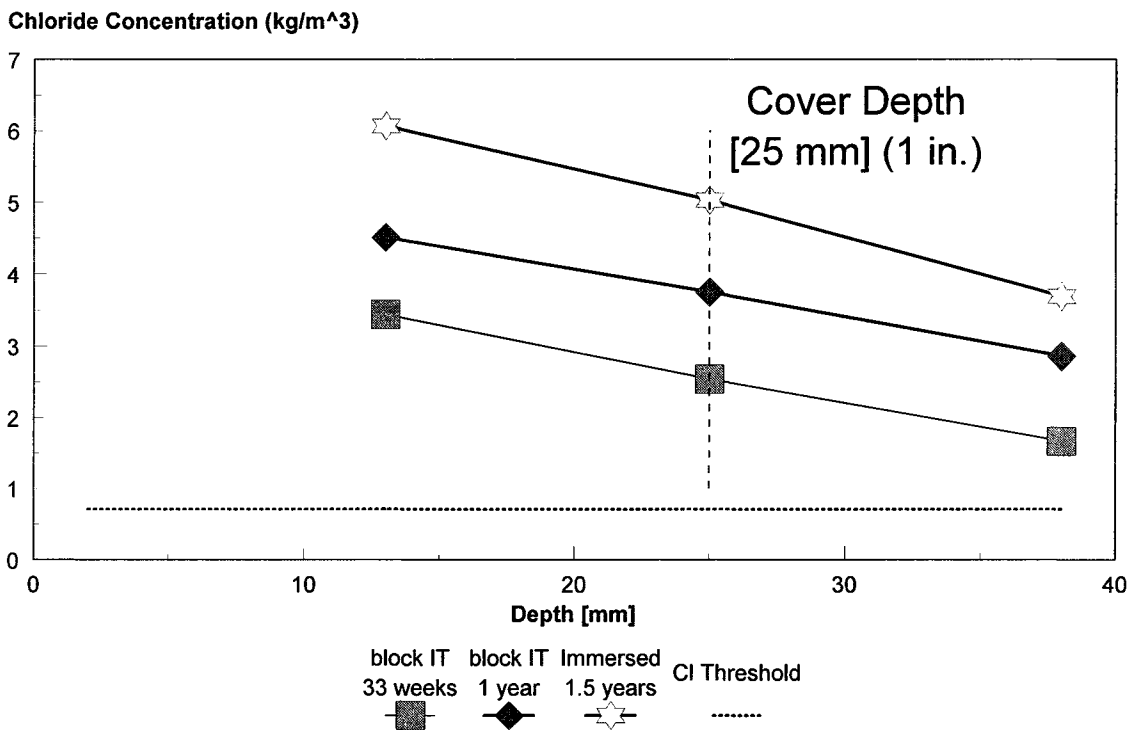


Figure 63. Chloride Concentrations, Immersed Zone, Concrete with w/c > 0.7, 6% NaCl Solution.

**Potentials: Deck**
BS-1 Specimen (Legs not Connected)
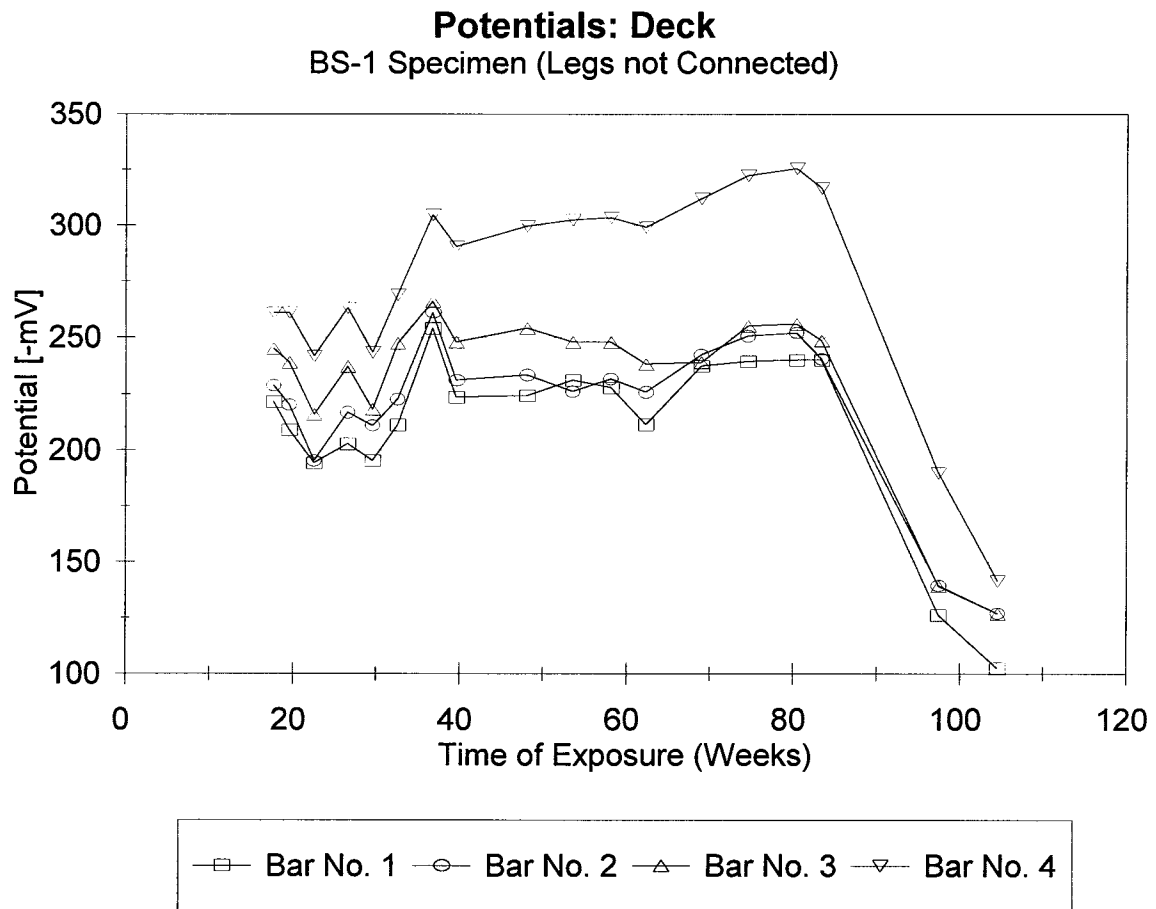
Figure 64. Corrosion Potentials in the Horizontal Zone, BS-1 Specimen (Control 1).

**Potentials: Deck**

BS-2 Specimen (Legs Connected)
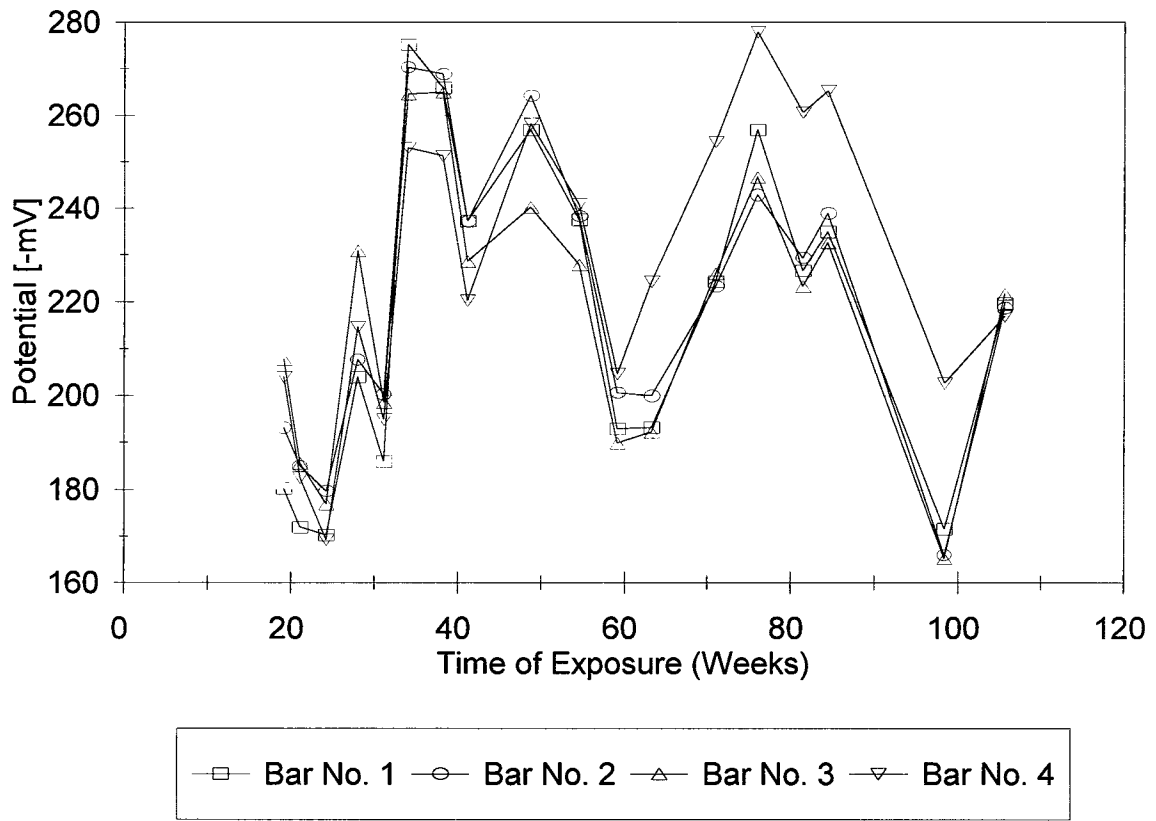
Figure 65. Corrosion Potentials in the Horizontal Zone, BS-2 Specimen (Control 2).
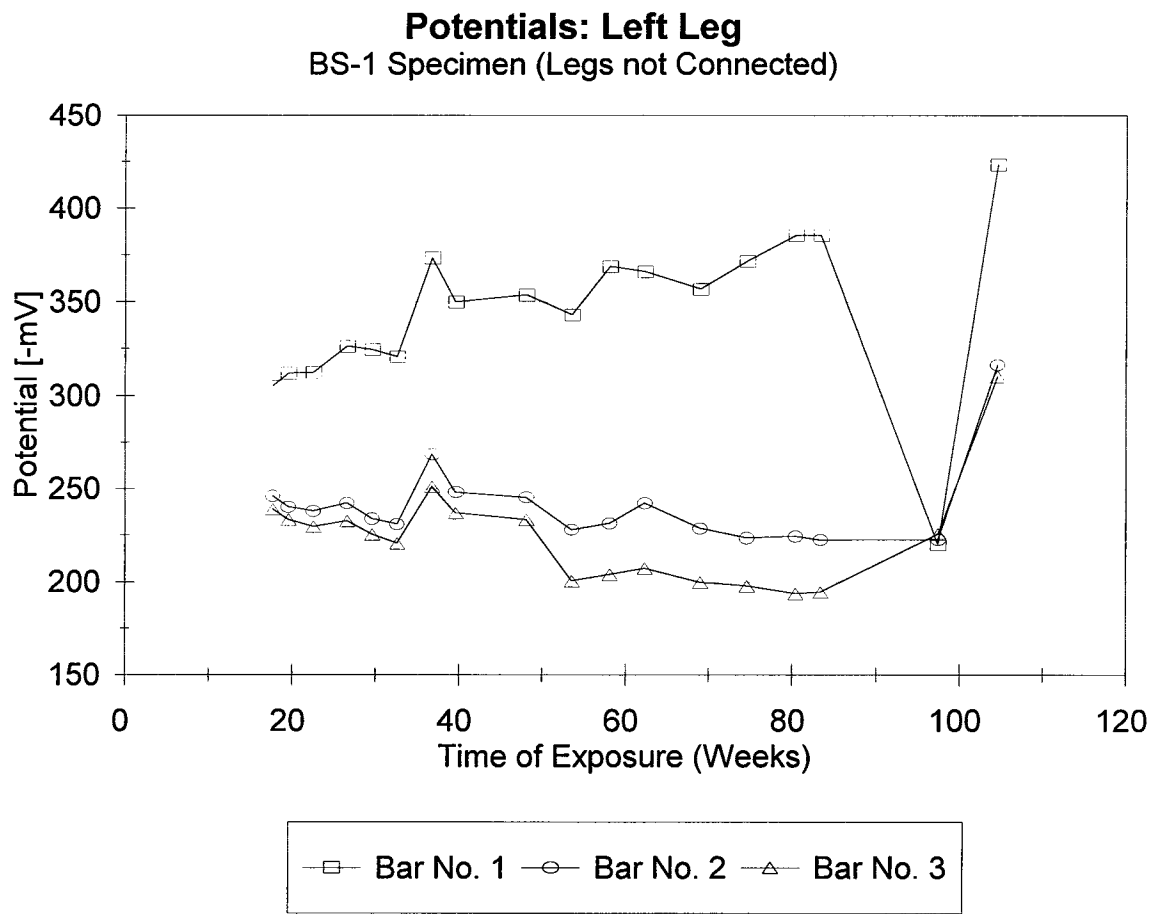
Figure 66. Corrosion Potentials in the Vertical Zone, Left Leg, BS-1 Specimen (Control 1).
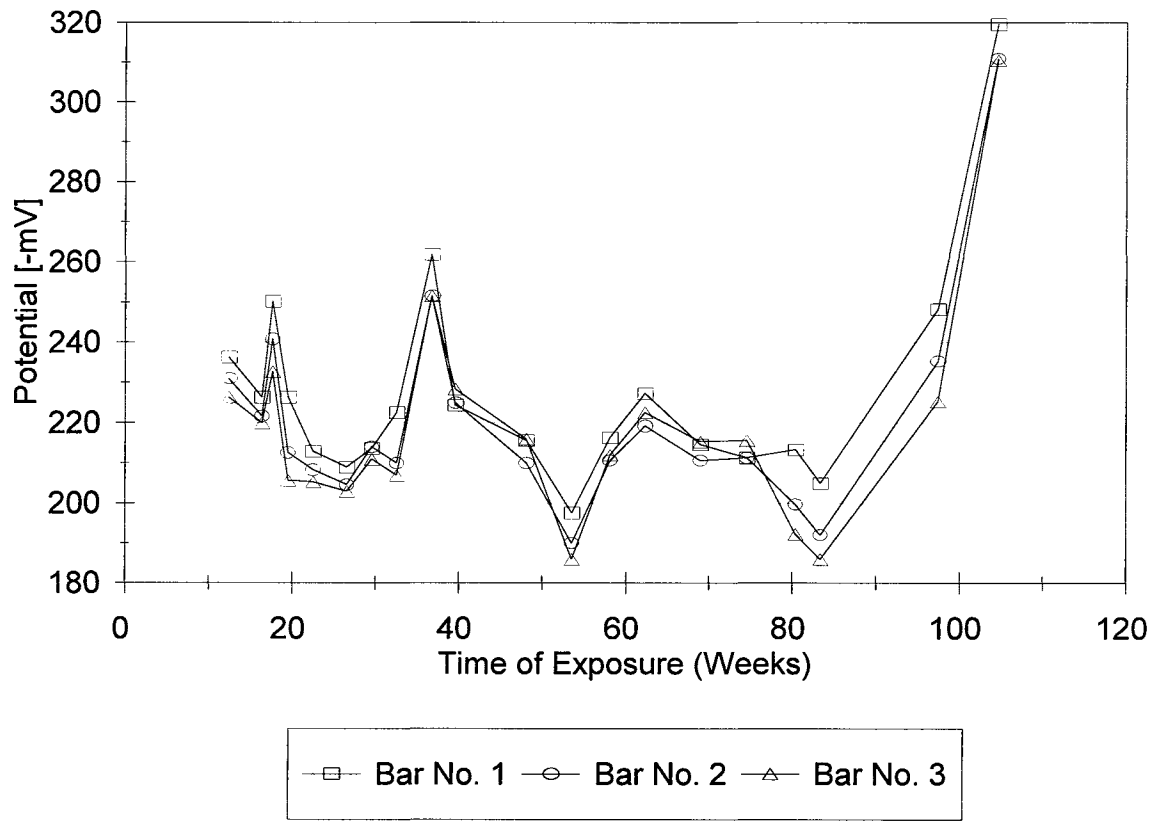
Figure 67. Corrosion Potentials in the Vertical Zone, Right Leg, BS-1 Specimen (Control 1).
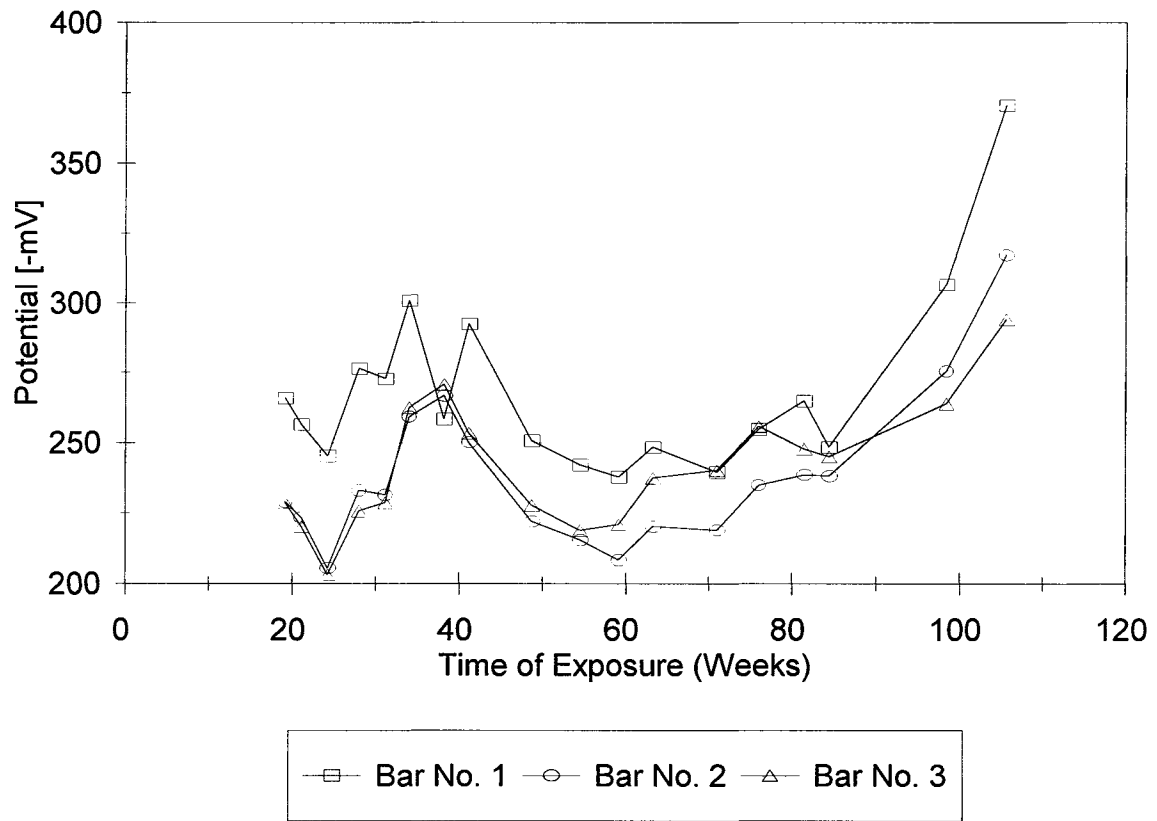
Figure 68. Corrosion Potentials in the Vertical Zone, Left Leg, BS-2 Specimen (Control 2).

**Potentials: Right Leg**

BS-2 Specimen (Legs Connected)
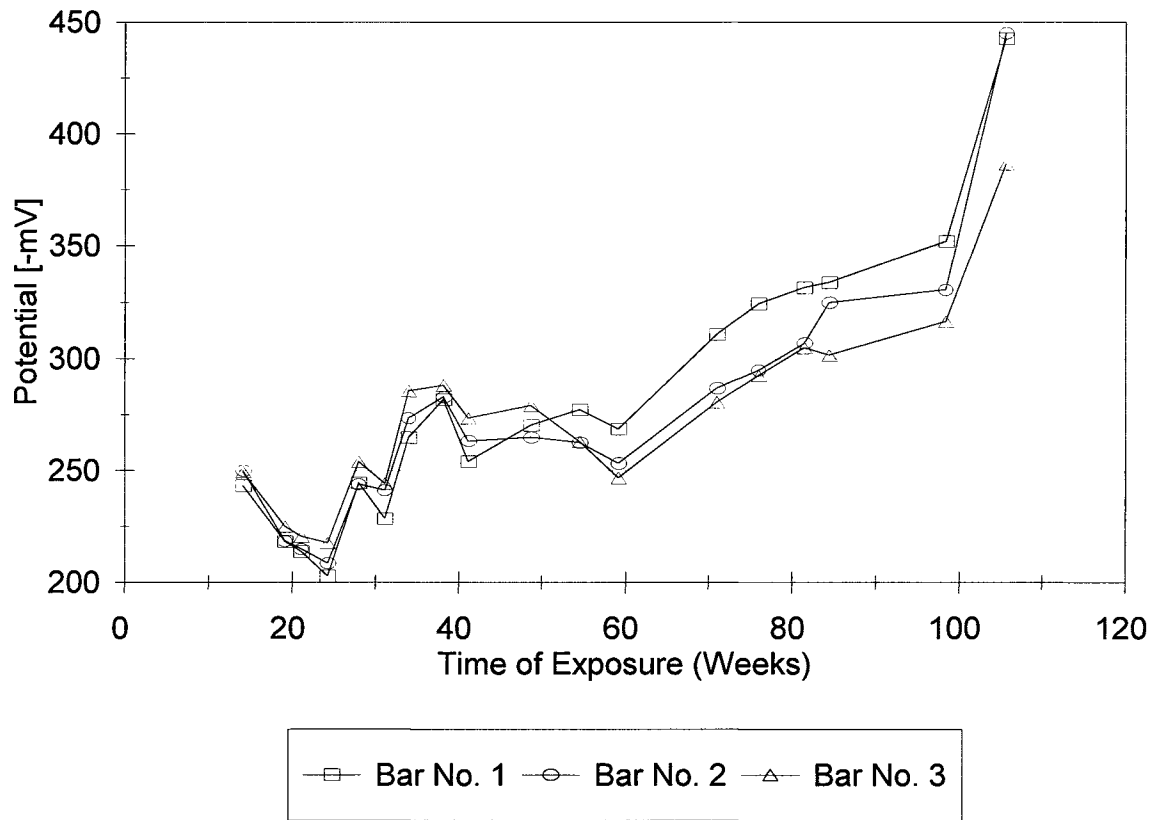
Figure 69. Corrosion Potentials in the Vertical Zone, Right Leg, BS-2 Specimen (Control 2).

**Control Specimens**

Exposure: Immersed Zone
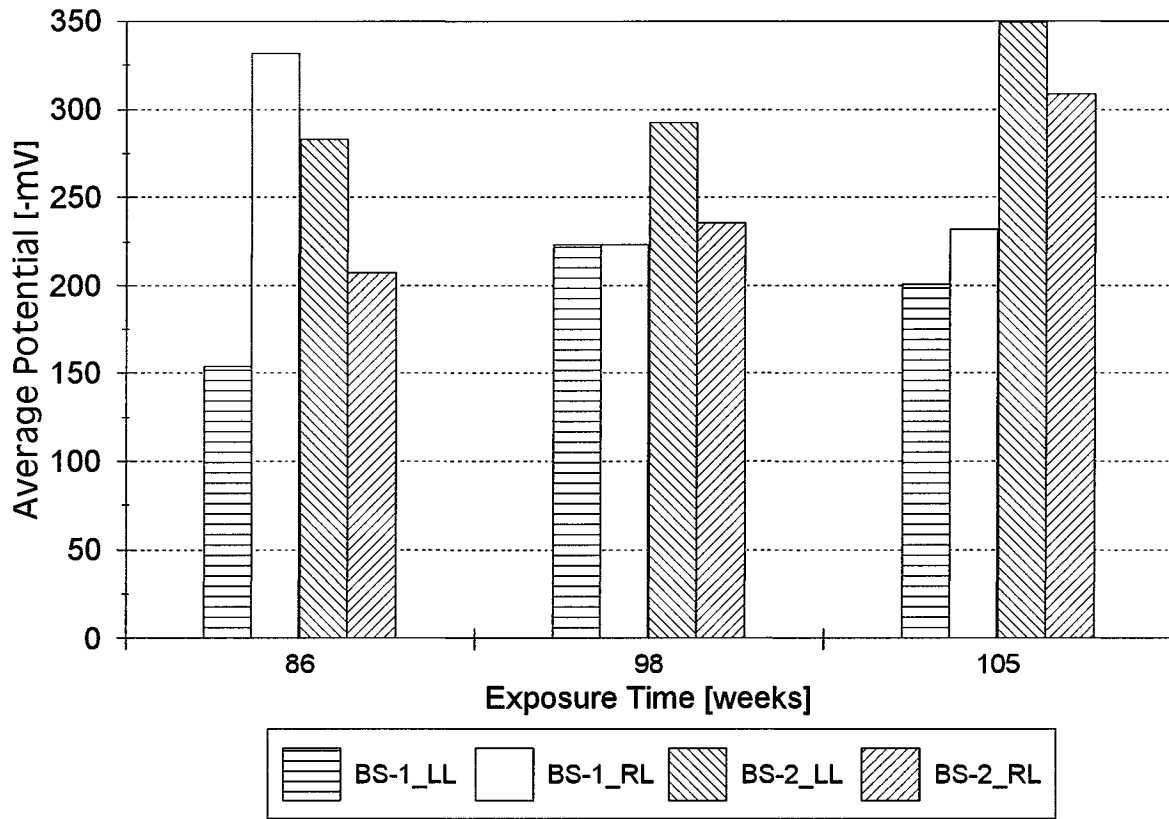
Figure 70. Corrosion Potentials in the Immersed Zone, Left and Right Legs, BS-1 and BS-2 Specimens.
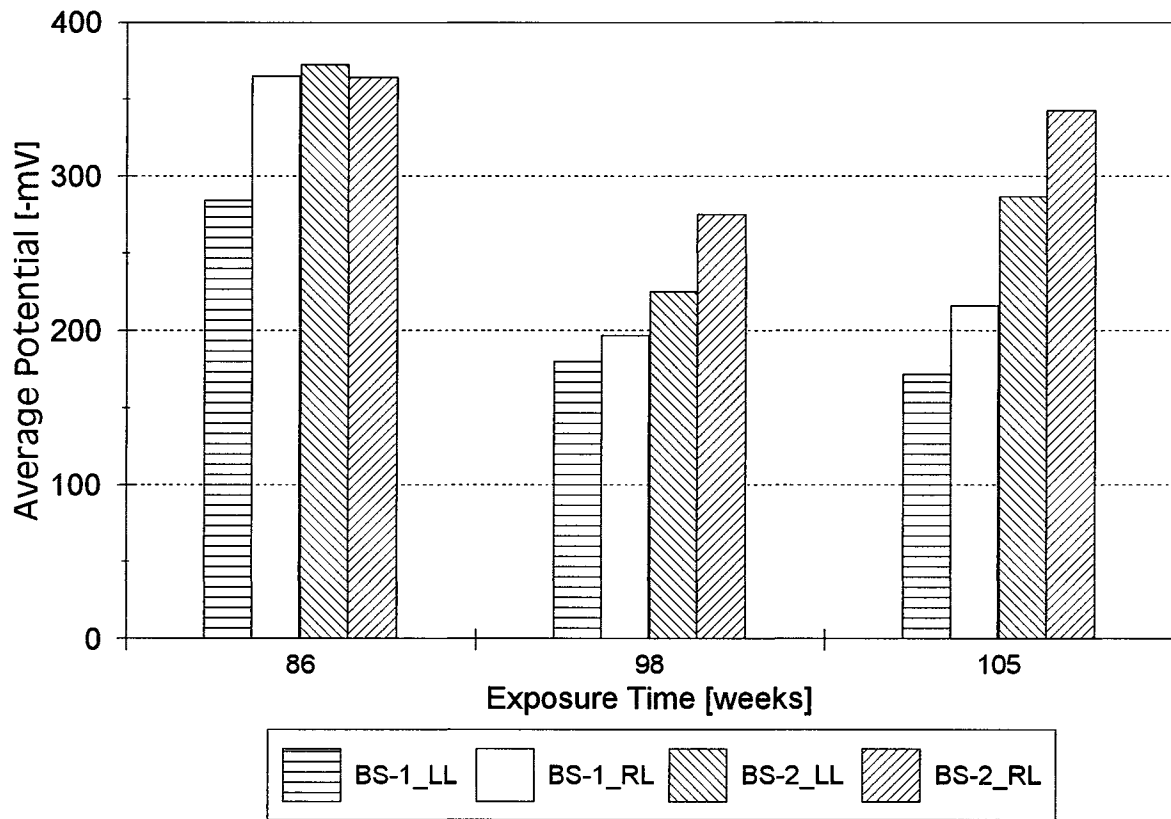
Figure 71. Corrosion Potentials in the Tidal Zone, Left and Right Legs, BS-1 and BS-2 Specimens.
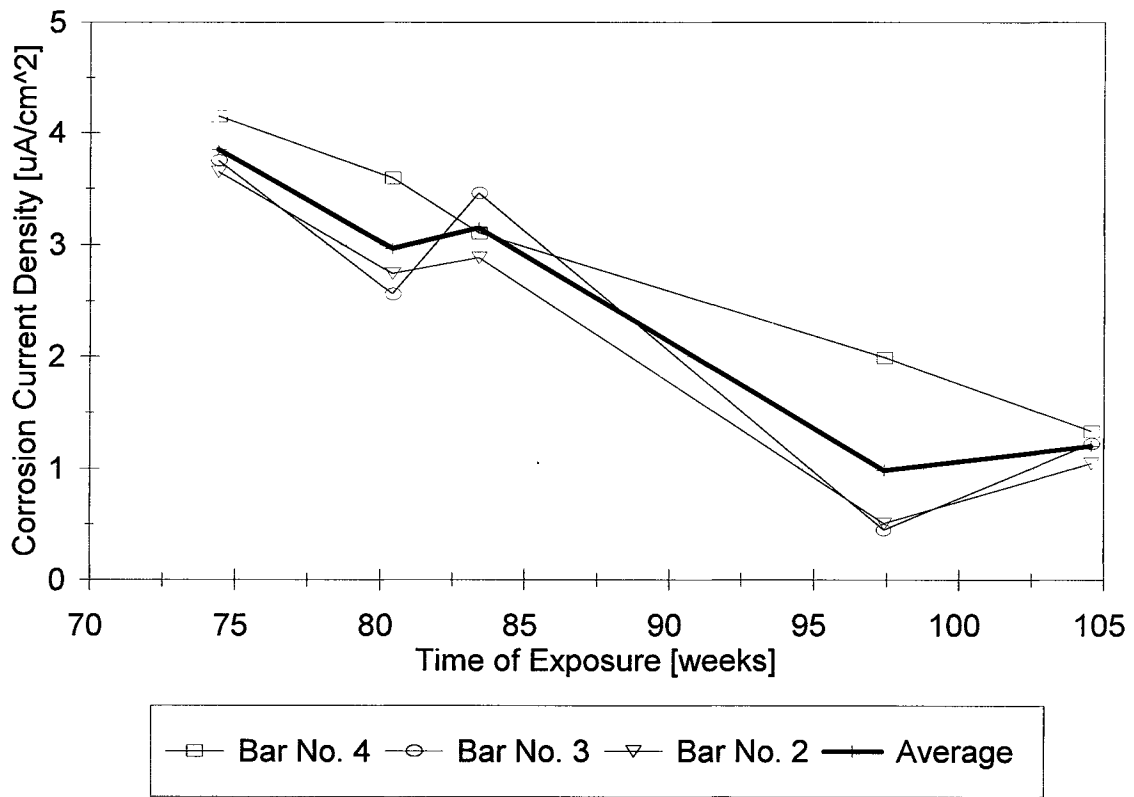
Figure 72. Corrosion Rates in the Horizontal Zone, BS-1 Specimen.
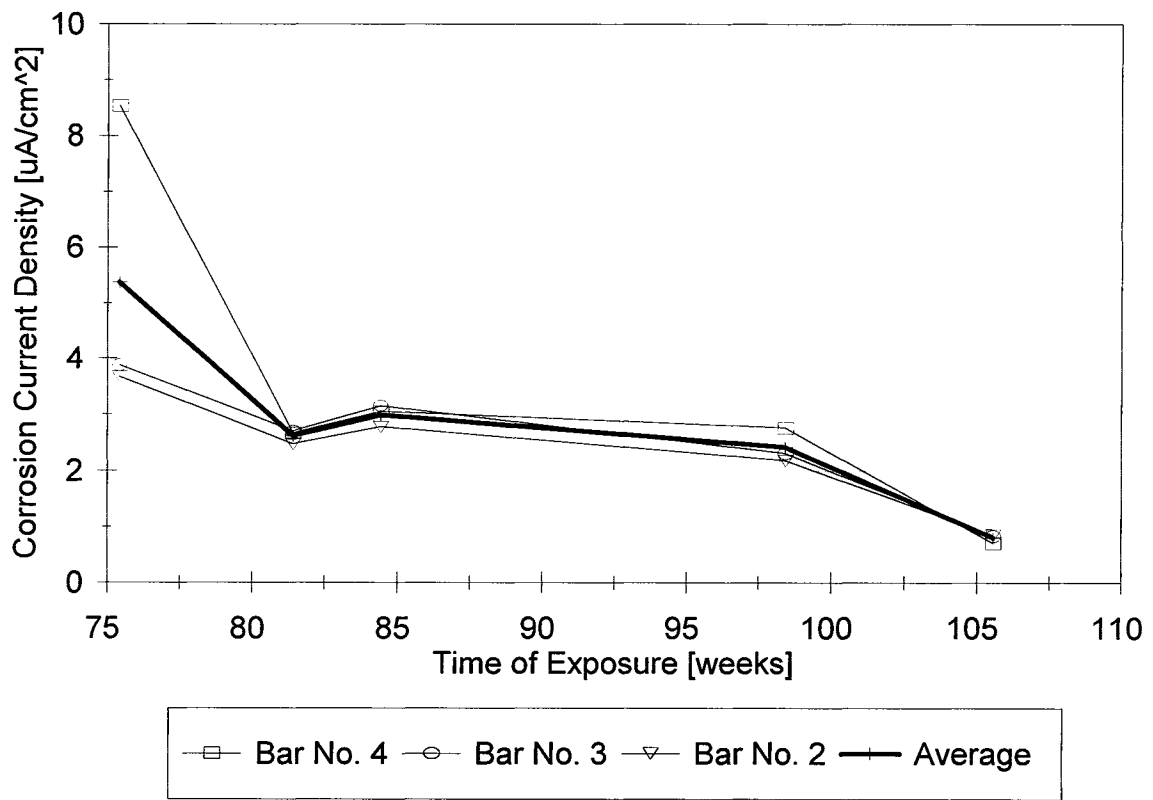
Figure 73. Corrosion Rates in the Horizontal Zone, BS-2 Specimen.

# Control 1 [BS-1]

## Vertical Zone, Right Leg
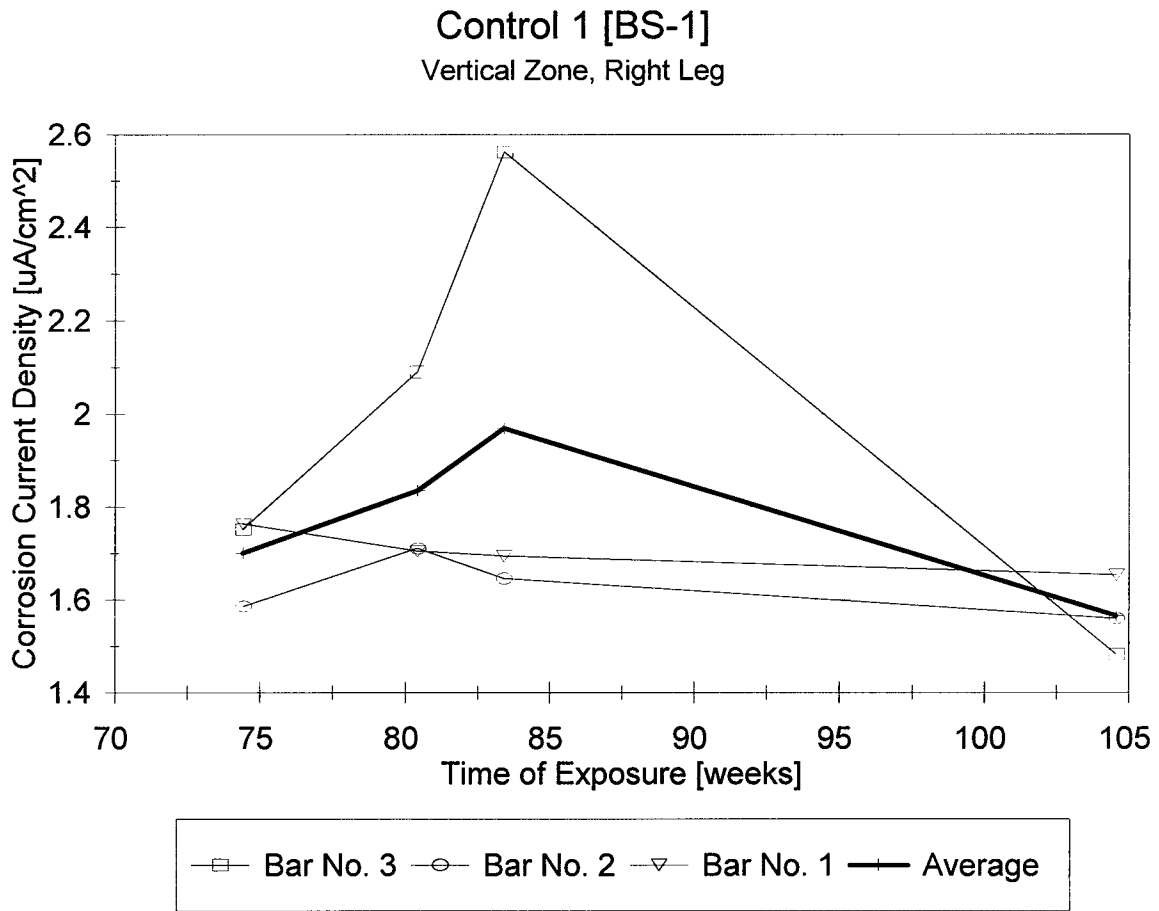


Figure 74. Corrosion Rates in the Vertical Zone, Right Leg, BS-1 Specimen.

## Control 1 [BS-1]
### Vertical Zone, Left Leg
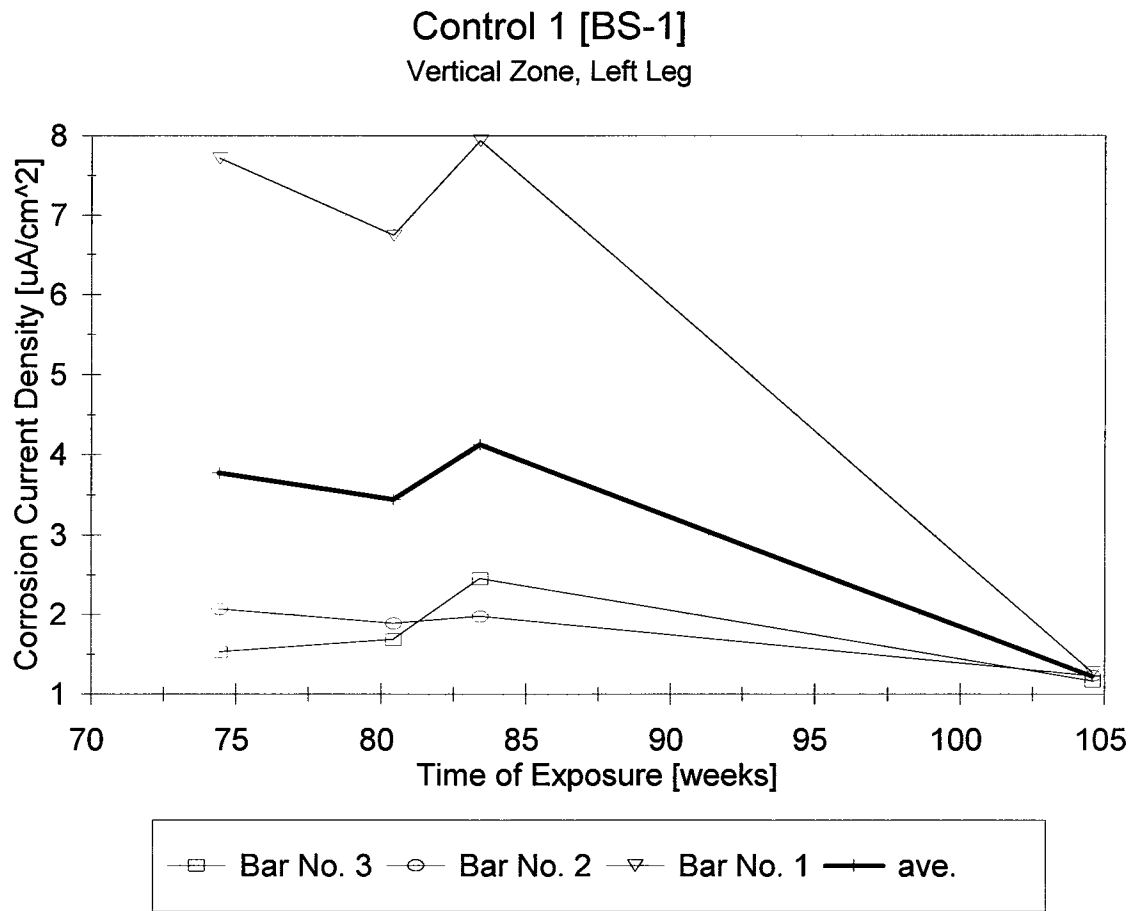


Figure 75. Corrosion Rates in the Vertical Zone, Left Leg, BS-1 Specimen.

Figure 76. Corrosion Rates in the Vertical Zone, Right Leg, BS-2 Specimen.

# Control 2 [BS-2]
## Vertical Zone, Left Leg
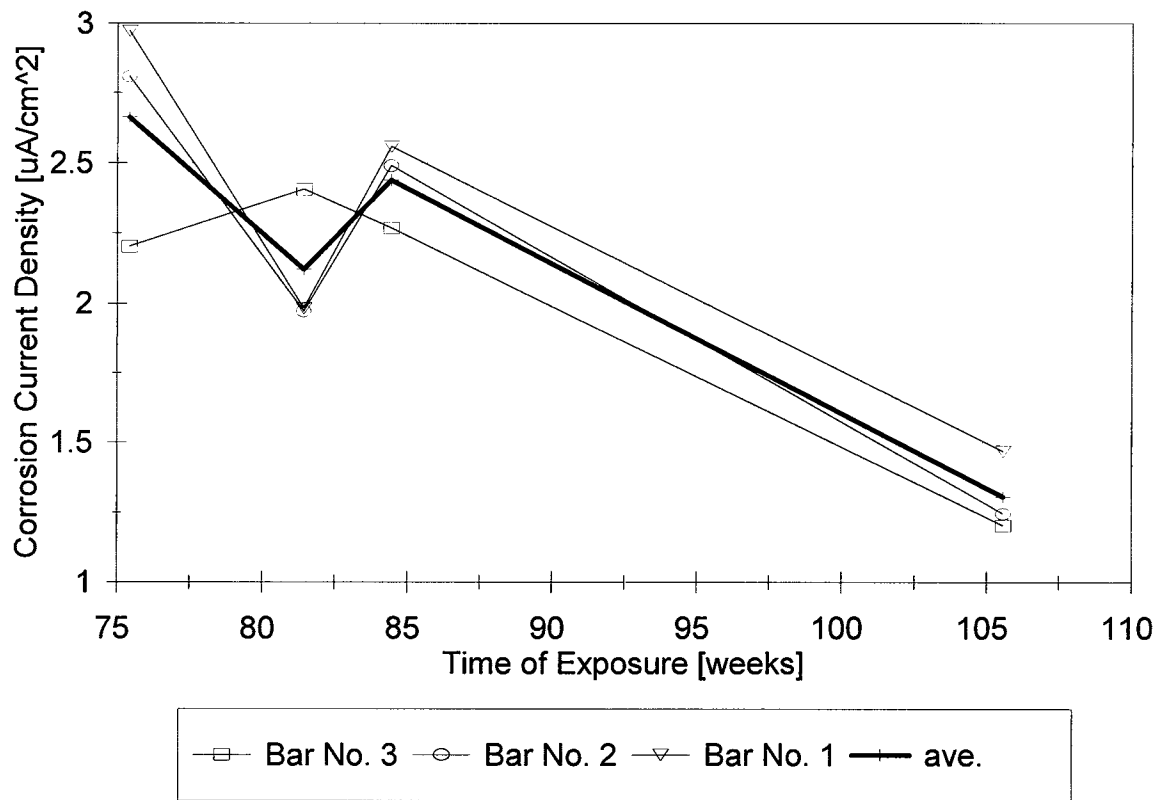


Figure 77. Corrosion Rates in the Vertical Zone, Left Leg, BS-2 Specimen.

Control 1 [BS-1]

Immersed Zone, Right Leg
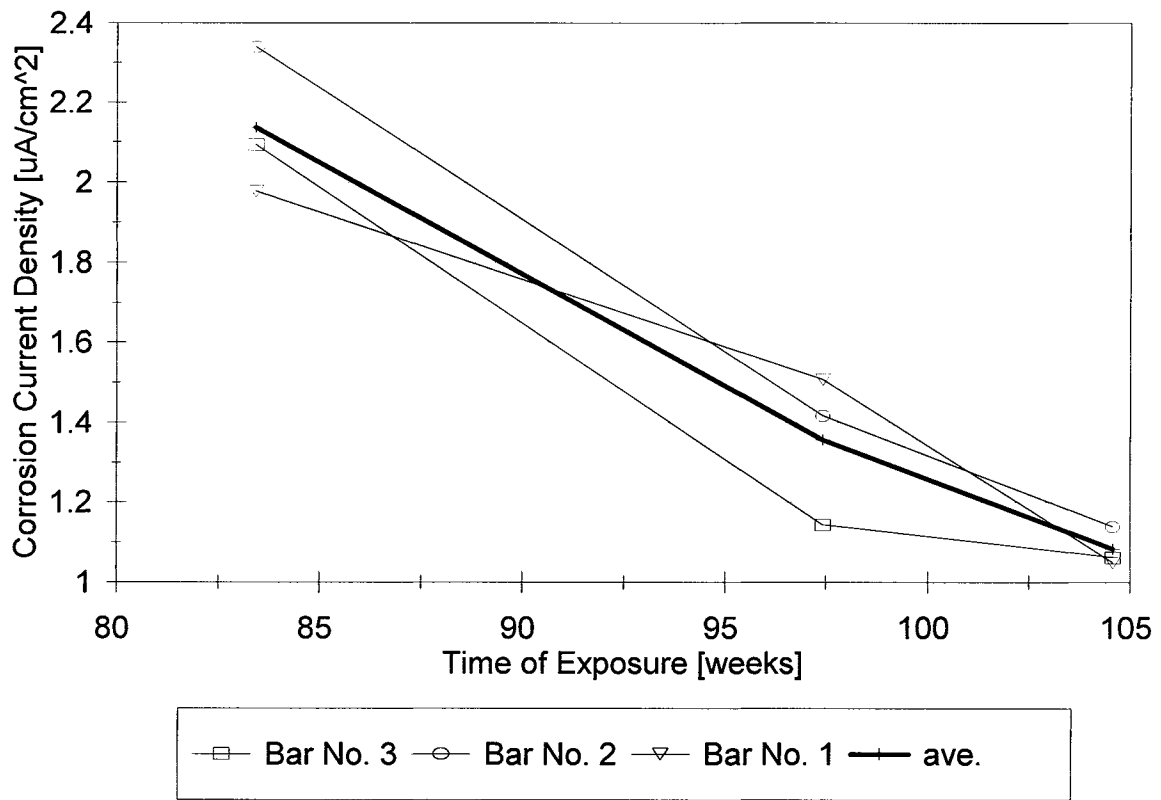
Figure 78. Corrosion Rates in the Immersed Zone, Right Leg, BS-1 Specimen.

**Control 1 [BS-1]**

Immersed Zone, Left Leg
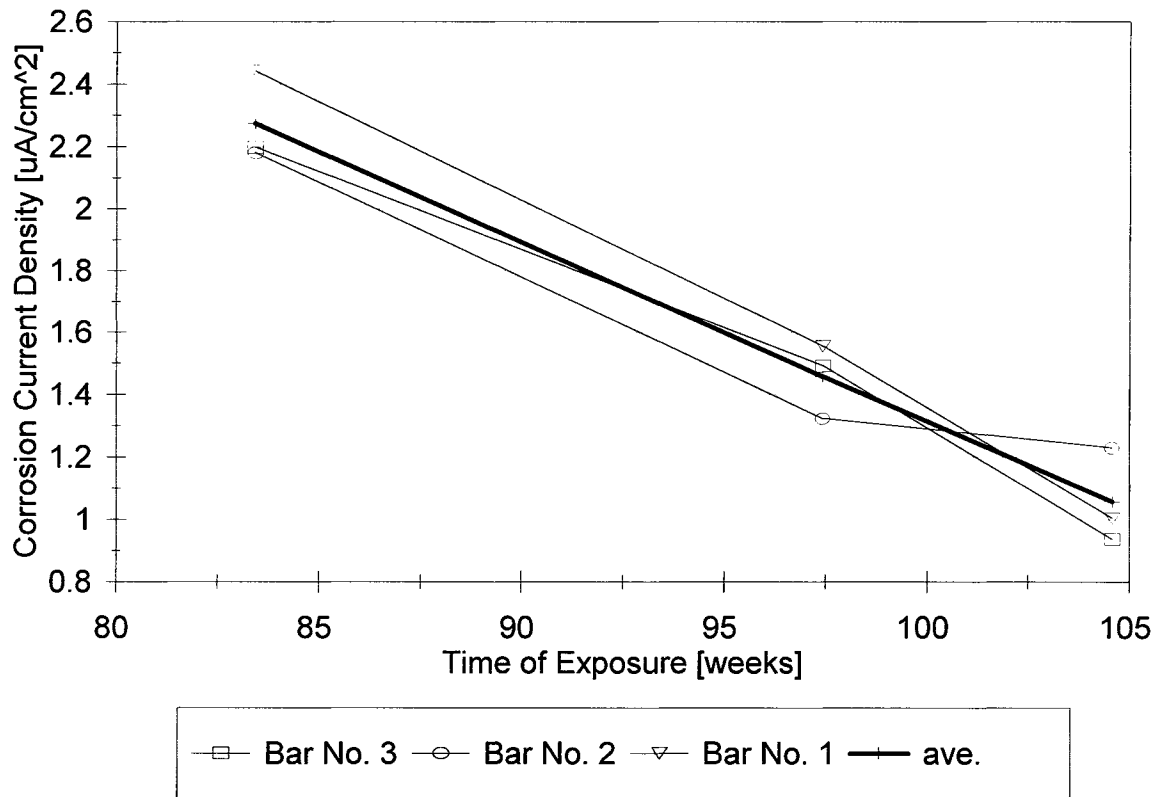
Figure 79. Corrosion Rates in the Immersed Zone, Left Leg, BS-1 Specimen.
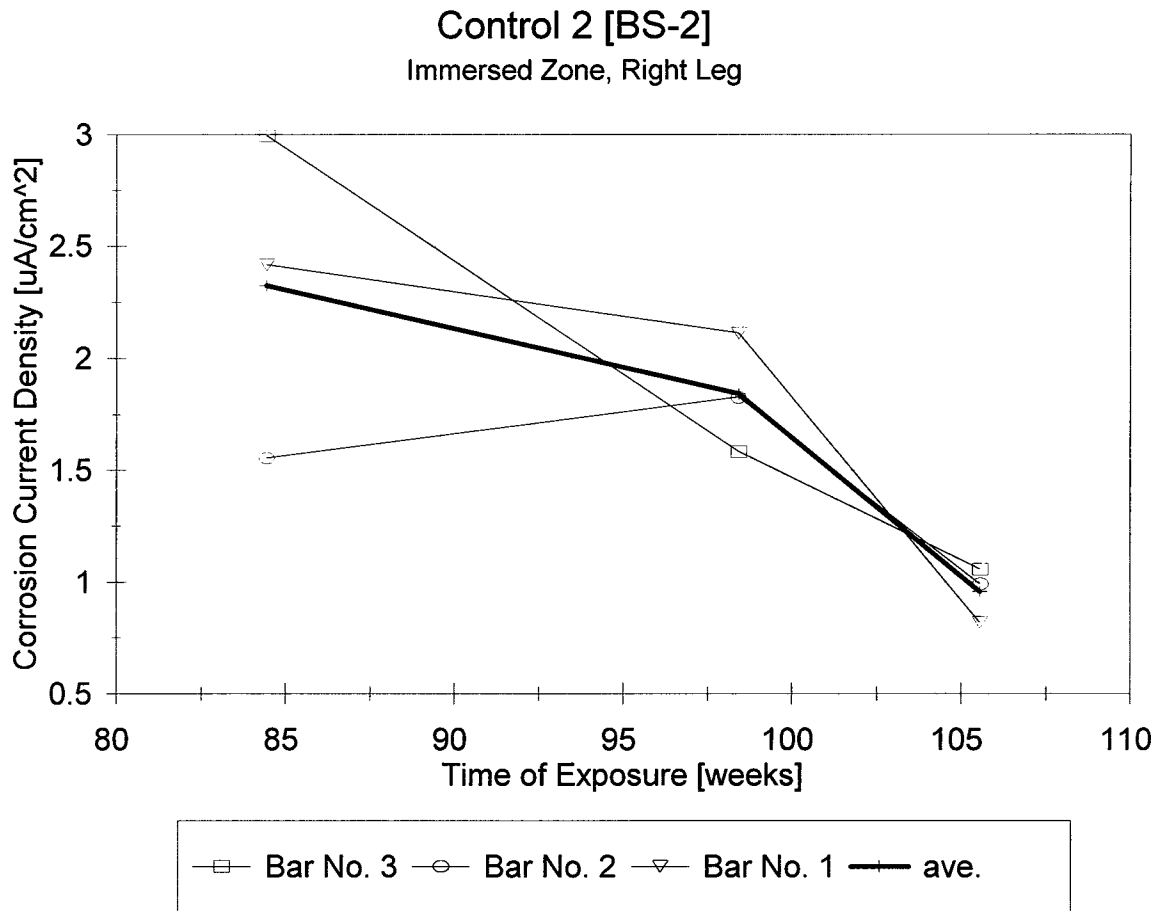
Figure 80. Corrosion Rates in the Immersed Zone, Right Leg, BS-2 Specimen.
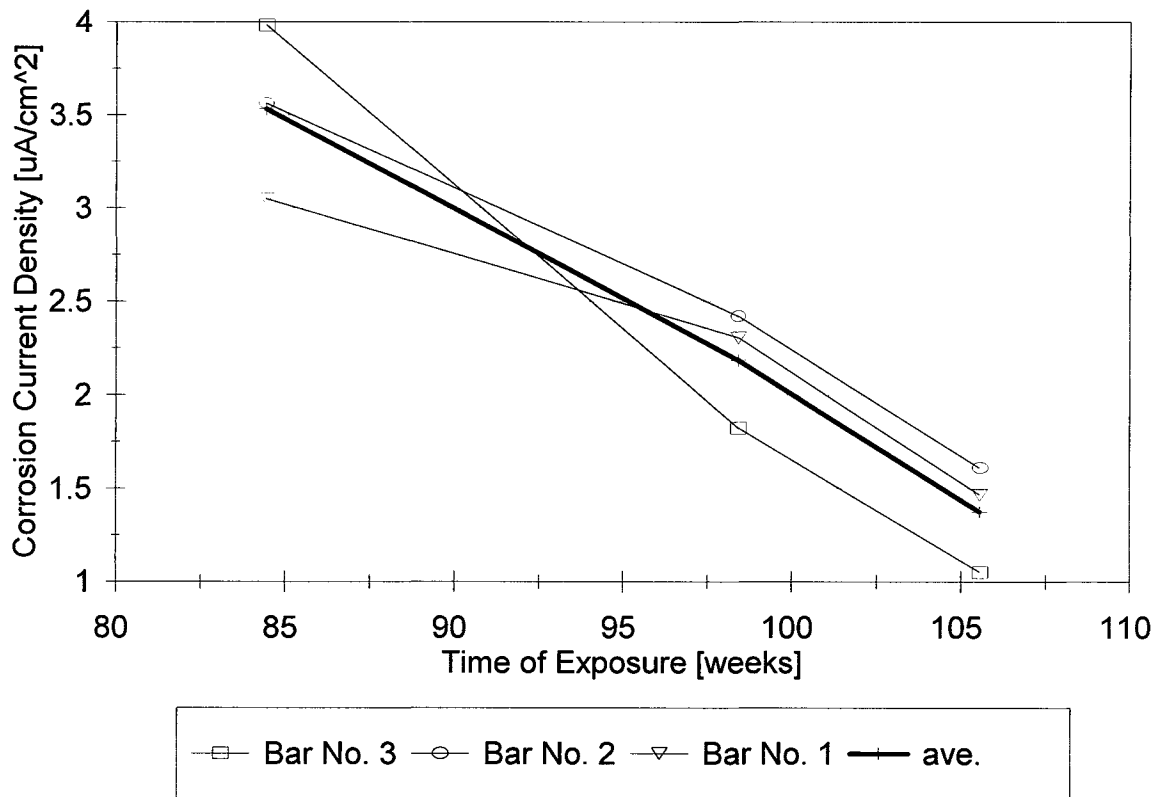
Figure 81. Corrosion Rates in the Immersed Zone, Left Leg, BS-2 Specimen.

## Control 1 [BS-1]
### Tidal Zone, Right Leg
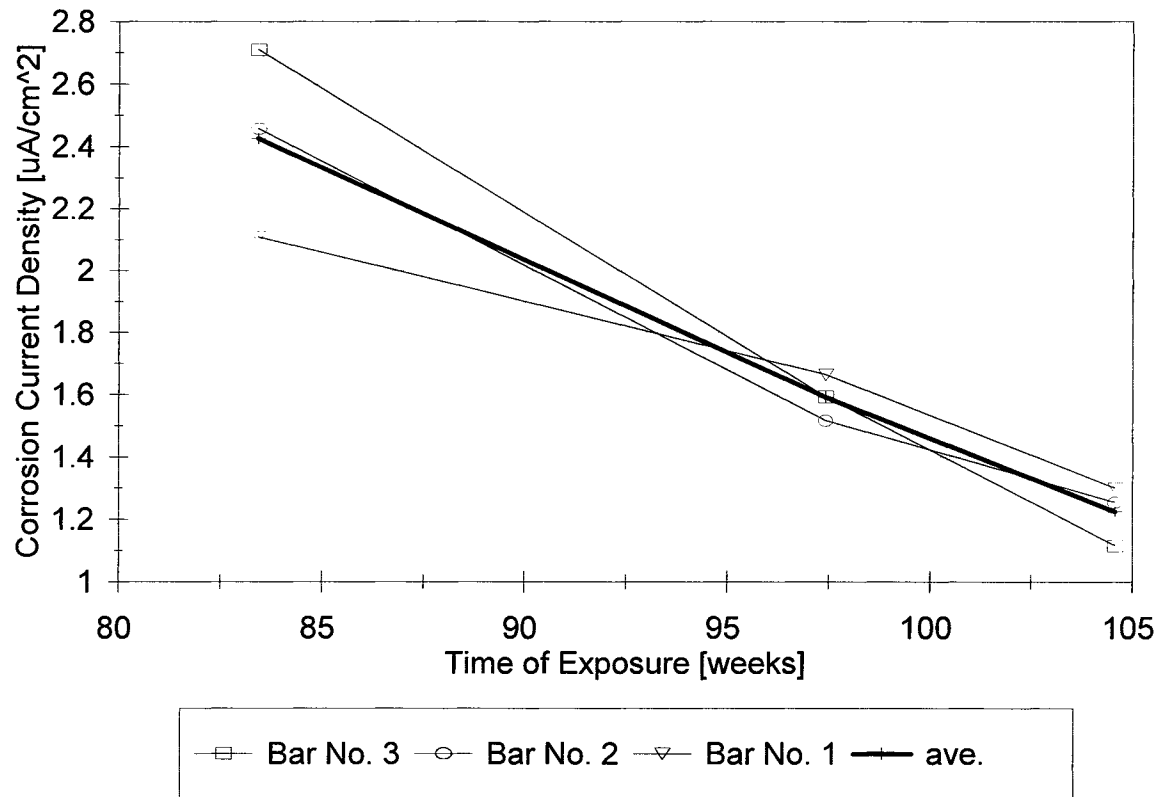
Figure 82. Corrosion Rates in the Tidal Zone, Right Leg, BS-1 Specimen.

# Control 1 [BS-1]

## Tidal Zone, Left Leg
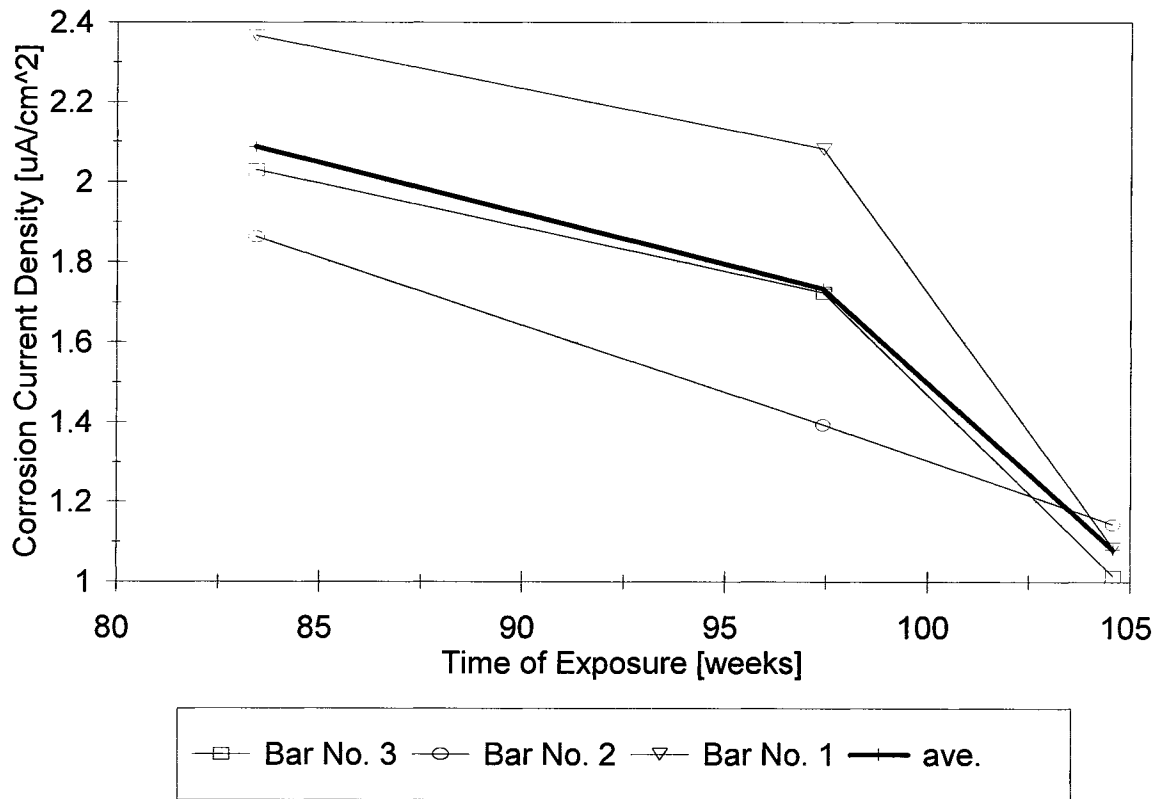


Figure 83.  Corrosion Rates in the Tidal Zone, Left Leg, BS-1 Specimen.

# Control 2 [BS-2]
## Tidal Zone, Right Leg
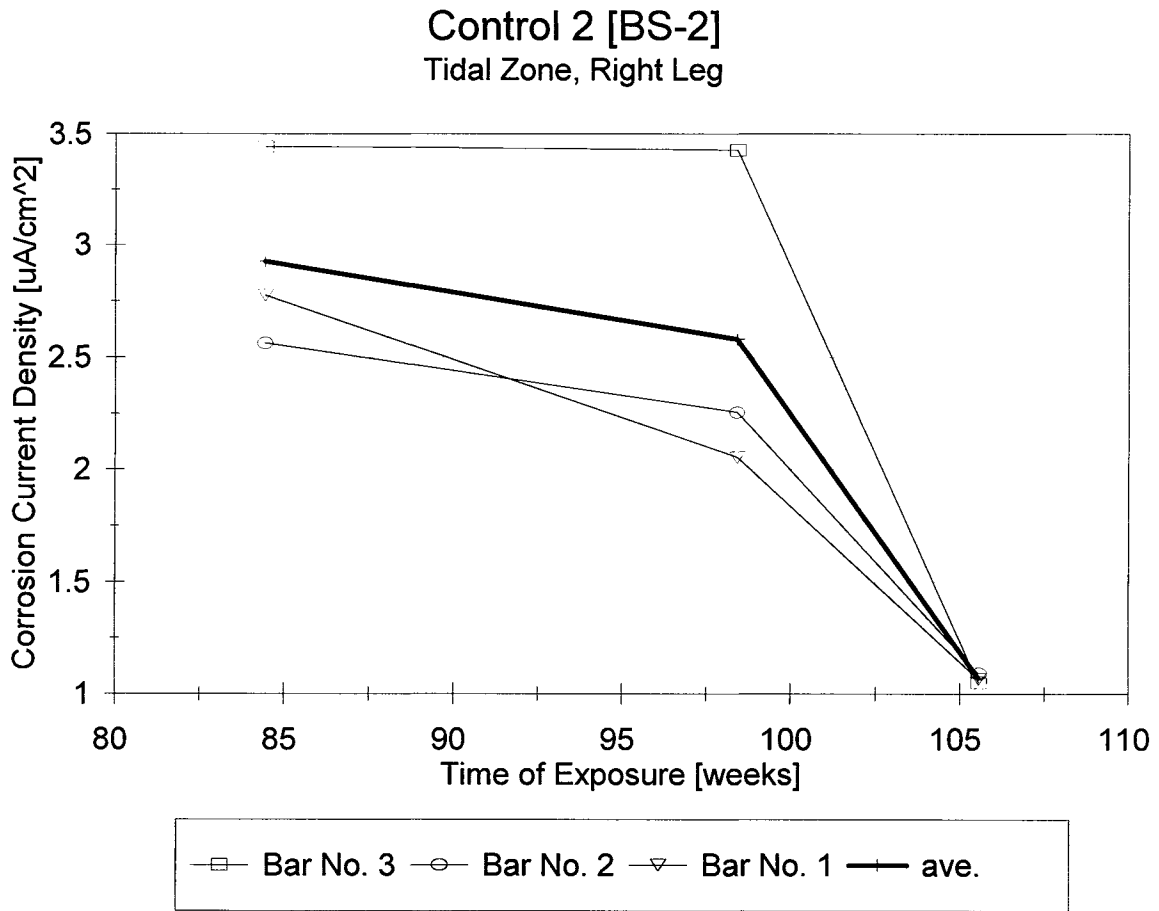


Figure 84.  Corrosion Rates in the Tidal Zone, Right Leg, BS-2 Specimen.

**Control 2 [BS-2]**
Tidal Zone, Left Leg
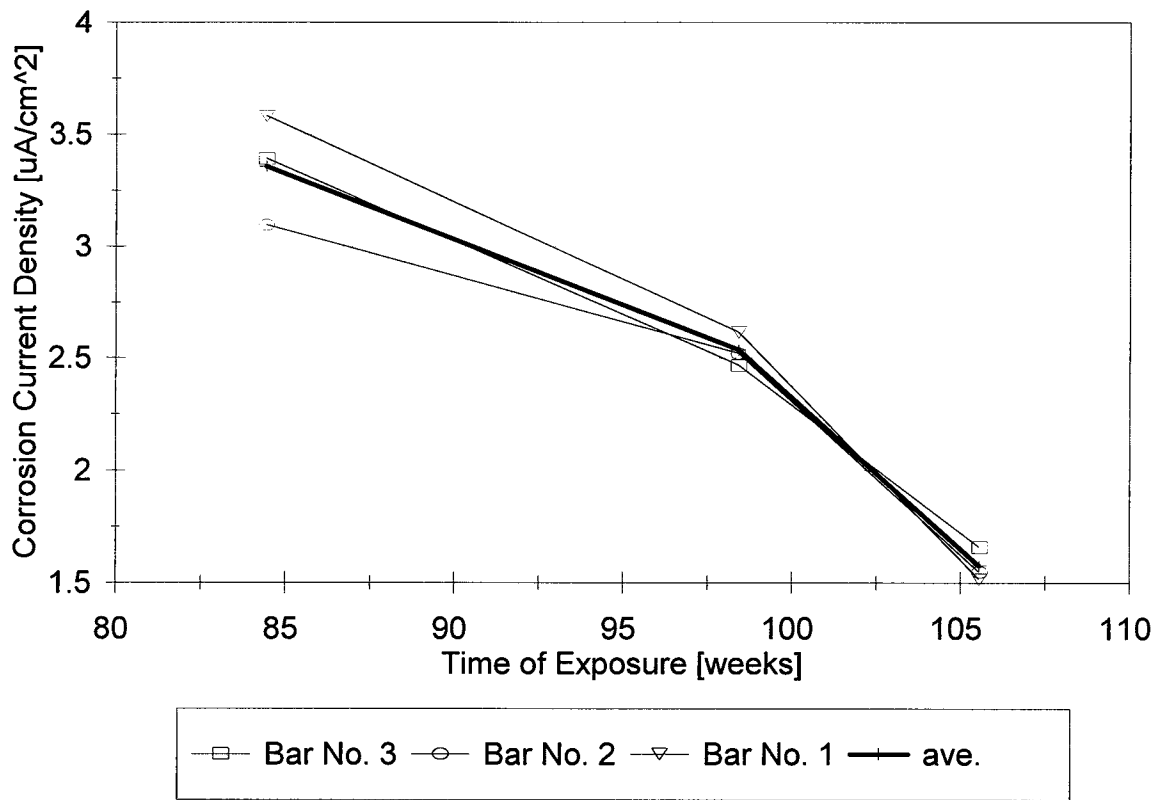
Figure 85. Corrosion Rates in the Tidal Zone, Left Leg, BS-2 Specimen.

**Rapid Concrete Permeability at 28 Days**
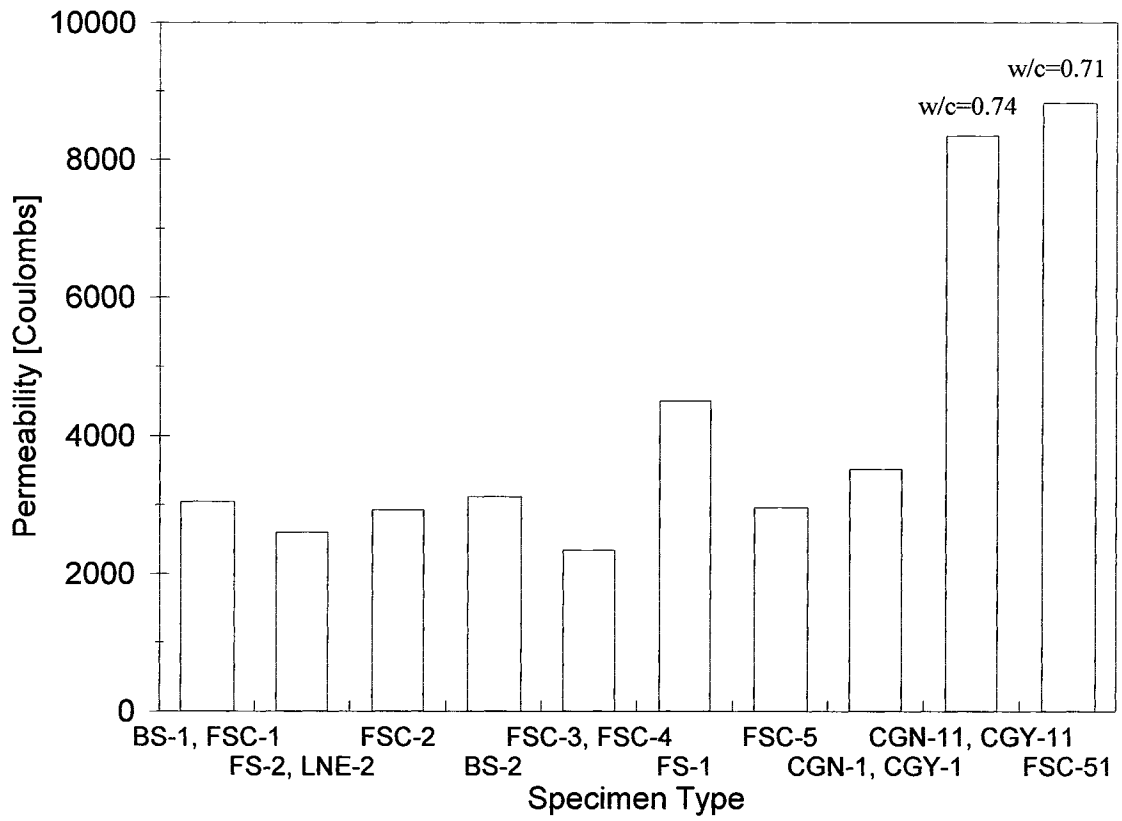
Figure 86. Rapid Concrete Chloride Permeability at 28 Days.

## Rapid Concrete Permeability at 1 Year
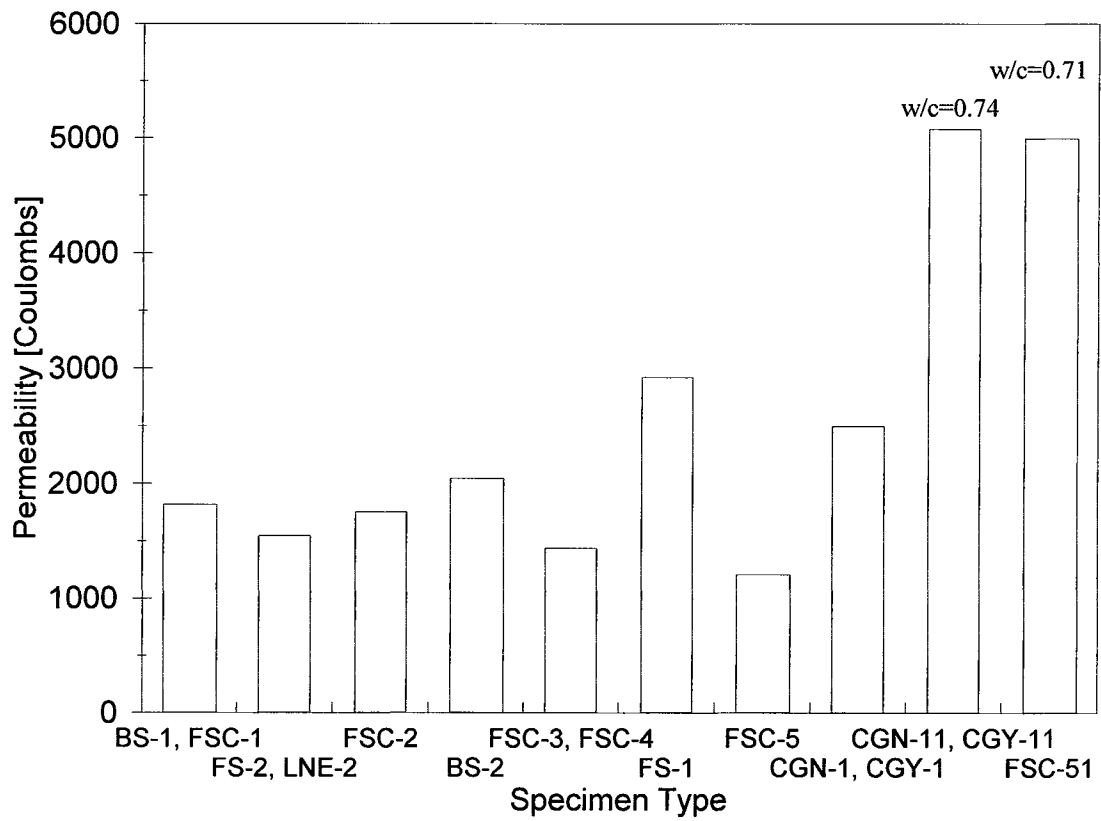


Figure 87. Rapid Concrete Chloride Permeability at 1 Year.
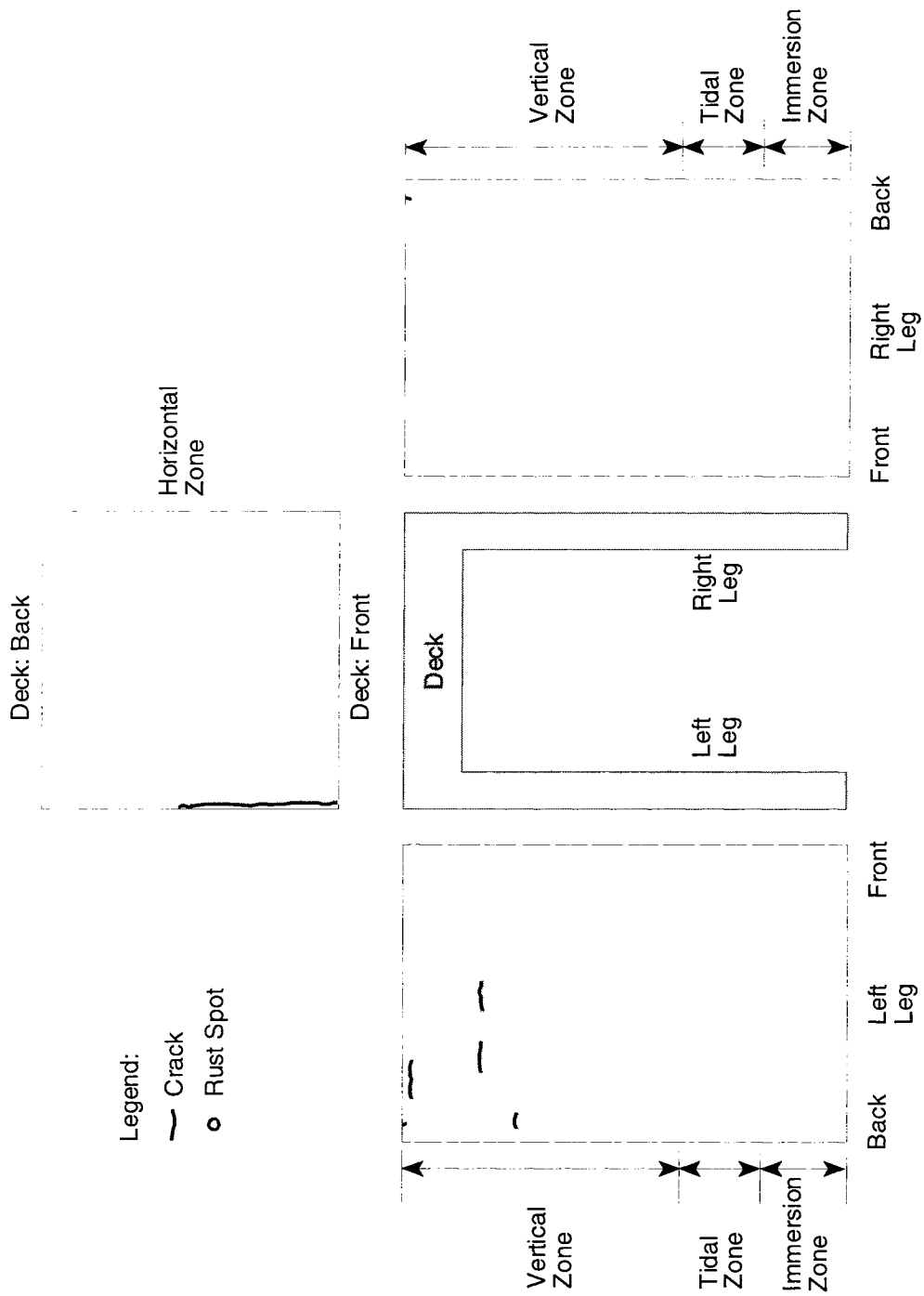
Figure 88.  Visual Observations: October 1996.  Cracking and Rust Spots in the BS-1 Specimen.

Legend:

⌒ Crack

o Rust Spot

Deck: Back

Horizontal
Zone

Deck: Front

Deck

Left
Leg

Right
Leg

Vertical
Zone

Tidal
Zone

Immersion
Zone

Back        Front

Left        Right
Leg          Leg

Front        Back

Vertical
Zone

Tidal
Zone

Immersion
Zone
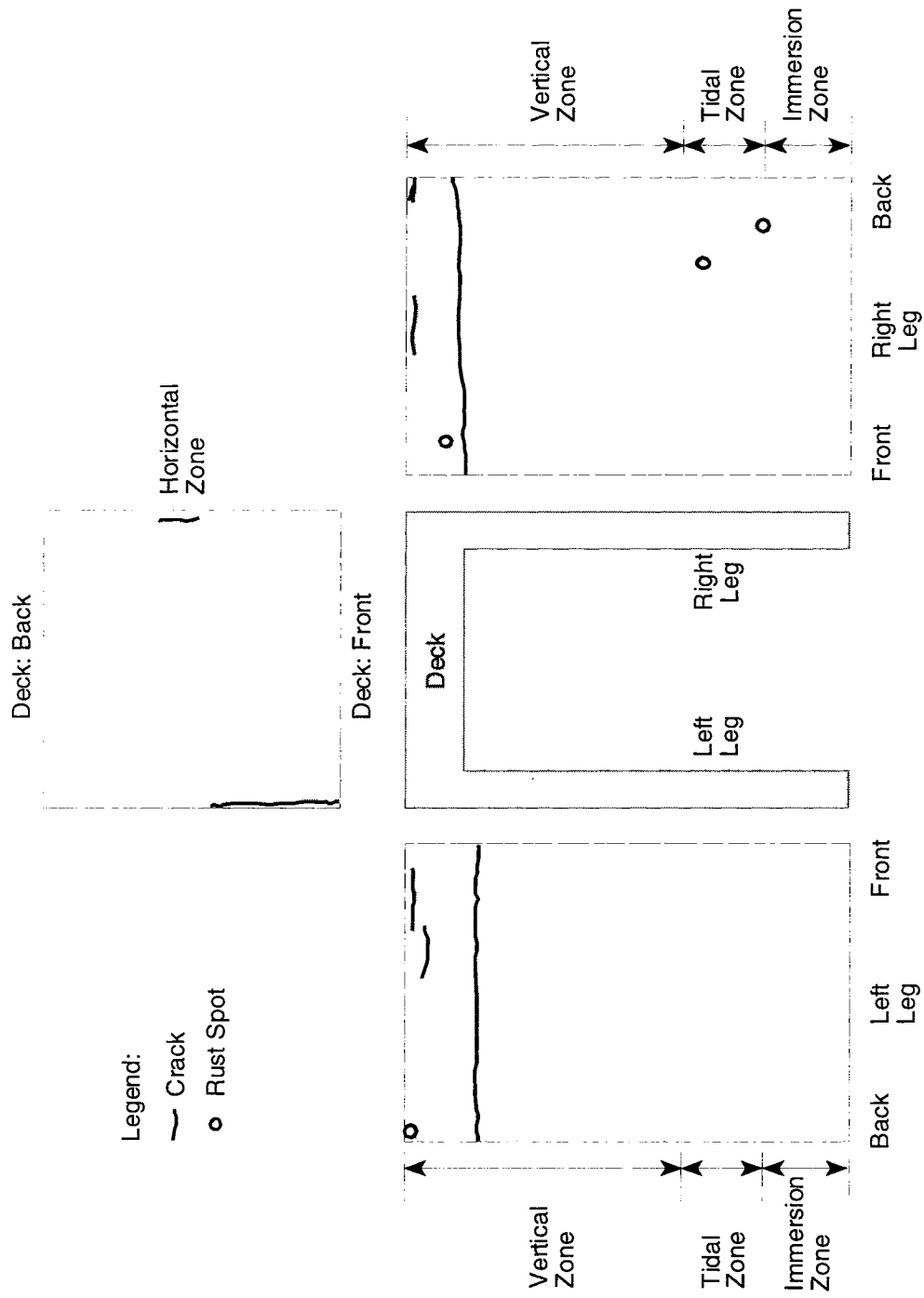
Figure 89.    Visual Observations: October 1996.  Cracking and Rust Spots in the BS-2 Specimen.
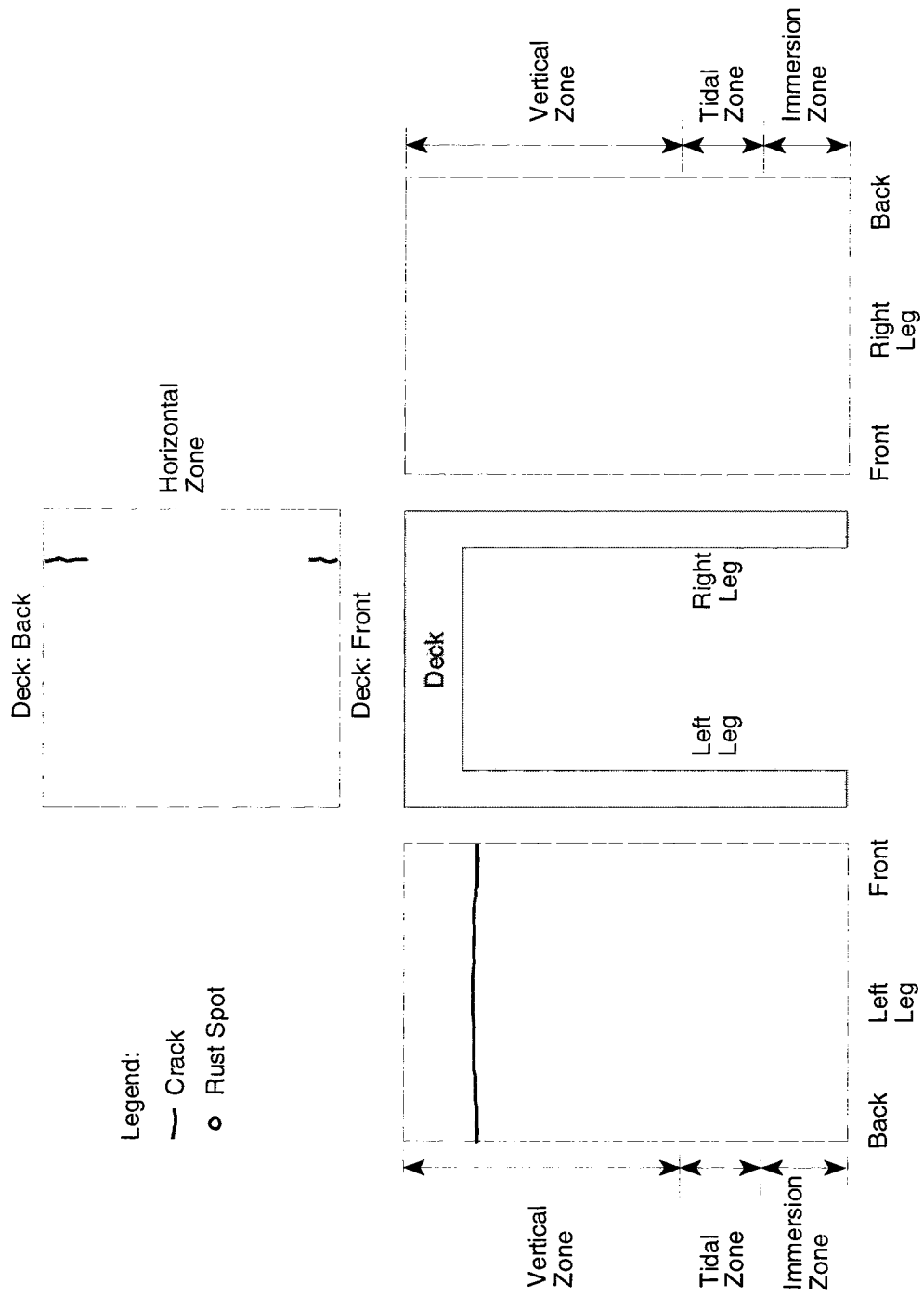
Figure 90.  Visual Observations: October 1996.  Cracking and Rust Spots in the FSC-2 Specimen.
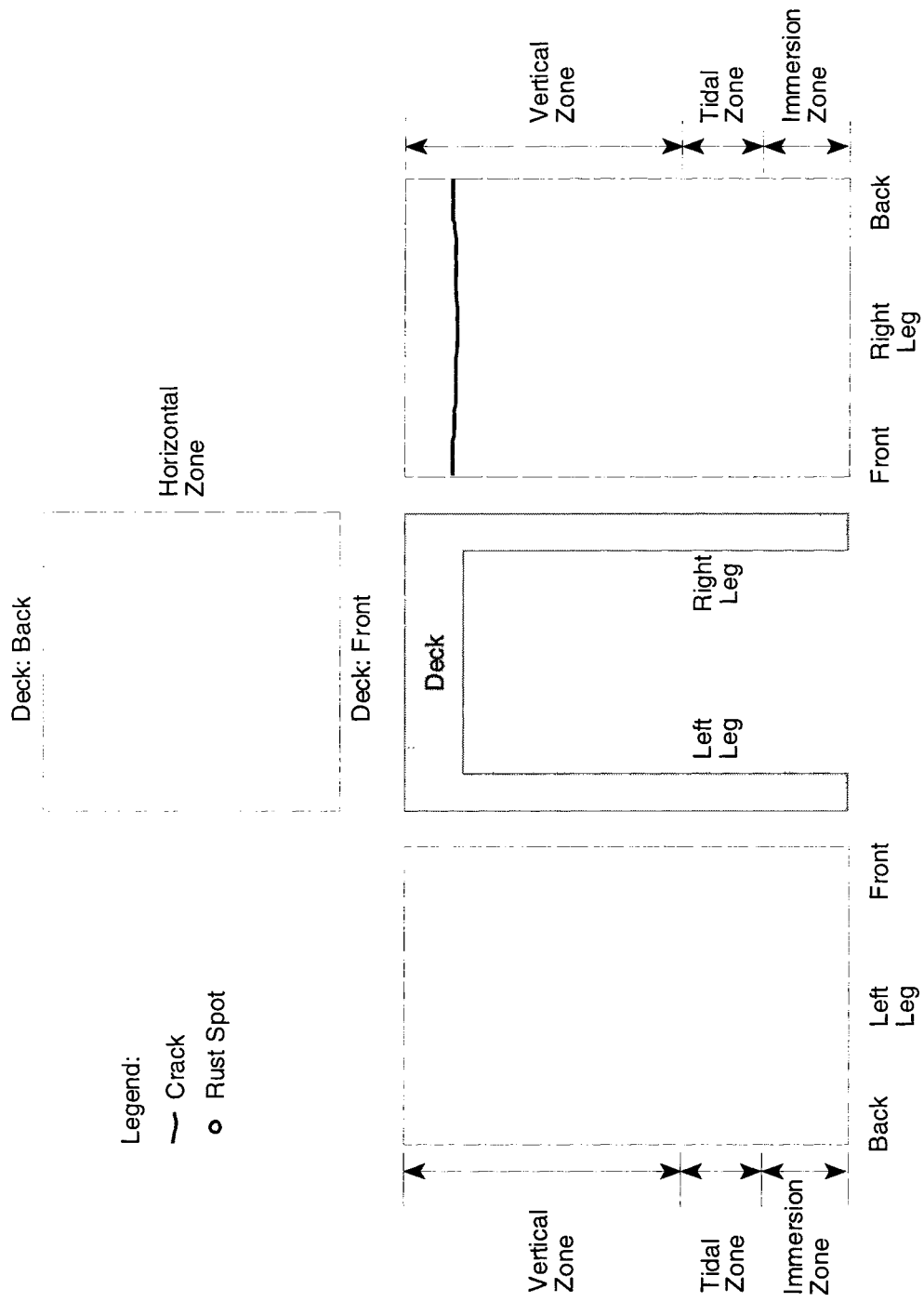
Figure 91.   Visual Observations: October 1996.   Cracking and Rust Spots in the FSC-3 Specimen.

Deck: Back

Horizontal
Zone

Deck: Front

Legend:
⌐ Crack
○ Rust Spot

Vertical
Zone

Tidal
Zone

Immersion
Zone

Deck

Left
Leg

Right
Leg

Back      Left      Front
          Leg

Vertical
Zone

Tidal
Zone

Immersion
Zone

Front      Right      Back
           Leg
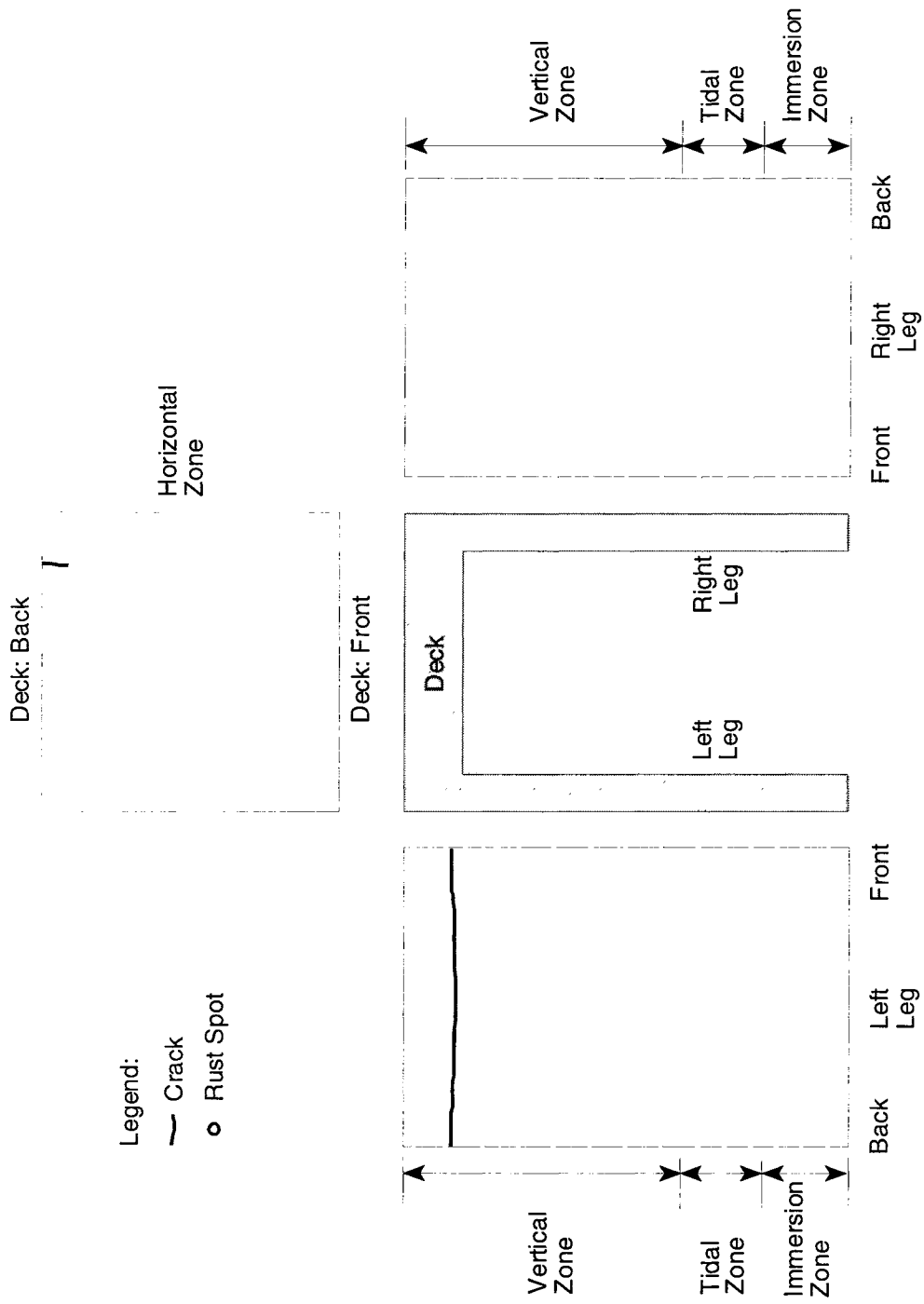
Figure 92.    Visual Observations: October 1996.   Cracking and Rust Spots in the FSC-5 Specimen.

Deck: Back

Horizontal
Zone

Deck: Front

Legend:

‒ Crack

o Rust Spot

Deck

Left
Leg

Right
Leg

Vertical
Zone

Tidal
Zone

Immersion
Zone

Back

Left
Leg

Front

Front

Right
Leg

Back

Vertical
Zone

Tidal
Zone

Immersion
Zone
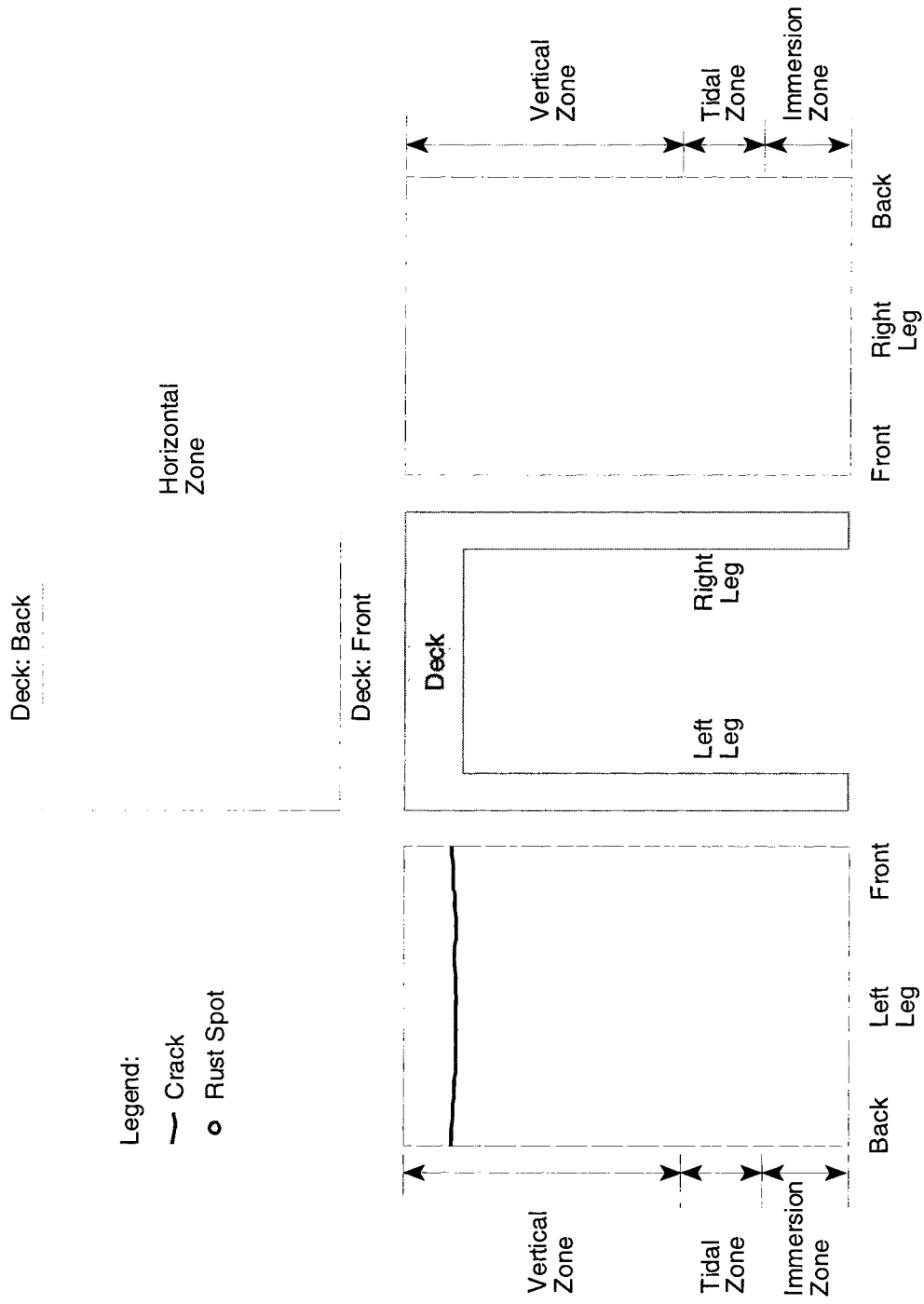
Figure 93.    Visual Observations: October 1996.   Cracking and Rust Spots in the LNE-2 Specimen.
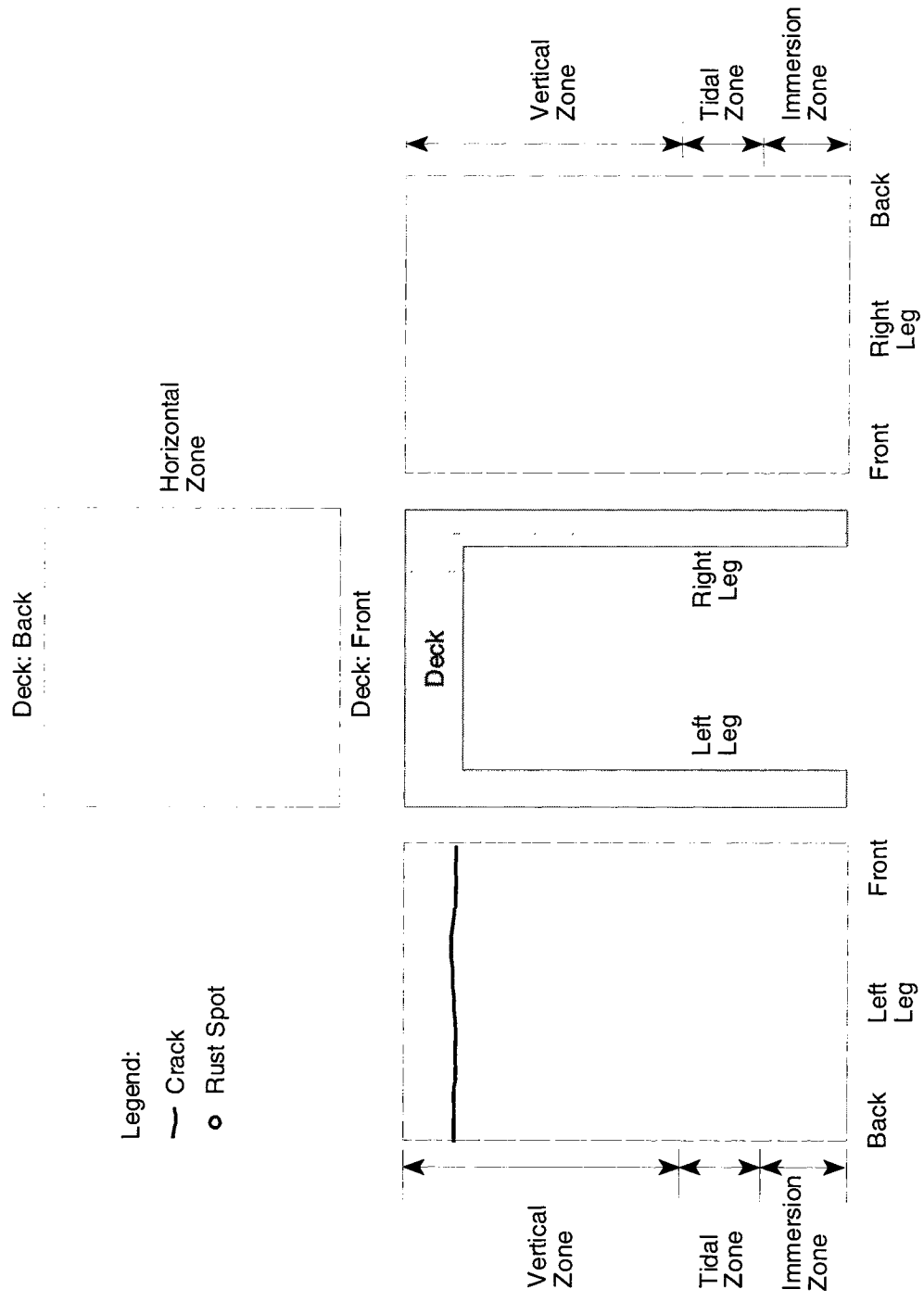
Figure 94.    Visual Observations: October 1996.  Cracking and Rust Spots in the FS-1 Specimen.
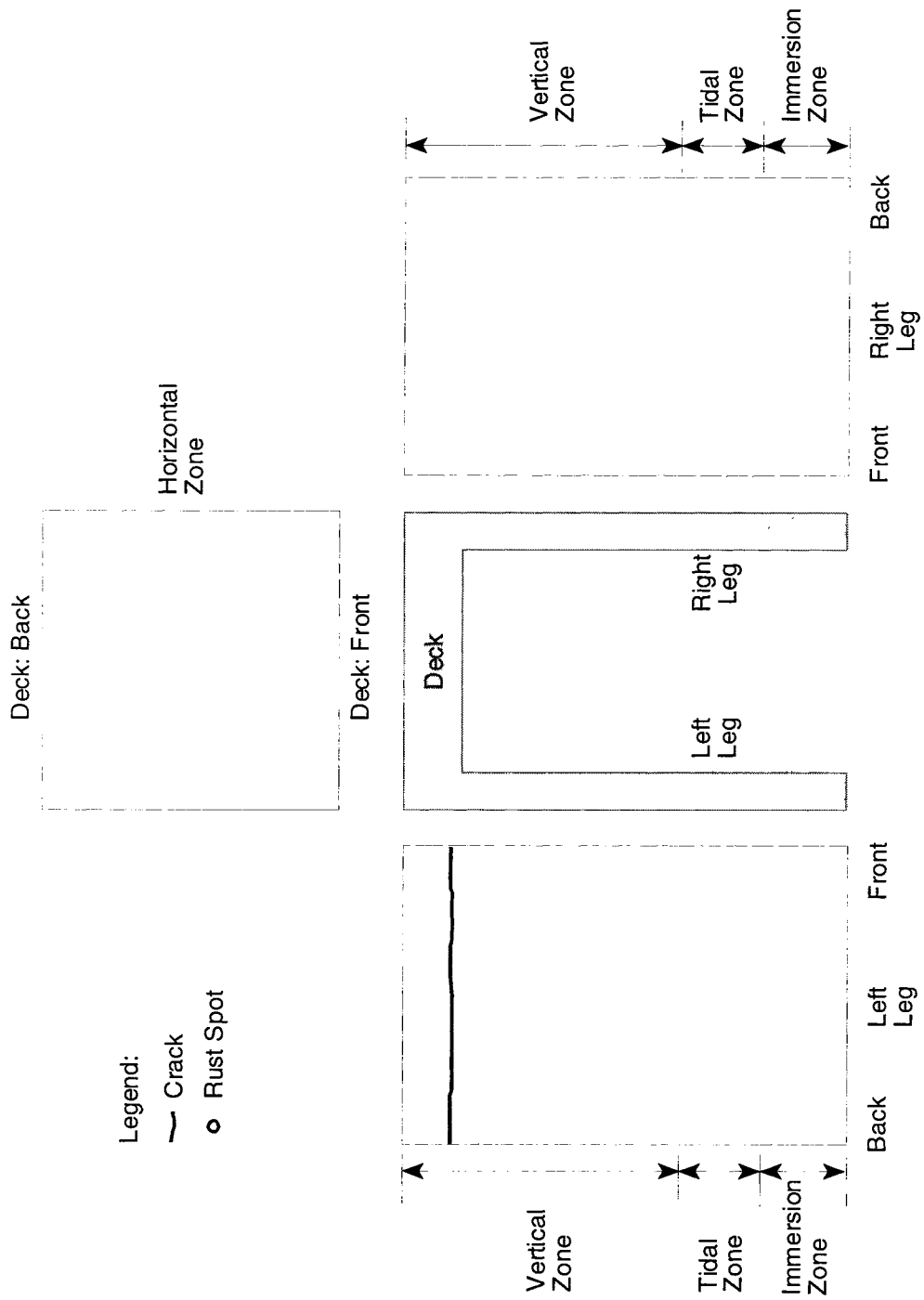
Figure 95. Visual Observations: October 1996. Cracking and Rust Spots in the FS-2 Specimen.

Legend:
— Crack
o Rust Spot

Deck: Back

Horizontal
Zone

Deck: Front

Deck

Left
Leg

Right
Leg

Vertical
Zone

Tidal
Zone

Immersion
Zone

Back    Left    Front
        Leg

Vertical
Zone

Tidal
Zone

Immersion
Zone

Front    Right    Back
         Leg
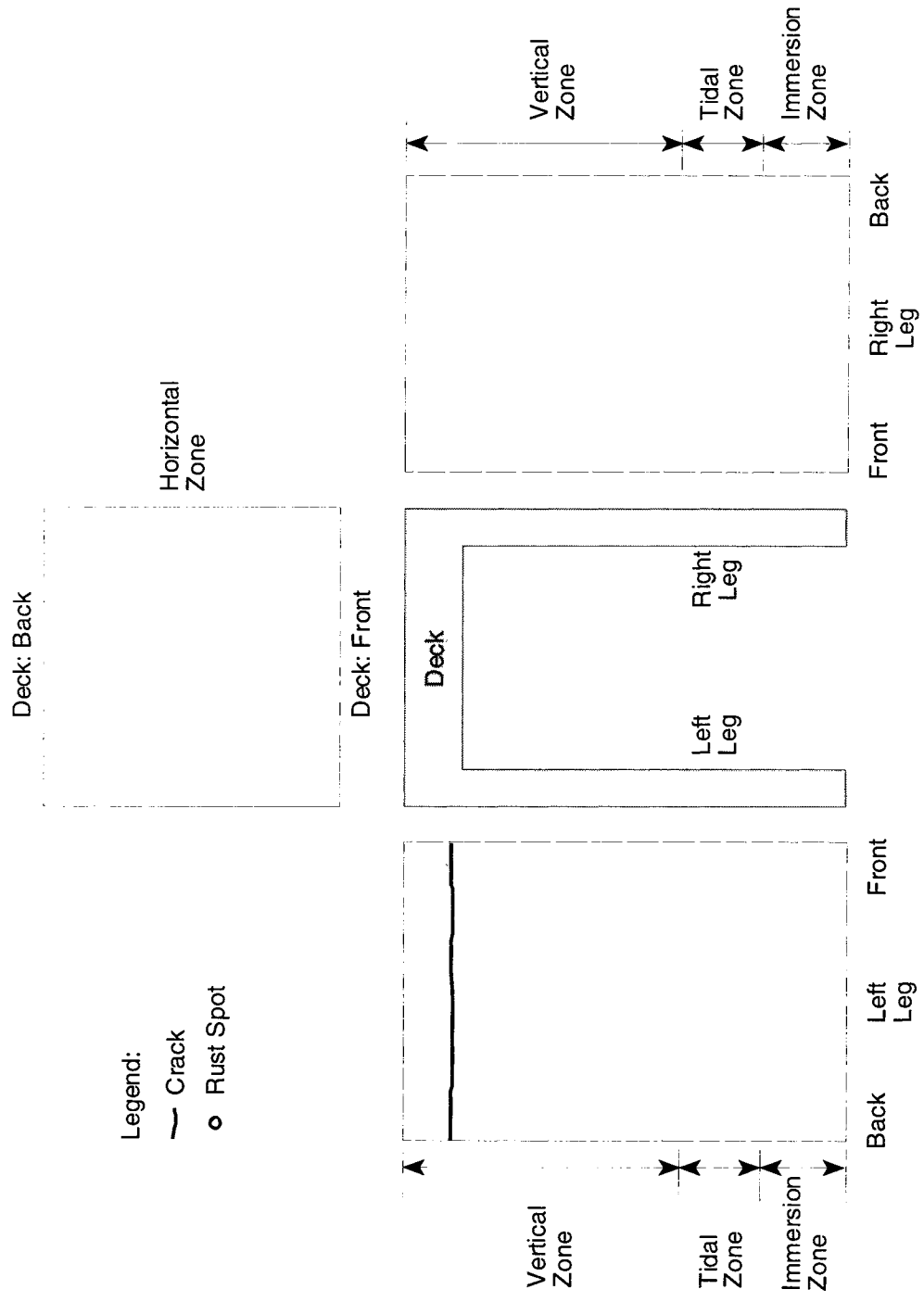
Figure 96.    Visual Observations: October 1996.  Cracking and Rust Spots in the CGY-1 Specimen.
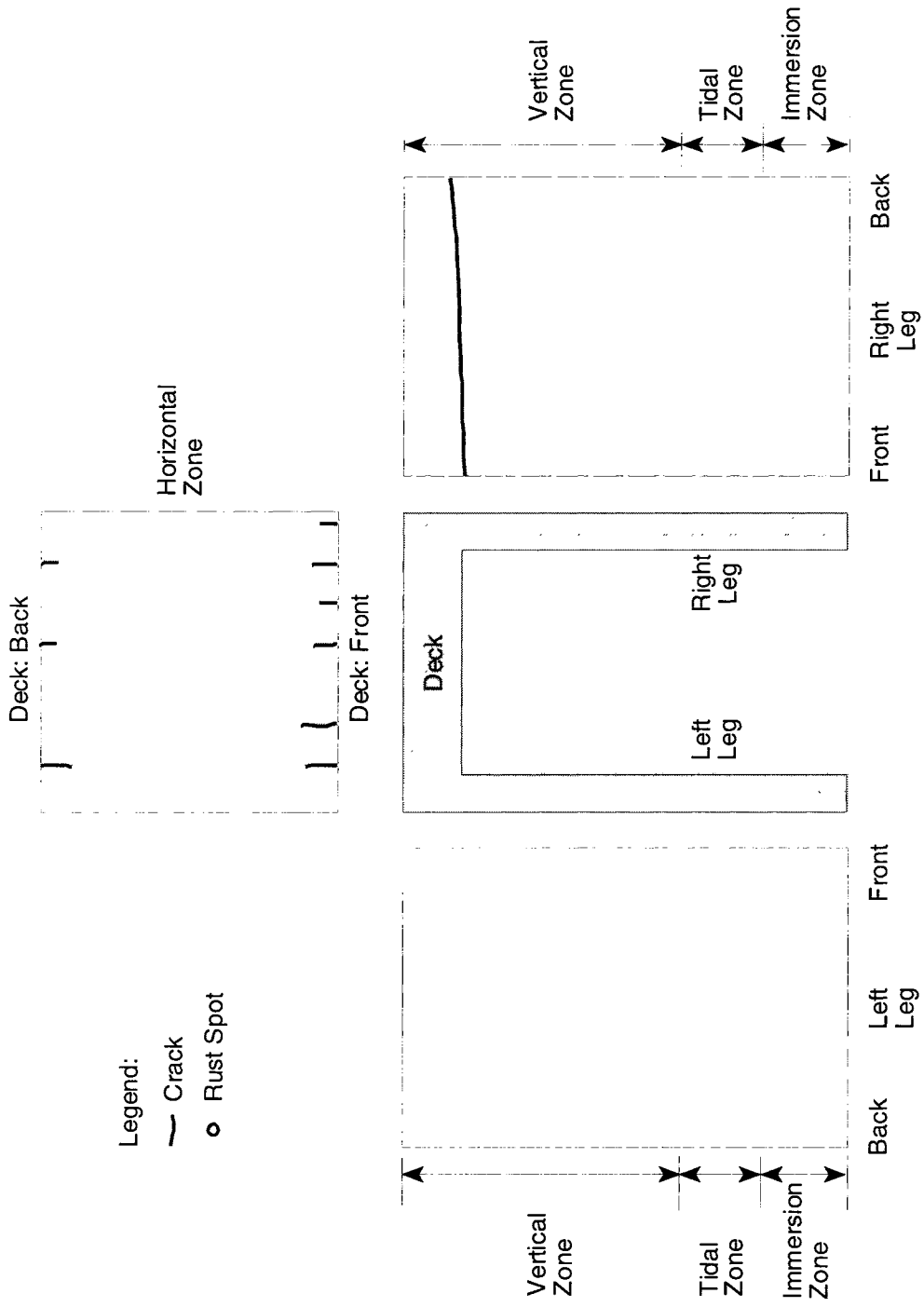
Figure 97. Visual Observations: October 1996. Cracking and Rust Spots in the FSC-51 Specimen.
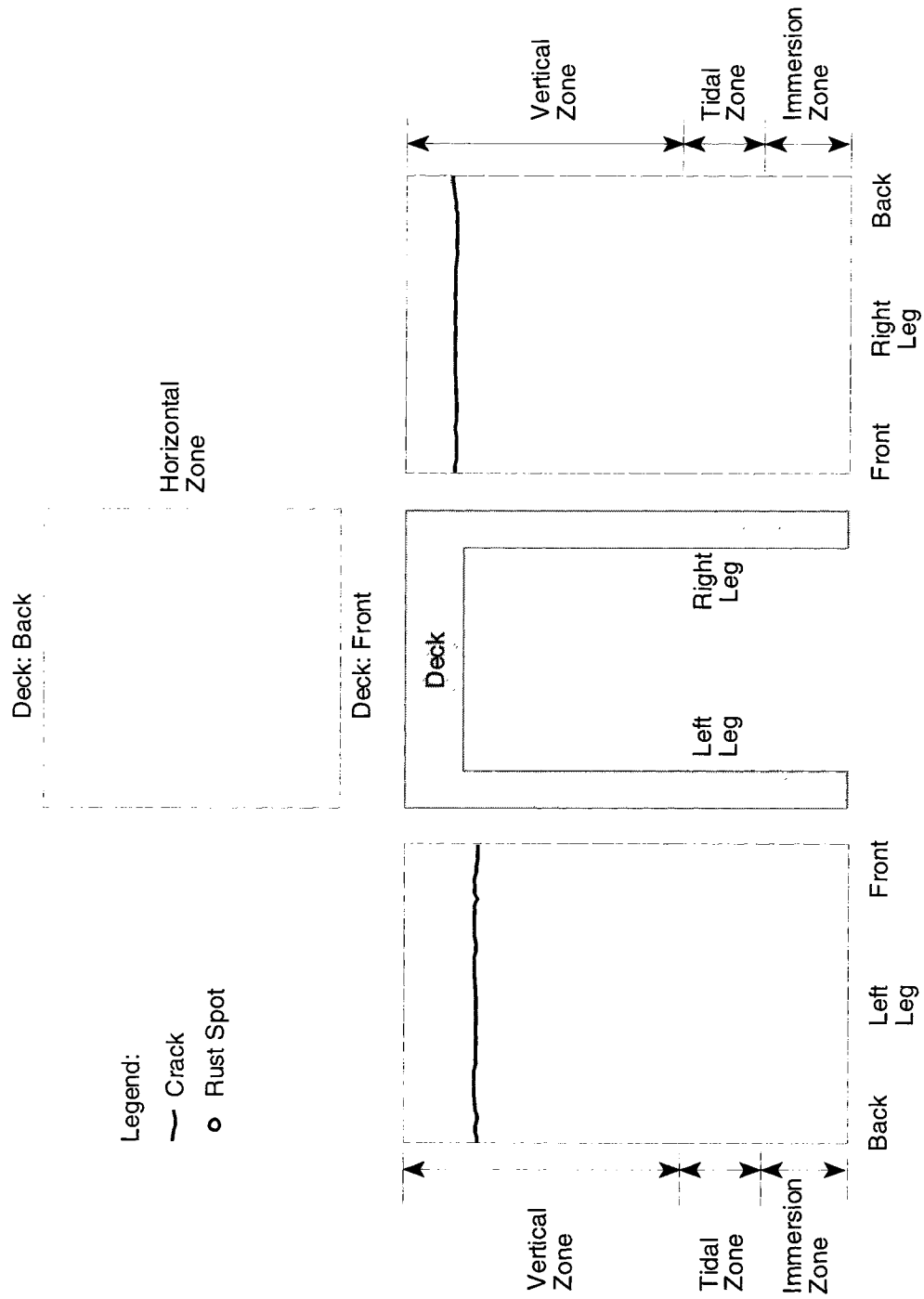
Figure 98. Visual Observations: October 1996. Cracking and Rust Spots in the CGN-11 Specimen.

Legend:

— Crack

○ Rust Spot

Deck: Back

Horizontal
Zone

Deck: Front

Deck

Left
Leg

Right
Leg

Vertical
Zone

Tidal
Zone

Immersion
Zone

Back

Left
Leg

Front

Vertical
Zone

Tidal
Zone

Immersion
Zone

Front

Right
Leg

Back

Figure 99. Visual Observations: October 1996. Cracking and Rust Spots in the CGY-11 Specimen.

Deck: Back

Legend:

⌒ Crack

o Rust Spot

Horizontal
Zone

Deck: Front

Deck

Vertical
Zone

Left
Leg

Right
Leg

Tidal
Zone

Immersion
Zone

Left
Leg

Back        Front

Deck

Front        Back

Right
Leg

Vertical
Zone

Tidal
Zone

Immersion
Zone

Figure 99.    Visual Observations: October 1996.  Cracking and Rust Spots in the CGY-11 Specimen.